

Fascin implements the distinction between two sensory neuron morphologies

Dissertation

der Fakultät für Biologie
der Ludwig–Maximilians–Universität München
Angefertigt am Max-Planck-Institut für Neurobiologie,
Abteilung Molekulare Neurobiologie,
Arbeitsgruppe Dendritische Differenzierung

Vorgelegt von
Julia Nagel
München 2011

Erstgutachter: Prof. Dr. Rüdiger Klein

Zweitgutachter: Prof. Dr. Rainer Uhl

Dissertation eingereicht am: 04.07.2011

Tag der mündlichen Prüfung: 25.11.2011

Hiermit erkläre ich ehrenwörtlich, dass ich die vorliegende Dissertation selbständig und ohne unerlaubte Hilfe angefertigt habe. Ich habe weder anderweitig versucht, eine Dissertation oder Teile einer Dissertation einzureichen beziehungsweise einer Prüfungskommission vorzulegen, noch mich einer Doktorprüfung zu unterziehen.

München, den

Julia Nagel

Die vorliegende Arbeit wurde zwischen April 2007 und Juni 2011 unter Anleitung von Dr. Gaia Tavoranis am Max Planck Institut für Neurobiologie in Martinsried durchgeführt.

Table of Content

Index of figures	10
Index of tables	11
Abbreviations	12
1 Summary	13
2 Introduction	14
2.1 Dendrites	14
2.2 Dendrite differentiation	15
2.2.1 Transcription factors	15
2.2.1 Guidance receptors and ligands	15
2.2.2 Establishment of dendritic branches	16
2.3 Md-da neurons of the <i>Drosophila</i> PNS	18
2.3.1 Morphological characterisation	18
2.3.2 Transcriptional code affecting md-da dendrite morphology	21
2.4 Actin cytoskeleton	23
2.4.1 Basic dynamic properties of actin	23
2.4.2 Actin-regulating proteins in dendrite development	24
2.4.3 Formation of filopodia	26
2.5 Fascin	29
2.5.1 Fascin structure	29
2.5.2 Actin bundling through fascin	30
2.5.3 Fascin regulation through phosphorylation	30
2.5.4 Fascin regulation by small GTPases	32
2.5.5 Biological role of fascin	32
2.5.6 Singed, the <i>Drosophila</i> fascin homologue	33
2.5.7 Fascin and its potential role in dendrite differentiation	34
3 Results	36
3.1 Singed expression in the <i>Drosophila</i> PNS	37
3.1.1 Endogenous Singed in the md-da neurons	37
3.1.2 Localization of fluorescently tagged Singed in terminal branchlets of md-da neurons	40

3.2	Terminal branchlets of class III and class IV neurons	43
3.2.1	Cytoskeletal organization	43
3.2.2	Terminal branchlet bending	46
3.3	Singed in class III neurons	48
3.3.1	Singed affects the number and density of class III spiked protrusions	48
3.3.2	Singed controls terminal branchlet morphology and dendrite complexity	49
3.3.3	Singed does not affect the general cytoskeletal organization in class III neurons	52
3.3.4	MARCM	54
3.3.5	Singed accumulation is correlated with the outgrowth of spiked protrusions	55
3.4	Singed in class IV neurons	58
3.4.1	<i>Singed</i> loss of function does not affect class IV dendritic branching	58
3.4.2	Overexpression of Singed can induce spiked protrusions in class IV neurons	59
3.5	Singed activity is modulated by phosphorylation	62
3.5.1	Regulation through phosphorylation in class III neurons	62
3.5.2	Regulation through phosphorylation in class IV neurons	64
3.6	The transcription factor Cut is acting through Singed in spiked protrusion formation	66
4	Discussion	69
4.1	Summary of the results	69
4.2	The role of Singed in class III neurons	70
4.2.1	Singed is required for the bundling of actin-filaments in class III neurons	70
4.2.2	Singed does not influence the overall dendrite extension	71
4.2.3	Dynamic Singed accumulation on dynamic spiked protrusions	72
4.3	Molecular regulation of Singed	73
4.3.1	Regulation through phosphorylation of the conserved Serine52	73
4.3.2	Regulation by small GTPases	73
4.4	Singed and the transcription factor Cut	75
4.4.1	Cut is acting through Singed in the formation of spiked protrusions	75
4.4.2	Possible regulation of Singed through Cut	76
4.5	What is the difference in class IV neurons?	78
4.5.1	Distinct and similar properties of class III and class IV dendrites	78
4.5.2	Singed in class IV neurons	78
4.5.3	Possible mechanisms for terminal branchlet formation in class IV neurons	79
4.6	Singed as a molecular switch between class III and class IV dendritic branching pattern	81
4.6.1	Singed defines class III characteristic morphology	81

4.6.2 Singed does not facilitate a complete transformation between the two classes	81
4.7 Specific versus general mechanisms in dendritic branch formation	83
4.8 A model for Singed in dendrite formation	84
5 Materials and Methods	86
5.1 Materials	86
5.1.1 Chemicals	86
5.1.2 Buffers and Solutions	87
5.1.3 Media	88
5.1.4 Enzymes and DNA standards	90
5.1.5 Plasmids and DNA library	90
5.1.6 Primer	91
5.1.7 Antibodies	92
5.1.8 Commercial kits	92
5.1.9 Equipment	92
5.2 Drosophila stocks	94
5.2.1 Fly stocks	94
5.2.2 Genotypes analysed	95
5.3 Methods	96
5.3.1 Molecular procedures	96
5.3.2. Gal4 UAS system	101
5.3.3 MARCM	102
5.3.4 Immunohistochemistry	104
5.3.5 Confocal imaging	105
5.3.6 Image analysis and statistics	105
6 References	107
7 Acknowledgements	116
8 Curriculum vitae	117

Index of figures

Figure 2.1:	The <i>Drosophila</i> peripheral nervous system	20
Figure 2.2:	Schematic drawing of fascin structure	31
Figure 2.3:	Singed bristle phenotype	34
Figure 3.1:	Singed is expressed in all md-da neurons	38
Figure 3.2:	Singed localizes to the terminal branchlets of class III neurons	39
Figure 3.3:	Functionality of the fluorescently tagged Singed construct	41
Figure 3.4:	Fluorescently tagged Singed localizes to class III spiked protrusions	42
Figure 3.5:	Actin localization in class III and class IV neurons	44
Figure 3.6:	Tubulin localization in class III and class IV neurons	45
Figure 3.7:	Curvature of terminal branchlets of class III and class IV neurons	47
Figure 3.8:	Loss of <i>singed</i> leads to the loss of class III spiked protrusions	49
Figure 3.9:	Singed controls spiked protrusion length and curvature	50
Figure 3.10:	Singed controls dendrite complexity	51
Figure 3.11:	Futsch extension is not altered upon loss of <i>singed</i>	53
Figure 3.12:	<i>singed</i> MARCM clones	55
Figure 3.13:	Singed accumulates within extending branchlets of class III neurons	57
Figure 3.14:	Singed is not required for class IV terminal branching	59
Figure 3.15:	Singed overexpression in class IV neurons	61
Figure 3.16:	Singed is partially regulated by phosphorylation in class III neurons	63
Figure 3.17:	Singed is partially regulated by phosphorylation in class IV neurons	65
Figure 3.18:	Singed is essential for the formation of Cut-induced spiked protrusions	67
Figure 3.19:	Singed localizes to ectopic spiked protrusions induced by Cut	68
Figure 4.1:	Model for Singed in dendrite formation	85
Figure 5.1:	Cloning strategy for mKO tagged Singed	96
Figure 5.2:	Gal4 UAS system	102

Index of tables

Table 5.1:	Chemicals used in this study	86
Table 5.2:	Media	88
Table 5.3:	Enzymes and DNA standards	90
Table 5.4:	Plasmids and DNA library	90
Table 5.5:	Primer	91
Table 5.6:	Antibodies	92
Table 5.7:	Commercial kits	92
Table 5.8:	Microscope systems	92
Table 5.9:	Consumables	93
Table 5.10:	Fly stocks	94
Table 5.11:	Genotypes analysed in this study	95

Abbreviations

ADP	adenosine diphosphate
ATP	adenosine triphosphate
CNS	central nervous system
C-terminal	carboxyl-terminal
DNA	deoxyribonucleic acid
dNTP	deoxynucleoside triphosphate
<i>Drosophila</i>	<i>Drosophila melanogaster</i>
EM	electron microscopy
FA	formaldehyde
F-actin	filamentous actin
FCS	fetal calf serum
G-actin	globular actin
GFP	green fluorescent protein
GTP	guanosine triphosphate
kb	kilobase
kDa	kilodalton
MARCKS	myristilated alanine rich C-kinase substrate
MARCM	mosaic analysis with repressible cell marker
md-da	multidendritic dendritic arborisation
mKO	monomeric Kushabira Orange
NMDA	N-methyl-D-aspartic acid
N-terminal	amino-terminal
PCR	polymerase chain reaction
PKC	protein kinase C
PNS	peripheral nervous system
PSD	post synaptic density
RNA	ribonucleic acid
SD	standard deviation
UAS	upstream activating sequence

1 Summary

For the proper formation of neuronal circuits, the precise interconnection of axonal processes with dendritic branches is indispensable. To achieve this, one important aspect is the establishment of a cell type specific dendritic branching pattern, capable to fulfil the required function.

In the last years, numerous studies identified molecules and mechanisms that are required in the formation of dendritic trees. However, regarding the huge variety of dendritic morphologies, we are still far from understanding how distinct types of dendritic branches are formed. Especially, studies in the *Drosophila* Peripheral Nervous System (PNS) suggest that specific dendritic morphologies are coming along with distinct transcriptional codes. But how these transcriptional programs are implemented and which molecules underlie the establishment of distinct dendritic branches remains to be solved.

In this work, I investigated the role of the conserved actin bundling molecule fascin, called Singed in *Drosophila*, in the development of specific dendritic morphologies. Focussing on two distinct neuronal classes, the class III and class IV neurons of the *Drosophila* PNS, I found that the terminal branchlets of these two neuronal classes are made by distinct molecular mechanisms: class III neurons require *singed* for their terminal branchlets, while class IV neurons do not. Moreover, Singed defines the morphological distinction between terminal branchlets of these two classes as revealed by loss and gain of function experiments. Finally, the transcription factor Cut, a regulator of class specific dendritic branching patterns in these neurons was found to act through Singed to define the class III specific morphology.

Here, I could show for the first time that an actin-regulating molecule is implementing the morphological distinction of two different sensory neuron classes. Furthermore, my experiments suggest that that molecularly distinct regulation of cytoskeletal function is the basis for type-specific dendritic arborization.

2 Introduction

2.1 Dendrites

Neurons are highly polarized cells with specialized subcellular compartments: they develop an axon that is able to connect to very distant targets and one or more dendrites that can reach high complexity. While the axon is responsible for the transmission of information to other neurons, the dendrites are receiving and processing this information. To be able to fulfill its complex tasks, it is not surprising that the nervous system consists of an enormous number of neurons that differ in shape, size, position and connectivity.

To connect the neurons into a functional circuit, precise targeting as well as the appropriate dendritic and axonal morphology are indispensable. Targeting of dendrites to particular regions of the nervous system contributes to the selection of connecting partners and, thereby, defines the types of received information. Moreover, the dendrite arborization pattern determines the number and arrangement of the sensory or synaptic input (London and Hausser 2005). Even timing or special arrangement of input that comes on a single dendritic branch or a subdomain of the dendritic arbor can influence the way the neuron integrates and processes the information (Magee 2000; Branco, Clark et al. 2010).

The formation of a dendritic tree includes several processes that all need to be tightly regulated to achieve the desired branching pattern that allows for a functional circuit. These processes include outgrowth and retraction of filopodia, stabilization of single branches, elongation and sometimes also remodeling of already formed branchlets (Corty, Matthews et al. 2009).

Within the last years, progress has been made to identify molecules and underlying mechanisms that are required to establish a dendritic tree. But we still do not know how morphologically and probably also functionally different dendritic branches are formed.

2.2 Dendrite differentiation

2.2.1 Transcription factors

Intrinsic properties of cells are determined by the expression of a defined set of transcription factors, and also specific dendritic arborization patterns have been shown to be controlled by distinct transcriptional regulation. Due to the availability of suitable genetic tools in *Drosophila*, candidate-prompted as well as large scale screens, revealed that class specific dendritic branching patterns of larval PNS neurons are determined by distinctive transcriptional codes (reviewed in (Jan and Jan 2010)). Nevertheless, built-in regulation of dendrite morphology by specific transcription factors was also identified in other systems. Interestingly, the *Drosophila* transcription factor *cut* and also its vertebrate homologues *Cux1* and *Cux2* were reported to regulate dendritic branching in defined sets of neurons (Grueber, Jan et al. 2003; Cubelos, Sebastian-Serrano et al. 2010). Additionally, *Neurogenin2*, a bHLH transcription factor was identified to be required for proper dendrite formation of pyramidal neurons in the rodent cortex. There, it defines the unipolar dendritic morphology, which is characteristic for these pyramidal neurons (Hand, Bortone et al. 2005).

2.2.2 Guidance receptors and ligands

Besides transcription factors, receptors that sense the environment for specific cues affecting growth, are crucial to specify dendritic morphology. Indeed, dendrites of mammalian pyramidal neurons respond to a wide range of different neurotrophins (McAllister, Lo et al. 1995).

Several guidance/receptor pairs that are known to function in axonal guidance are also important for dendritic development. For example, the guidance molecule Slit and its receptor Robo have been shown to play a general role in the development and targeting of dendritic branches of the *Drosophila* CNS and PNS neurons (Furrer, Kim et al. 2003; Furrer, Vasenkova et al. 2007; Dimitrova, Reissaus et al. 2008; Brierley, Blanc et al. 2009; Mauss, Tripodi et al. 2009). Likewise, in cultured neurons from the rodent cortex, Slit and Robo signaling is important for the elongation and branching of the dendritic tree (Whitford, Marillat et al. 2002). Moreover, the ligand receptor pair Netrin

and Frazzled and its homologues Unc-6 and Unc-5 have been shown to regulate dendritic targeting in neurons of *Drosophila* and *C. elegans* (Furrer, Kim et al. 2003; Brierley, Blanc et al. 2009; Mauss, Tripodi et al. 2009; Mrkusich, Osman et al. 2010; Teichmann and Shen 2011). While in mammalian cortical pyramidal neurons the receptor Neuropilin-1 directs dendritic growth towards a source of Semaphorin-3A to apical regions, different levels of Semaphorin-1 guide *Drosophila* projection neuron dendrites to defined areas of the antennal lobe (Polleux, Morrow et al. 2000; Komiyama, Sweeney et al. 2007).

2.2.3 Establishment of dendritic branches

The elaboration of a dendritic tree is a very dynamic process where short branchlets or filopodia are constantly formed and retracted until selected ones get stabilized and become a durable part of the dendritic tree. Like in axonal development, interstitial branching, where new branches are formed on the side of existing ones, as well as growth cone splitting have been observed in dendrite development. In the dendrites of *Xenopus* optical tectal neurons, for example, small branches are rapidly added and retracted on the axis of an existing branch during the development (Wu, Zou et al. 1999). Also developing pyramidal neurons of rat hippocampal slices add and retract branches on their primary dendrite (Dailey and Smith 1996). *Drosophila* PNS class IV neurons develop their complex dendritic trees through splitting of their tips combined with interstitial branching (Sugimura, Yamamoto et al. 2003; Dimitrova, Reissaus et al. 2008).

The selection of the filopodia that are stabilized to form proper dendritic branches is thought to happen in an activity-dependent way. For instance, the long-standing synaptotrophic hypothesis is based on the idea that synaptic input controls the development of a dendritic tree. It was originally stated by Vaughn in 1989 and is supported strongly by several *in vivo* imaging studies of developing dendrites. For example, in *Xenopus* optic tectal neurons, glutamate receptor activity is required for the elaboration of a proper dendritic tree, as the blocking of NMDA receptor activity decreases dendritic dynamics (Rajan and Cline 1998; Rajan, Witte et al. 1999). Moreover, dendritic arbors in the optic tectum of zebrafish larvae develop via dynamic

filopodia that are stabilized at sites of perdurable PSD accumulation and develop into new branches (Niell, Meyer et al. 2004). Also spontaneous waves of activity associated with mammalian brain development argue for the importance of synaptic input for the development of precise neuronal circuits, including proper dendritic and axonal targeting (Katz and Shatz 1996; Feller 1999).

The architecture of the dendritic tree itself, however, is formed by the underlying cytoskeleton. Not surprisingly, regulators of actin and microtubule cytoskeleton have been linked to dendrite development. Especially the studies on the small GTPases Rac1, Cdc42 and RhoA pointed out the importance of the actin cytoskeleton in this process (Luo 2000; Lee, Li et al. 2003; Scott, Reuter et al. 2003; Andersen, Li et al. 2005).

2.3 Md-da neurons of the *Drosophila* PNS

2.3.1 Morphological characterization

One of the best studied model systems in dendrite differentiation is a defined subset of neurons of the *Drosophila* PNS, the multidendritic dendritic-arborization (md-da) neurons. Md-da neurons are located in between the epidermis and the muscular body wall and grow and branch in two dimensions (Fig. 2.1 A). They start to develop their dendritic tree in the embryo and reach their maximal dendritic complexity in the transparent third instar larvae, with the experimental advantage of imaging the whole animal without dissection. Unlike the mammalian peripheral sensory endings, that are predominantly axon-like, the *Drosophila* peripheral sensory endings are dendritic-like compartments (Bodmer, Barbel et al. 1987). They do not receive synaptic input, but they transduce signals from the external environment, like mechanical input or heat. A fundamental marker for mammalian dendrites is the mixed population of microtubules: plus- and minus-ends of microtubules are directed towards the periphery of dendrites. In axons instead, most microtubules are directed with the plus-ends towards the growth cone (Baas, Deitch et al. 1988). The sensory endings of the md-da *Drosophila* PNS neurons as well as *Drosophila* mushroom body neuron dendrites, which actually receive axonal input in the brain, also show mixed microtubule polarity. In the md-da neurons, even most of the dendritic microtubules are directed with their minus-ends distally (Lee, Winter et al. 2000; Andersen, Li et al. 2005; Mattie, Stackpole et al. 2010).

There are 15 md-da neurons per larval hemisegment, which were divided into four different classes according to the complexity of their dendritic tree (Grueber, Jan et al. 2002)(Fig. 1C). Class I neurons have the least complex dendrites and usually show one long primary dendrite which is directed dorsally, and several secondary branches with anterioposterior orientation. Class I neurons are important for a sensory feedback loop, that reports successful contraction of the larval muscles, which is essential for coordinated crawling (Hughes and Thomas 2007; Cheng, Song et al. 2010). Class II neurons have relative long, symmetrically bifurcated dendrites that extent to distant targets and only show few higher order branches. Class III neurons show a similar basic

branching pattern as class II neurons, but are decorated with numerous spiked protrusions, short terminal branchlets, along their main branches. So far, a clear functional role for class II or class III neurons was not found. The most complex dendritic trees are established by the class IV neurons, which are space filling and cover the larval body wall completely. Class IV neurons are important for sensation of pain, heat and light (Hwang, Zhong et al. 2007; Xiang, Yuan et al. 2010)(Fig. 2.1 B, C). The four different classes of md-da neurons have extensively overlapping dendritic trees. However, it was shown for class III and class IV neurons that neurons of the same class avoid dendritic territories of the neighboring neuron, a phenomenon called tiling. Additionally, these neurons show a high self-avoidance, meaning that there are only rare cases where dendritic braches of the same cell cross each other (Grueber, Jan et al. 2002).

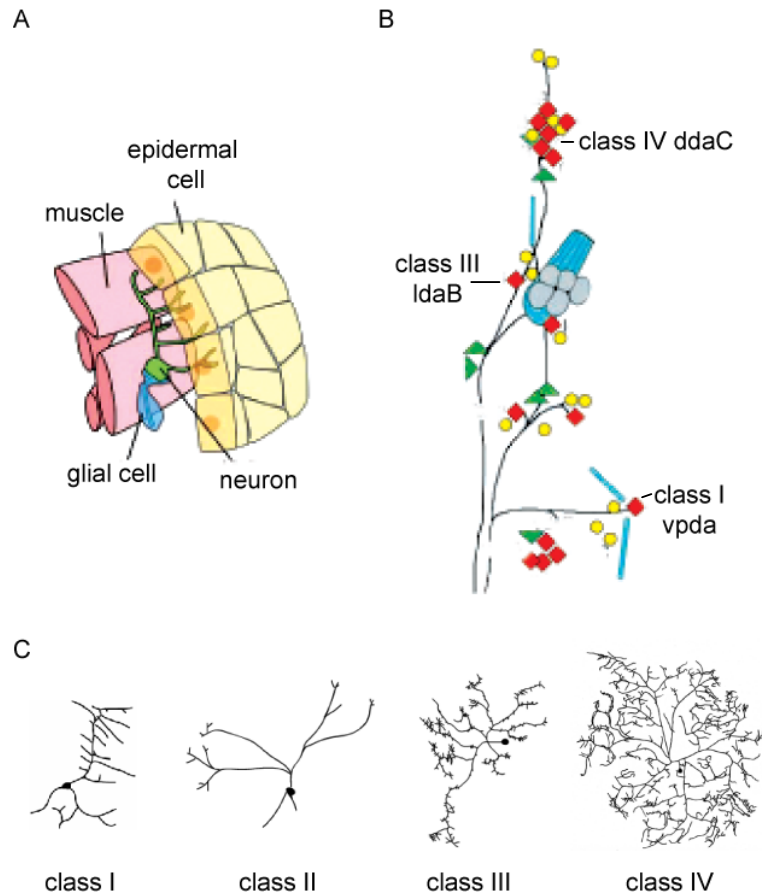


Figure 2.1: The *Drosophila* peripheral nervous system

(A) The neurons of the *Drosophila* PNS are squeezed in between the epidermis and the muscular body wall. Picture adapted from Yamamoto (Yamamoto, Ueda et al. 2006). (B) Diagram of the *Drosophila* abdominal PNS, one larval hemisegment is represented. Md-da neurons: red diamonds. External sensory neurons: yellow circles. Other multidendritic neurons: green triangles. Chordotonal organs: blue rectangles. Important neurons for this work are indicated. Taken from Grueber (Grueber, Jan et al. 2002). (C) Representative dendritic branching patterns of the four classes of md-da neurons.

2.3.2 Transcriptional code affecting md-da dendrite morphology

Interestingly, the specific and distinct dendritic morphology of the different classes of md-da neurons is controlled by distinct transcriptional codes.

For example, the transcription factor *Abrupt* is only expressed in class I neurons and is responsible for their simple dendritic branching pattern. Ectopic expression of *Abrupt* in the complex classes III and IV leads to a simplification of their dendritic trees (Sugimura, Satoh et al. 2004).

Spineless, instead, is a transcription factor that is expressed in all md-da neurons, though with different effects on the distinct classes. In the simpler class I and class II neurons, mutants of *spineless* give rise to more complex dendritic trees. The complex class III and class IV neurons show a reduced dendritic branching pattern in *spineless* mutants. On top, overexpression of *Spineless* in class IV neurons also results in a decreased dendritic branching pattern. Possibly, *Spineless* is activated by different upstream factors in different cell types, which could result in the class specific morphologies dependent on this transcription factor (Kim, Jan et al. 2006).

Similar to *Spineless*, the transcription factor *Cut* is also expressed in several classes of neurons. While in class I neurons *Cut* is absent, class II, class III and class IV neurons show different *Cut* expression levels. Highest levels of *Cut* can be detected in class III neurons. Accordingly, loss of *cut* leads to the complete loss of the typical class III spiked protrusions and to defects in the outgrowth of the main dendritic branches. Medium expression levels of *Cut* are detected in class IV neurons where mutations of *cut* also lead to a decreased complexity and total dendrite length. Class II neurons only show a weak *Cut* expression, however, their morphology is strongly affected by the loss of *cut*. Class II neurons, which are mutant for *cut*, seem to fail almost completely to extend their dendrites; nonetheless they are still capable to branch. Ectopic overexpression of *Cut* induces the formation of numerous small terminal branchlets in class I, II and class IV neurons that resemble the typical class III spiked protrusions. Taken together, *cut* promotes md-da neuron dendritic complexity and the formation of small terminal branchlets (Grueber, Jan et al. 2003).

Class III and class IV neurons both express *cut* but still have very different dendritic morphologies. For the morphological distinction between class III and class IV neurons an additional transcription factor, called *knot/collier*, is required. It is only expressed in

class IV neurons and is responsible for the complex branching pattern of this class possibly by regulating microtubule dynamics (Hattori, Sugimura et al. 2007; Jinushi-Nakao, Arvind et al. 2007; Crozatier and Vincent 2008).

These examples show that dendritic complexity is likely the consequence of the combined actions of a large number of regulatory genes. Indeed, a RNA interference based screen identified 76 transcription factors that influence the dendritic morphology of class I neurons (Parrish, Kim et al. 2006).

2.4 Actin cytoskeleton

Although the specific branching pattern of dendrites is controlled by a number of intrinsic and extrinsic factors, the final dendritic morphology is regulated by dynamic changes in the cytoskeleton. There are three main cytoskeletal components: actin filaments, microtubules and intermediate filaments, but in *Drosophila* only actin and microtubules can be found. Long actin filaments are located beneath the plasma membrane where they build the cell cortex, and are responsible for the shape and motility of the cell. A variety of cellular protrusions is formed by actin filaments: filopodia, lamellipodia, microvilli and hair cell stereocilia (Shibayama, Carboni et al. 1987; Tilney, Tilney et al. 1992; Small, Rohlf et al. 1993). Filopodia and lamellipodia are highly motile structures that extend and retract from the cell surface (Small, Stradal et al. 2002). To carry out these dynamic changes, filamentous actin displays intrinsic dynamics that is enhanced and controlled by regulators of the actin cytoskeleton.

2.4.1 Basic dynamic properties of actin

Actin is a 43 kDa monomeric globular protein, though under physiological conditions actin monomers assemble into long and stable filaments. However, the initial step of polymerization is slow because small oligomers are very unstable (Sept and McCammon 2001). Filamentous actin consists a helical polymer of globular subunits, all arranged in a head to tail fashion resulting in a polarized filament. Based on the arrowhead pattern created by decoration with myosin, an F-actin binding motor protein, one end is called barbed end and the other one pointed end (Small, Isenberg et al. 1978).

Actin monomers assemble at both ends of the filaments but with different kinetics. At the barbed end, which is also called plus end, actin monomers are incorporated faster into the filament than at the pointed end, also called minus end (Pollard 1986). The free actin monomers in the cell are bound to ATP or ADP. As soon as an ATP bound actin monomer is incorporated into the filament at the barbed end, ATP is hydrolyzed (Blanchoin and Pollard 2002). The γ -phosphate dissociates later as the integrated molecule travels away from the barbed end and ADP-actin finally dissociates from the filament at the pointed end (Pollard 1986; Carlier and Pantaloni 1988; Fujiwara,

Takahashi et al. 2002). The result is a slow treadmilling of subunits from the barbed end where the subunits are added to the pointed end at which the subunits are lost.

2.4.2 Actin regulating proteins in dendrite development

Actin dynamics is regulated by a big group of actin-regulating proteins, that are capable of maintaining a pool of actin monomers, initiating polymerization, regulating the assembly and turnover of actin filaments, and cross-linking filaments into networks or bundles (Pollard and Cooper 2009). These actin-regulating proteins can in turn be regulated by small GTPases that respond to a variety of extracellular stimuli. Especially the role of Cdc42, Rac1 and RhoA, small GTPases of the Rho family, in dendrite development has been extensively studied in the past years.

Investigating Rac1, most studies support a general positive regulatory role in the formation a dendritic tree. For example, triple mutants for all three *Drosophila* Rac1 related genes, *rac1*, *rac2* and *mtl*, in mushroom body neurons, show reduced dendritic length and branching (Ng, Nardine et al. 2002). Similarly, *rac1* mutant md-da neurons of the *Drosophila* larvae exhibit reduced dendritic branching, whereas overexpression of Rac1 promoted branching. However, *rac1* did not affect early stages of dendrite development in the embryo what could be due to functional redundancy with the other Rac1 related genes (Lee, Li et al. 2003; Andersen, Li et al. 2005). Other studies mainly implemented constitutively active or dominant negative forms of Rac1. In *Xenopus* optic tectal neurons overexpression of a constitutively active form of Rac1 leads to increased branch additions and retractions and a dominant negative form only to increased retractions (Li, Van Aelst et al. 2000). In cultured rat cortical neurons the effect is even more drastic, the constitutively active form Rac1 leads to increased primary and basal dendrites and the dominant negative form to a reduction in the number of primary dendrites (Threadgill, Bobb et al. 1997). However, there is also experimental data that interferes with the idea of Rac1 being a general positive regulator of dendrite branching and outgrowth. For instance, overexpression of constitutively active Rac1 in the *Drosophila* md-da neurons results in a reduced number of secondary branches and a primary branch that fails to extend properly, what could be

also due to non-specific effects generated by strong overexpression of the construct (Gao, Brenman et al. 1999).

Cdc42 can act either positive or negative on dendrite development, depending on the observed cell type. Analysis of constitutively active Cdc42 suggests a positive role of dendrite development in chick primary spinal neurons and *Xenopus* optic tectal neurons (Kuhn, Meberg et al. 2000; Li, Van Aelst et al. 2000). Vice-versa dominant negative Cdc42 is reducing the number and length of *Xenopus* retinal ganglion dendrites and also argues for a positive role of Cdc42 in this process (Ruchhoeft, Ohnuma et al. 1999). Other studies suggest a negative regulation of Cdc42 on dendrite formation. For example expression of constitutively active Cdc42 leads to reduced dendritic branching and outgrowth in *Drosophila* md-da neurons and *Xenopus* retinal ganglion cells (Luo, Liao et al. 1994; Gao, Brenman et al. 1999; Ruchhoeft, Ohnuma et al. 1999). Strikingly, *cdc42* mutant vertical sensory neurons of the *Drosophila* visual system show increased dendritic length while maintaining a normal dendritic complexity (Scott, Reuter et al. 2003). The contrasting effects of Cdc42 on dendrite development could be possibly explained by different ways of activation existing in different types of cells (Govek, Newey et al. 2005). However, in most cases the analysis of Cdc42 mutant cells is missing which could rule out possible side-effects of the dominant-negative or constitutively active forms.

RhoA seems to be a general suppressor of dendrite growth. Mutants and dominant-negative forms of RhoA result in increased dendritic branch length in *Drosophila* mushroom body neurons, *Xenopus* optic tectal neurons and hippocampal neurons in culture (Lee, Winter et al. 2000; Li, Van Aelst et al. 2000; Ahnert-Hilger, Holtje et al. 2004). Consistently, constitutively active RhoA or activation of endogenous RhoA results decreased branch extension and complexity in these cell types (Lee, Winter et al. 2000; Li, Van Aelst et al. 2000; Pilpel and Segal 2004). Endogenous Rho signalling should therefore be low to allow dendrite growth and activated Rho signalling could locally limit dendrite growth when needed (Govek, Newey et al. 2005).

The direct role of diverse actin-regulating molecules on dendrite development was investigated in the *Drosophila* md-da neurons. For example, *ena* encodes a protein that belongs to a conserved family of actin regulatory proteins that associate with the barbed ends of actin filaments and antagonize filament capping by capping protein (CapZ) and

thereby allow prolonged elongation (Krause, Dent et al. 2003). In all classes of md-da neurons, mutations of *ena* result in a reduction of dendritic branching, suggesting that the prolonged elongation of actin filaments is required for the formation of dendritic branches (Li, Li et al. 2005).

Tropomyosin, an F-actin stabilizing protein, binds as a dimer along the length of actin filaments (Pruyne, Schott et al. 1998). A mutation of *tropomyosin II*, a gene encoding multiple Tropomyosin isoforms, fails to restrict the dendritic field size of class I and class IV neurons and is therefore important to preserve the overall extension of the dendritic branches. In the absence of Tropomyosin, F-actin might be less stabilized, what could allow for increased dendrite growth (Li and Gao 2003).

Cofilin can disassemble actin by severing and depolymerizing actin-filaments. However without the recycling of the Cyclase-Associated Protein (CAP), cofilin remains bound to G-actin (Moriyama and Yahara 2002; Balcer, Goodman et al. 2003). Mutations in the Drosophila CAP orthologue *capulet* lead to abnormal actin aggregates in md-da dendrites, interfering with microtubule based mitochondria transport (Medina, Worthen et al. 2008). These experiments show that also minor changes in the regulation of the actin-cytoskeleton that do not directly lead to changes in the dendritic branching pattern could affect other important cellular functions, like in this study, energy supply. Importantly, even though the morphologies of the distinct classes of md-da neurons are quite different and are regulated by defined transcriptional codes, the actin-regulating molecules investigated so far seem to have similar effects on the different classes and thus a general function on dendrite branching.

2.4.3 Formation of filopodia

Filopodia are short and thin actin-based cellular protrusions, which are especially important for cells to probe their environment and allow for directed cell migration. Neuronal growth cones exhibit numerous filopodia, which are essential for sensing gradients of guidance cues to turn the neurites in a preferred direction of growth (Gundersen and Barrett 1980; Bentley and Toroian-Raymond 1986; Zheng, Wan et al. 1996). Besides playing an important role for growth cone turning, the formation of filopodia is thought to be in general the initial step of dendritic branching (Heiman and Shaham 2010).

Characteristic for filopodial protrusions are long, parallel and tightly bundled actin filaments where the fast growing barbed ends are directed towards the membrane pushing it outwards during filament growth (Lewis and Bridgman 1992; Pollard and Borisy 2003).

Different mechanisms underlying the generation of filopodial protrusions are discussed in the field (Gupton and Gertler 2007; Mattila and Lappalainen 2008; Faix, Breitsprecher et al. 2009). On the one hand, EM studies of melanoma cells led to the “convergent elongation model”. In this model filopodial actin bundles are thought to emerge from the branched cortical actin network, facilitated by the Arp2/3 complex that allows nucleation on the side of existing filaments (Svitkina, Bulanova et al. 2003). Knockdown of Arp2/3 complex in primary neurons and neuroblastoma cells inhibited initiation and dynamics of filopodia supporting earlier EM studies (Korobova and Svitkina 2008).

According to the “convergent elongation model” some of the barbed ends in the cortical actin network are bound by capping proteins to terminate elongation, while others are bound by a tip complex that allows continuous elongation and linking of the filaments (Schafer, Jennings et al. 1996; Bear, Svitkina et al. 2002). Actin bundling molecules, especially Fascin, are thought to provide stiffness to the bundle for pushing the membrane outwards (Vignjevic, Kojima et al. 2006).

On the other hand, another model, the “filament nucleation model” proposes filopodia formation independent of Arp2/3 and the branched actin network. Instead, actin filaments are thought to be nucleated *de novo* by formins. Supporting experimental data come from *Dictyostelium discoideum* and mammalian cells, where filopodia can form in the absence of Arp2/3 complex (Steffen, Faix et al. 2006). Moreover, in *Dictyostelium* the formin Dia2 is essential for filopodia formation (Schirenbeck, Bretschneider et al. 2005). Cryo-electron tomography of *Dictyostelium* filopodia also revealed a different actin organization than the EM studies of melanoma cells. In *Dictyostelium* the shaft of the filopodium consists of discontinuous actin filaments that are shorter than the protrusion itself. Nevertheless, they are arranged in parallel bundles, possibly cross-linked by Fascin. (Medalia, Beck et al. 2007).

Despite this controversy about the initiation of filopodia, certain core activities seem to be required for the formation of a filopodium (Faix, Breitsprecher et al. 2009).

Especially important are actin bundling proteins that are necessary to generate a force that can protrude the membrane (Mogilner and Rubinstein 2005). In melanoma cells, Fascin has been identified as the major actin-cross linker in filopodia. Even though other actin cross-linking proteins as Fimbrin and Espin are also localized to filopodia, Fascin knock down was shown to affect strongly filopodia formation (Vignjevic, Kojima et al. 2006). Likewise, in various other cell types, Fascin localizes to filopodia including neurons, HeLa and epithelial cells (Yamashiro-Matsumura and Matsumura 1986; Sasaki, Hayashi et al. 1996; Cohan, Welnhofner et al. 2001). Moreover, Fascin is one of three components, including Fascin, Arp2/3 complex and the activator of the Arp2/3 complex WASP, that could together initiate filopodia-like bundles *in vitro* (Vignjevic, Yarar et al. 2003).

2.5 Fascin

Fascin forms tight and stable bundles with F-actin and was therefore named after the Latin *fasciculus*, which means bundle (Otto, Kane et al. 1979). It was identified in extracts of the cytoplasm of sea urchin eggs while Kane tried to polymerize microtubules but instead got highly organized needle-like structures consisting of fascin and actin (Hartwig and Stossel 1975; Kane 1975; Mabuchi and Kane 1987).

2.5.1 Fascin structure

Fascin is a monomeric 55 kDa protein and belongs to the group of β -trefoil molecules which consists of a number of functional unrelated proteins (Yamashiro-Matsumura and Matsumura 1985). Characteristic for these proteins is the β -trefoil fold, a structure consisting of six two stranded β -hairpins, where three of them form a barrel and the remaining three build a cap on the barrel (Graves, Hatada et al. 1990; Eriksson, Cousens et al. 1991; Ponting and Russell 2000). The crystal structure of human fascin-1 was solved in 1999 and showed the presence of 4 β -trefoil folds, which pack to form a distorted tetrahedron organized in two lobes with a skew angle of approximately 56° (Sedeh, Fedorov et al. 2010).

For the actin-crosslinking function as a monomer, fascin needs two actin-binding sites. However, so far no structure of the fascin-F-actin complex is available which allows mapping the precise actin-binding sites. Nevertheless, one binding site was located by limited proteolysis experiments to the C-terminal part of the protein, between the residues 277 and 493 (Ono, Yamakita et al. 1997). These findings were supported by *in vivo* data from *Drosophila*, where mutations from Ser 289 to Asn or Gly 409 to Glu disrupted actin binding activity (Cant and Cooley 1996). Another putative actin binding site was mapped to the first β -trefoil where a highly conserved region shows similarity to the actin-binding site of myristylated alanine rich C-kinase substrate (MARCKS). (Yamakita, Ono et al. 1996; Ono, Yamakita et al. 1997)(Fig.2.2).

2.5.2 Actin bundling through Fascin

In vitro, fascin bundles actin in a hexagonal manner, so that each actin filament is linked to six neighbor filaments (DeRosier and Edds 1980). The hexagonal packing of these filaments produces a 11 nm periodic transverse banding pattern on the bundles (Bryan and Kane 1978; Edwards, Herrera-Sosa et al. 1995). Transmission electron microscope images show that in actin bundles cross-linked by fascin, unipolar F-actin filaments are very tightly packed together with a 8 nm spacing between the filaments (Bryan and Kane 1978; Maekawa, Endo et al. 1982; Cant, Knowles et al. 1994).

Saturation experiments revealed a protein ratio of 1 fascin molecule per 4.76 actin monomers, showing that fascin is incorporated in very high concentrations into the bundles (Bryan and Kane 1978). Corresponding results were achieved with human fascin-1, recombinant *Drosophila* fascin and recombinant mouse fascin (Yamashiro-Matsumura and Matsumura 1985; Cant, Knowles et al. 1994; Edwards, Herrera-Sosa et al. 1995). Interestingly, fascin as well as other F-actin crosslinking proteins modify the helical symmetry of actin filaments. The native form of a left-handed helix rotating through six turns per 13-monomer repeat is unfavorable for hexagonal symmetry achieved by fascin bundling. Indeed, fascin bundled actin filaments were shown to be overtwisted by roughly -0.01 monomers/turn (Purdy, Bartles et al. 2007; Shin, Purdy Drew et al. 2009).

2.5.3 Fascin regulation through phosphorylation

The actin-binding activity of fascin has been shown to be regulated by phosphorylation. In human fascin-1 a serine at position 39, which is located within the MARCKS homology motif, is the major site for phosphorylation by protein kinase C α (PKC α) (Fig. 2.2). This site is well conserved among fascins of different species, including human, mouse, *Xenopus* and *Drosophila*. The only exception is sea urchin fascin, which has a threonine instead of a serine at this position. Additionally, the sequence surrounding the phosphorylation site is the most conserved domain among these fascins (Ono, Yamakita et al. 1997; Sedeh, Fedorov et al. 2010).

Phosphorylation of Ser-39 reduces the actin-binding activity of human fascin *in vitro* (Yamakita, Ono et al. 1996). Additionally, a phosphomimetic S39D fascin mutant leads

to reduced formation of fascin-containing protrusions on matrix adherent cells (Adams, Clelland et al. 1999). Similar results were obtained in B16F1 melanoma cells where expression of the phosphomimetic mutant decreased the number of filopodia and resulted in loosely bundled actin filaments in the remaining filopodia. The non-phosphorylatable S39A mutant instead induced long, overabundant filopodia. (Vignjevic, Kojima et al. 2006). Additionally, it was shown that in N2a cells, phosphorylated fascin is mainly freely diffusing in the cytoplasm, whereas actin bundling in filopodia is performed by dephosphorylated fascin (Aratyn, Schaus et al. 2007).

Nonetheless, the regulation of fascin activity by phosphorylation seems to be more complex in vivo. In *Drosophila* the migration of blood cells is dependent on fascin, but not regulated by Serine phosphorylation. This phosphorylation however, is important for the development of *Drosophila* bristles (Zanet, Stramer et al. 2009).

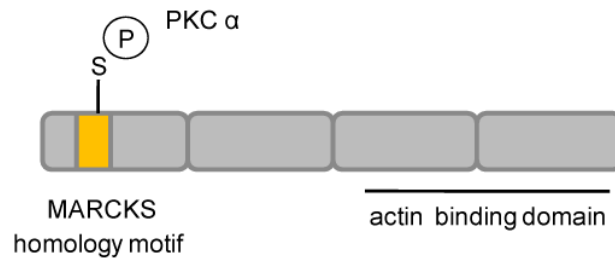


Figure 2.2: Schematic drawing of Fascin structure

Each grey box represents one β-trefoil fold.

2.5.4 Fascin regulation by small GTPases

The small GTPases, general regulators of the cytoskeleton, were also shown to be important for the regulation of fascin.

Myoblasts adhesive to the matrix glycoprotein thrombospondin-1 form fascin-containing microspikes that are dependent on Rac1 and Cdc42. Likewise expression of constitutively active forms of Rac1 and Cdc42 promotes the localization of fascin to lamellipodia and filopodia in this cell type (Adams and Schwartz 2000). Interestingly, the interaction of fascin and PKC was shown to be dependent on Rac1 but not on Cdc42 in colon carcinoma cells, suggesting an additional regulatory activity of Rac1 on fascin that influences its colocalization with PKC (Parsons and Adams 2008).

Another small GTPase, Rab35 was shown to affect the localization of fascin. Rab35 mediates intracellular vesicle trafficking and is able to recruit fascin to distinct subcellular compartments (Zhang, Fonovic et al. 2009).

2.5.5 Biological role of Fascin

Fascin is a key element in cell motility and cancer invasion. It organizes actin-based cellular structures like dynamic cortical cell protrusions and cytoplasmic microfilament bundles.

In humans there are three different fascin genes: fascin-1, retinal fascin (fascin-2) and testis fascin (fascin-3). Moreover, for mouse and bovine, tissue specific fascin genes were found as well, such as bovine retinal fascin (bovine fascin-2) and mouse testis fascin (mouse fascin-3) (Tubb, Bardien-Kruger et al. 2000; Kureishy, Sapountzi et al. 2002; Tubb, Mulholland et al. 2002). However, most studies on fascin take only fascin-1 into account. The only exception is human fascin-2, it was found to be linked with autosomal dominant retinitis pigmentosa (Wada, Abe et al. 2001).

In general, increased expression of fascin induces membrane protrusions and increases cell migratory activity (Yamashiro, Yamakita et al. 1998). Fascin is known to be upregulated in a number of highly motile cell phenotypes, such as invasive cancer cells and *Drosophila* migrating hemocytes and plasmatocytes (Adams 2004; Vignjevic and Montagnac 2008; Zanet, Stramer et al. 2009). Moreover, knockdown of fascin in human colon carcinoma cells results in reduced cell migration (Hashimoto, Parsons et

al. 2007). Additionally, cell types that form complex cellular protrusions express fascin at high levels, like antigen presenting dendritic cells and neurons (Mosialos, Hanissian et al. 1994; Edwards, Herrera-Sosa et al. 1995).

In the developing mouse embryo as well as in adult human tissues, fascin is highly expressed in neuronal cells (De Arcangelis, Georges-Labouesse et al. 2004; Zhang, Tao et al. 2008). Interestingly, fascin-1 deficient mice are viable and fertile and they do not show gross developmental abnormalities. However, fascin-1 is favorable for neonatal survival and dorsal root ganglion neurons derived from fascin-1 knockout mice have smaller growth cones and shorter filopodia when cultured (Yamakita, Matsumura et al. 2009). In several studies, fascin has been shown to be important for neuronal growth cone morphogenesis and reorganization (Cohan, Welnhof et al. 2001; Brown and Bridgman 2009). Recently, it was also shown that downregulation of fascin in the mouse olfactory bulb is linked to memory formation (Li, Mauric et al. 2010).

2.5.6 Singed, the *Drosophila* fascin homologue

In *Drosophila*, there is only one gene for fascin called *singed*, a name describing the obvious bristle phenotype of several severe *singed* mutants (Bryan, Edwards et al. 1993). The bristles and hairs on the head, thorax, legs and wings are gnarled, bent or kinked in varying degrees in *singed* mutant animals (Fig. 2.3). Additionally, *singed* affects the female germ line leading to sterility (Bender 1960). The defects in bristle formation and oogenesis result both from reduced actin bundling through the absence of the Singed protein. Nurse cells, deficient of *singed* lack cytoplasmic actin bundles during oogenesis, nurse cell nuclei are not kept in their position and finally block the cytoplasm flow into the oocyte (Cant, Knowles et al. 1994).

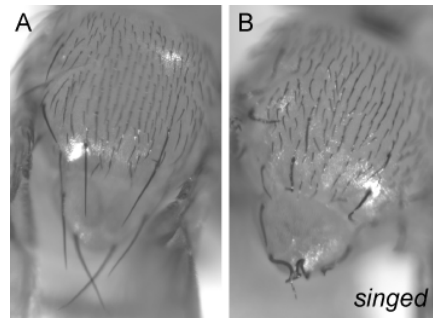


Figure 2.3: Singed bristle phenotype

(A) Thorax of wild type fly, bearing long and straight bristles. (B) Thorax of a *singed* mutant fly. The bristles are severely gnarled and bended.

Moreover, *singed* affects neurite shape and trajectory in cultured neurons of the mushroom body which has been shown to be important for olfaction and learning. Mutant neurons fail to grow out long and straight processes; instead the neurites are curled and bended. This is accompanied by altered F-actin localization. F-actin, which is usually localized to distinct branchlets, is abnormally broad and uniform in *singed* mutants (Kraft, Escobar et al. 2006).

On top, the migration ability of plasmatocytes is strongly inhibited in *singed* mutants; showing that also *in vivo* cell motility is affected by *singed*. In wildtype cells, Singed localizes to and is essential for the assembly of dynamic actin-rich microspikes within the plasmatocyte lamellae (Zanet, Stramer et al. 2009).

2.5.7 Fascin and its potential role in dendrite differentiation

As discussed above, the actin-bundling molecule fascin is highly expressed in neuronal tissue of several species, including mouse, human and *Drosophila* (De Arcangelis, Georges-Labouesse et al. 2004; Zhang, Tao et al. 2008; Zanet, Stramer et al. 2009). Moreover, fascin was found to be a structural component of axonal growth cones. Cultured dorsal root ganglion neurons of fascin-1 deficient mice are smaller and form less filopodia than usual (Yamakita, Matsumura et al. 2009). Also in *Drosophila*, MB neurons in culture show altered neurite outgrowth when lacking *singed*, the *Drosophila* Fascin homologue. Interestingly, neurites of axonal and dendritic character are both

affected, suggesting that *singed* might be also important for dendritic development (Kraft, Escobar et al. 2006). Also the conserved role of fascin in the formation of filopodia is suggesting a potential function in dendrite development, because filopodia are thought to be the first step of dendritic branching (Heiman and Shaham 2010). However, data to explain the role of fascin for the elaboration of dendritic branching patterns *in vivo* are missing. Fascin-1 mutant mice showed normal brain morphology as revealed by Nissl staining of serial coronal brain sections (Yamakita, Matsumura et al. 2009). Therefore, more detailed morphological analysis is required to shed light into the potential function of fascin for dendrite development.

3 Results

The initial and general step in the outgrowth of a dendritic branch is thought to be the generation of a filopodium (Heiman and Shaham 2010). The formation of filopodia in turn is dependent tightly bundled actin filaments, often through fascin, to allow protrusion of the membrane (Vignjevic, Kojima et al. 2006). Indeed, fascin expression is high in neuronal tissue of several species, however so far *in vivo* data that could link fascin with the formation of dendritic branches is missing. Studies on fascin in dendritic branch formation could give important insight into how dendritic branches are formed molecularly and if the variety of dendritic morphologies is really achieved by the same cytoskeletal regulation.

To address the role of the *Drosophila* fascin homologue, Singed, in dendrite development, I have investigated specific classes of md-da sensory neurons of the *Drosophila* larvae. The most important findings in my thesis are that different classes of md-da neurons are formed on the basis of molecularly separable mechanisms and that Singed, as an effector of the transcription factor Cut, defines the morphological distinction between two classes of neurons.

3.1 Singed expression in the *Drosophila* PNS

3.1.1 Endogenous Singed in the md-da neurons

To investigate if Singed might play a role in the formation of the dendritic branches in the *Drosophila* PNS neurons, I first looked at the expression pattern of *singed* in the *Drosophila* md-da neurons with monoclonal anti-Singed antibodies in wild type animals (Cant, Knowles et al. 1994). In third instar larval filets all cell bodies of the md-da neurons showed a clear Singed labeling with no detectable differences in the level of expression (Fig. 3.1 A-C). Additionally, epidermal cells were strongly labeled. As a mutant line I used the *sn*^{36a} mutation, resulting from a 5.5 kb P element insertion in the 5' untranslated region, which was reported to be a null mutation (Paterson and O'Hare 1991; Cant, Knowles et al. 1994)

In the *sn*^{36a} mutant larvae the staining of the md-da cell bodies and the epidermal cells was strongly reduced, however some residual protein was still detected (Fig. 3.1 D-F). Like many cytoskeletal elements in *Drosophila*, *singed* is maternally contributed. This could lead to residual protein levels even in the full mutant background. This observation was confirmed by Anastasia Tatarnikova (PhD student in the lab of Gaia Tavosanis, MPI of Neurobiology) by western blot analysis of single *sn*^{36a} mutant larvae, showing a reduced but still detectable amount of Singed protein.

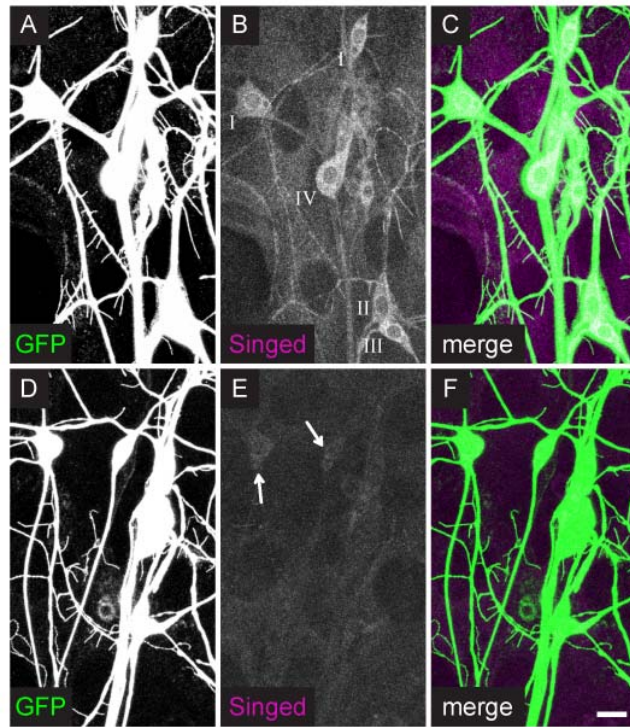


Figure 3.1: Singed is expressed in all md-da neurons

(A-F) Md-da neurons of the dorsal cluster highlighted with the diver reporter line 80G2. Immunolabeling of control third instar larval filets with anti-Singed and anti-GFP antibodies. Singed is detected in all four classes of md-da neurons. Roman numerals label the corresponding classes of neurons in (B). (D-F) Immunolabeling of *sn^{36a}* third instar larval filets with anti-Singed and anti-GFP antibodies. Residual Singed was faintly detected in some cell bodies (see arrows in E). Scale bar: 10 μ m.

Interestingly, in contrast to the broad expression pattern in the cell bodies, I found a much more specific labeling at the dendritic branches. The dendrites of class III md-da neurons carry numerous filopodia-like terminal branchlets, called spiked protrusions. Singed was clearly enriched in these class III spiked protrusions in comparison to the main dendritic branches (Fig. 3.2 A-C). The major fraction of spiked protrusions showed a clear labeling for Singed and only very few of them did not display Singed enrichment. In *sn^{36a}* mutant larvae the labeling of the spiked protrusions was completely gone (Fig. 3.2 D-F). Despite a clear expression of Singed in the cell bodies, in the most complex class of md-da neurons, the class IV neurons, I could never detect any enrichment of Singed at the dendrites, including main branches or small terminal

branchlets (Fig 3.2 G-I). The very simple class I neurons showed very faint Singed labeling at the main branches but the small terminal branchlets were not enriched in Singed. Additionally, I could detect some Singed labeling at the branching points, though the specificity of this localization was not further investigated (Fig. 3.2 J-L). Hence, due to the expression of Singed in the md-da neurons and moreover the specific localization of Singed to the terminal branchlets of class III neurons, *singed* could be a potential candidate for the regulation of dendritic branching.

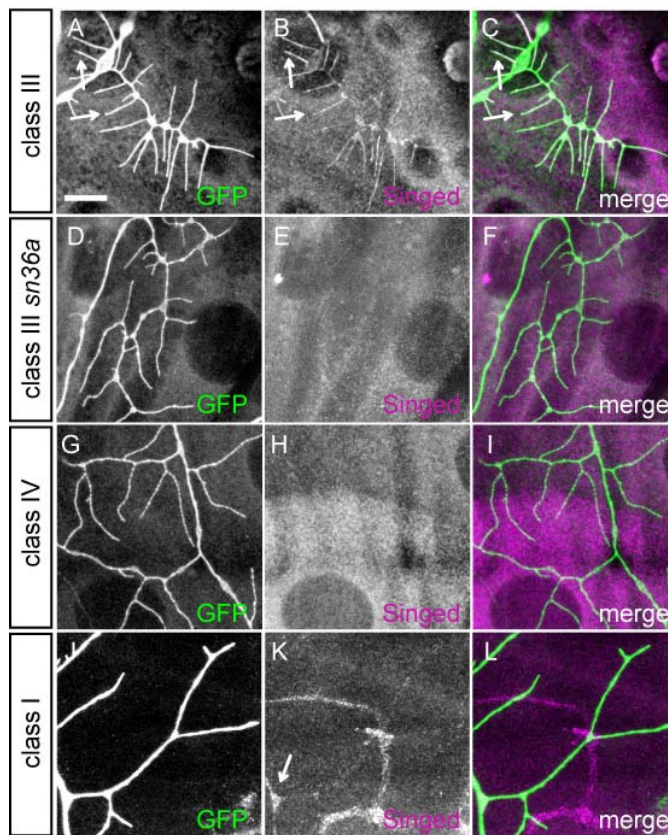


Figure 3.2: Singed localizes to the terminal branchlets of class III neurons

(A-F) Localization of endogenous Singed in class III neurons. (A-C) Wild type and (D-F) *sn^{36a}* mutant class III ldaB neurons of third instar larvae expressing membrane tagged *mCD8GFP* under the control of *c161Gal4*. Singed is localized to the spiky protrusions of the wild type class III neuron; in the *sn^{36a}* mutant this localization is lost and Singed is barely or no longer detected. (G-I) Localization of endogenous Singed in class IV ddaC neuron, expressing *UASmCD8GFP* under the control of *477Gal4*. In class IV neurons endogenous Singed can be detected within the cell body (see also Fig 3.1.), but not at the terminal branches. (J-L) Localization of endogenous Singed in class I vpda neurons, expressing *UASmCD8GFP* under the control of *2-21Gal4*, Singed can be detected at some branching points (arrow in K), but not at the terminal branchlets. Scale bar: 10 μ m

3.1.2 Localization of fluorescently tagged Singed in terminal branchlets of md-da neurons

The detection of endogenous Singed in the md-da neurons might be partially obscured by Singed expression in the epidermis or the underlying muscle. To exclude false negative results, I generated a fluorescently-tagged monomeric Kusabira-Orange *singed* construct (*mKO::sn*) which was cloned into the *pUAS* vector and inserted into the fly genome. With this expression vector system it was possible to drive the expression of the *mKO::sn* construct with different *Gal4* driver lines in the tissue of interest (Brand and Perrimon 1993). First, to test if this fusion protein was functional, I tried to rescue the extreme *sn*³ bristle phenotype by expressing the *mKO::sn* fusion protein in the broad expression pattern of the *actin-Gal4* driver. *sn*³ mutant flies have severely gnarled bristles; a phenotype due to reduced bundling of actin filaments during bristle development resulting from reduced Singed levels (Cant, Knowles et al. 1994) (Fig. 3.3 A). Neither the *UAS-mKO::sn* construct nor the *actin-Gal4* insertion on their own could rescue the bristle phenotype (Fig. 3.3 B, C). However, the combination of both resulted in the development of bristles with almost wild type appearance (Fig. 3.3 D-F). This experiment shows that the insertion of the *UAS* or the *Gal4* construct into the fly genome does not affect the *singed* mutant bristle phenotype, but the expression of mKO-tagged Singed in the *actin-Gal4* expression pattern can rescue the altered bristle morphology. Therefore, I considered the mKO::sn fusion protein as functional.

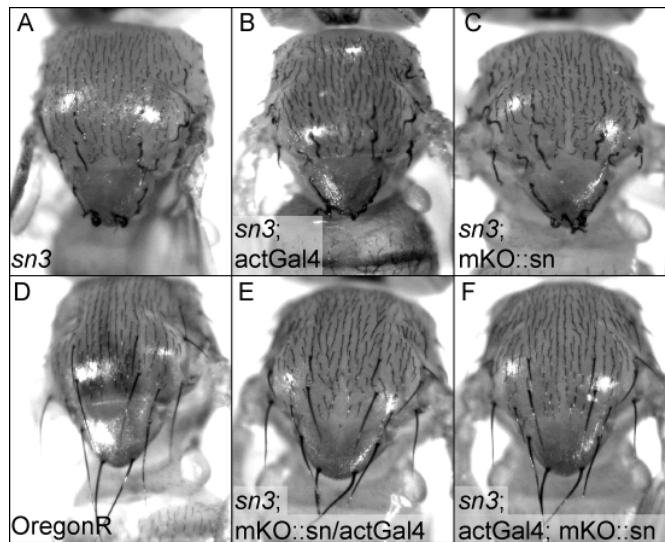


Figure 3.3: Functionality of the fluorescently tagged Singed construct

(A-F) Test for the functionality of the *mKO::sn* construct. The severe *sn*³ bristle phenotype (A) can be rescued by expressing *mKO::sn* under the control of *actinGal4* (E, F) to an almost wild type appearance (D). Neither *actinGal4* alone (B), nor *mKO::sn* alone (C) can rescue the bristle phenotype.

To test the localization of *mKO::sn* in the md-da neurons, I expressed the construct with different md-da neuron specific Gal4 driver lines. In class III neurons, I could confirm the localization of the endogenous protein revealed by antibody staining. Additionally to the localization to the cell bodies, fluorescently-tagged Singed localized to a vast majority of the spiked protrusions and was not enriched at the main branches (Fig. 3.4 A-C). In class IV neurons, fluorescently tagged Singed was visible in the cell bodies but did not localize to particular dendritic subdomains (Fig. 3.4 D-F). Expression of the Kushabira Orange tagged Singed in the simple class I neurons also resulted in the localization to the cell bodies and additionally, like the endogenous protein, to a faint localization at the branching points. At the observed levels of expression, *mKO::sn* seems not to lead to mislocalization or abnormal dendritic phenotypes.

Importantly, in spite of the fact that *singed* was expressed in all four classes of md-da neurons in the cell bodies, Singed was only localized to distinct dendritic domains of class III neurons, namely the spiked protrusions, suggesting that *singed* plays a specific role in the class III dendritic branching.

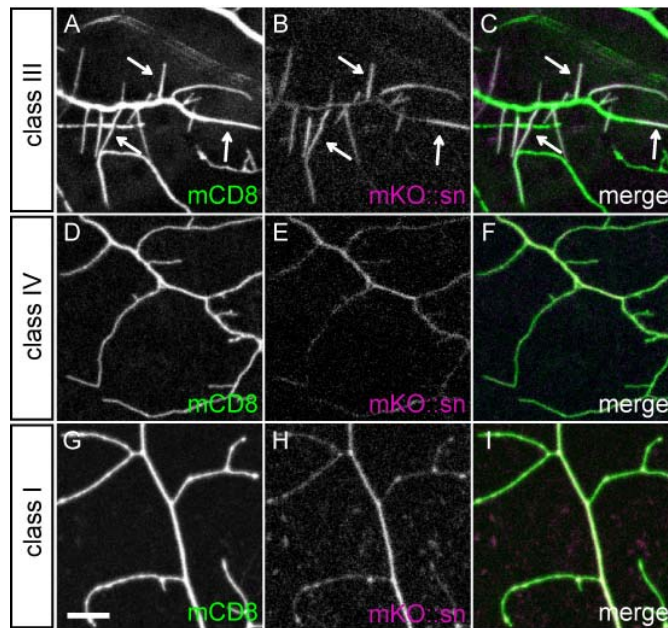


Figure 3.4: Fluorescently tagged Singed localizes to class III spiked protrusions

(A-C) Class III *ddaA* neuron highlighted with *80G2* and expressing monomeric KushabiraOrange-tagged Singed (*mKO::sn*). *mKO::sn* is enriched within the terminal branchlets of class III neurons (arrows). (D-F) Class IV *ddaC* neuron expressing *mCD8GFP* and *mKO::sn* under the control of *477Gal4*. *mKO::sn* shows no specific localization at terminal branches of class IV neurons. (G-H) Class I *ddaE* neuron expressing *mCD8GFP* and *mKO::sn* under the control of *c161Gal4*. *mKO::sn* is not enriched at terminal branches. There might be some enrichment at branching points. Scale bar: 10 μm .

3.2 Terminal branchlets of class III and class IV neurons

3.2.1 Cytoskeletal organization

The very specific localization of Singed to the spiked protrusions of class III neurons was surprising, because Singed expression was detected in all classes of md-da neurons. A possible explanation for this could be a different organization of the actin and microtubule cytoskeleton in the dendrites of the specific neuronal classes. Class I neurons were reported to have microtubule based dendritic trees, suggesting why the actin-bundling molecule Singed is not enriched in these branches (Jinushi-Nakao, Arvind et al. 2007).

To investigate, if the basic dendritic cytoskeleton of class III and class IV neurons differs in its organization, I compared the localization of GFP tagged actin and tubulin in these neurons. As shown before, a large fraction of the class III terminal branchlets were completely filled with actin-GFP and only few terminal branchlets showed low levels of actin (Andersen, Li et al. 2005; Li, Li et al. 2005; Medina, Swick et al. 2006; Medina, Worthen et al. 2008) (Fig. 3.5 A-C). Also the terminal branchlets of class IV neurons showed actin-GFP enrichment. However only in shorter branchlets it was also decorating the branch over the whole length. In longer branchlets the signal was more discontinuous and often only enriched in subdomains (Fig. 3.5 D-F).

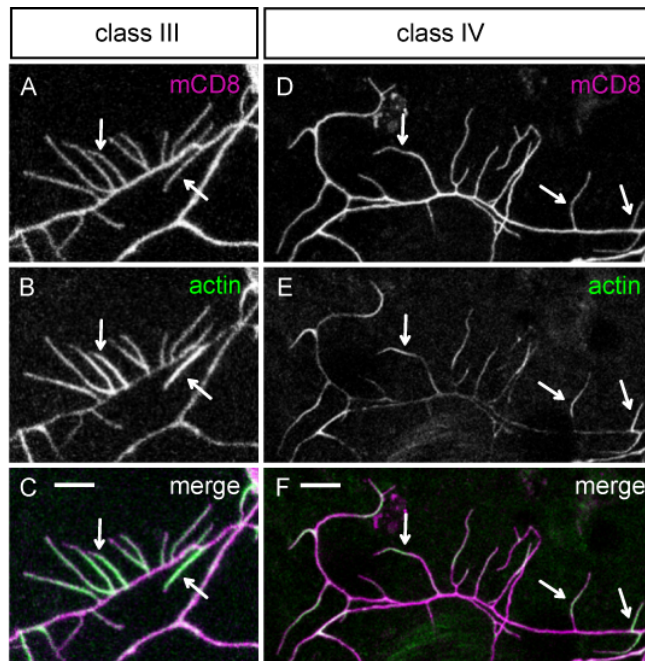


Figure 3.5: Actin localization in class III and class IV neurons

(A-F) Actin localization in terminal branchlets of class III (A-C) and class IV (D-F) neurons in the third instar larvae. The neurons express *UAS-actinGFP* and *UASmCD8cherry* under the control of *109(2)80-Gal4*. (A-C) Actin-GFP localizes to the terminal branchlets of class III neurons. Arrows point to spiked protrusions where Actin-GFP is enriched over the whole length of the branchlet. Scale bar: 5 μ m. (D-F) Actin-GFP localizes to terminal branchlets of class IV neurons, mainly within defined subdomains (arrows). Scale bar: 10 μ m.

In contrast to the localization of actin to the spiked protrusions of class III neurons, tubulin-GFP only labelled the main branchlets and did never invade the short terminal branchlets (Fig. 3.6 A-C). This was consistent with previous results where the microtubule binding proteins Futsch and Tau could only be detected at the main branches of class III neurons (Andersen, Li et al. 2005; Li, Li et al. 2005). In class IV neurons, tubulin-GFP also localized to the main branches. Lots of terminal branchlets were completely devoid of tubulin, however, the signal in class IV neurons seemed to be weaker and more diffuse than in class III neurons (Fig. 3.6 D-F).

Thus, the general cytoskeletal organization of class III and class IV neurons is similar in that actin localizes to the terminal branchlets and tubulin to the main branchlets. Moreover, the distinct localization of Singed to the terminal branchlets of the two

classes cannot be simply explained by a different basic localization actin and microtubules. Possibly, specific factors are missing in class IV neurons that could allow Singed to localize to distinct dendritic domains.

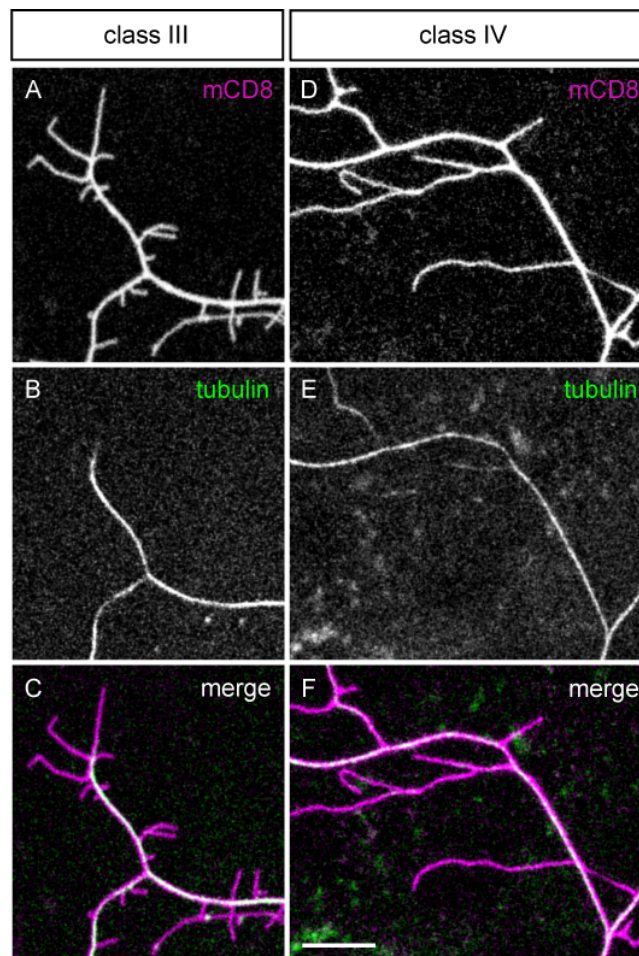


Figure 3.6: Tubulin localization in class III and class IV neurons

(A-F) Tubulin localization in dendritic branches of class III (A-C) and class IV (D-F) neurons in the third instar larvae. The neurons express *UAS-tubulinGFP* and *UASmCD8cherry* under the control of *109(2)80-Gal4*. (A-C) Tubulin-GFP localizes to the main branches of class III neurons, the spiked-protrusions are devoid of Tubulin-GFP. (D-F) Tubulin-GFP localizes to main branches of class IV neurons; in many of the terminal branchlets Tubulin-GFP is not detectable. Scale bar: 10 μm .

3.2.2 Terminal branchlet bending

Even though the general cytoskeletal organization of class III and class IV neurons is quite similar, class III and class IV neurons have many distinct morphological properties some of which were previously described. In comparison to class III, class IV dendrites have a larger dendritic field size and are more complex, judged by their higher dendrite branch order and number of dendrite termini (Grueber, Jan et al. 2002). Moreover, the terminal branches have clear and distinctive characteristics. Class III terminal branchlets, the spiked protrusions, are short, on average 5 μm and straight. In contrast the terminal branchlets of class IV neurons are longer, 15 μm on average and often bent (Fig. 3.5). For a quantitative evaluation of the curvature of the terminal branchlets Friedrich Förstner (former PhD student in the lab of Alexander Borst, MPI of Neurobiology) implemented the TREES toolbox and calculated the convex area delimited by a terminal branchlet (Cuntz, Forstner et al. 2010). Curved branchlets give rise to a higher convex area than straight terminal branchlets. To equal out the length differences of the terminal branchlets of class III and class IV neurons the convex area was normalized over the terminal branch length. Indeed, class IV neuron terminal branchlets showed a significantly larger convex hull/branch length than class III neurons (Fig. 3.7).

These results show that the morphology of the terminal branchlets, especially their length and curvature, is a clear and distinctive feature between class III and class IV neurons. Since Singed is only localized to the class III terminal branchlets, it might also be responsible for the class III spiked protrusions and their specific morphology.

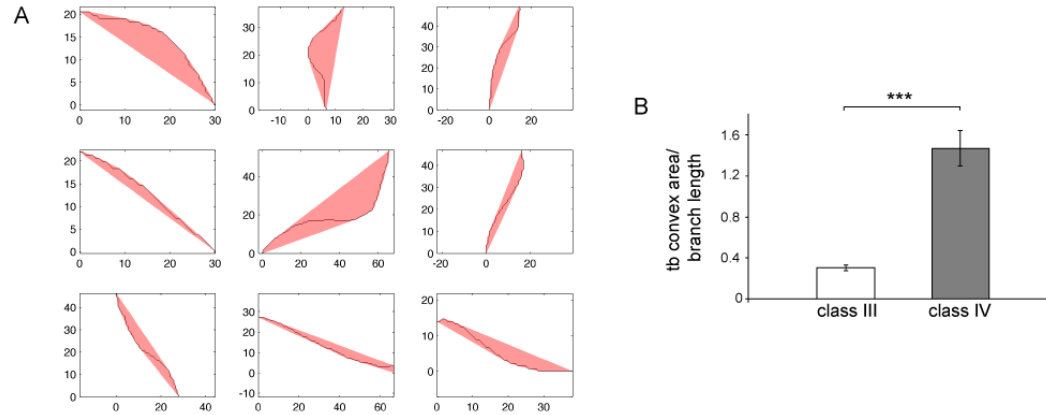


Figure 3.7: Curvature of terminal branchlets of class III and class IV neurons

(A) Examples of class IV terminal branchlets (dark red) enveloped by their convex hulls (light red). The path-normalized convex hull can be used as a measure for the curvature of a terminal branchlet. Axes are set in micrometers. (B) Quantification of the curvature of terminal branchlets of class III and class IV neurons, shown as the terminal branch (tb) convex area normalized over the branch length. Class III neuron terminal branchlets have significantly smaller convex area/branch length compared to class IV neurons. In this and all subsequent figures:

* $p < 0.05$, ** $p < 0.01$, *** $p < 0.001$. SD is indicated.

3.3 Singed in class III neurons

3.3.1 Singed affects the number and density of class III spiked protrusions

The examination of the Singed expression pattern showed that Singed is expressed in all classes of md-da neurons, but only localized to the terminal branchlets of one specific class, the class III neurons. In order to analyze, if *singed* plays a role in the class III specific spiked protrusions, I used loss of function approach. I investigated two different alleles, the sn^3 fertile hypomorph and the sn^{36a} sterile null mutation (Paterson and O'Hare 1991; Cant, Knowles et al. 1994). The dendrites of class III ldaB neurons of third instar larvae exhibit lots of short, actin rich spiked-protrusions along their main branches (Fig. 3.5 A-C and Fig. 3.8 A, A', D-F; number: 238 ± 29 ; density: $0.1/\mu\text{m}$). In the sn^3 hypomorph the number and density of these protrusions was reduced (Fig. 3.7 B, D-F; number: 179 ± 30 ; density: $0.07/\mu\text{m}$). However, this reduction was not statistically significant. In contrast, the sn^{36a} null mutant showed a significantly reduced number and density of spiked protrusions compared to the control (Fig. 3.8 C, D-F number: 130 ± 42 ; $p < 0.01$; density: $0.04/\mu\text{m}$; $p < 0.01$). This defect in the number of spiked protrusions was not due to a general problem in dendrite extension, because the overall branch length of the dendritic tree was not affected in sn^{36a} mutant larvae (control: $3888 \mu\text{m} \pm 332$; sn^{36a} : $3981 \mu\text{m} \pm 575$; $p > 0.5$).

sn^{36a} and sn^3 full mutant larvae showed a clear reduction in the density of spiked protrusions of class III ldaB neurons. However, the *Drosophila* PNS neurons are localized in between the epidermis and the muscular body wall and are therefore in close contact with these tissues. Thus, it was possible that the observed phenotype was non-cell autonomous, especially, because antibody staining revealed that Singed is also expressed in the epidermis (Fig. 3.1). To test for a cell autonomous effect of Singed in the ldaB class III neurons, I tried to rescue the spiked protrusion phenotype by combining the sn^{36a} mutant with one copy of Kushabira Orange tagged Singed specifically expressed in these neurons with the *c161Gal4* driver line. This driver line only activates expression in class I, class II and class III neurons and not in epidermal or muscle cells. One copy of the *mKO::sn* construct in sn^{36a} mutant background restored the number of spiked protrusions (240 ± 56 ; $p > 0.05$) and protrusion density ($0.1/\mu\text{m}$ of branch length; $p > 0.05$) to control levels (Fig. 3.8 D, E-F). This experiment

revealed that the mutation of *singed* was responsible for the observed phenotype in reduction of spiked protrusion number and density, and that it acts in a cell autonomous manner.

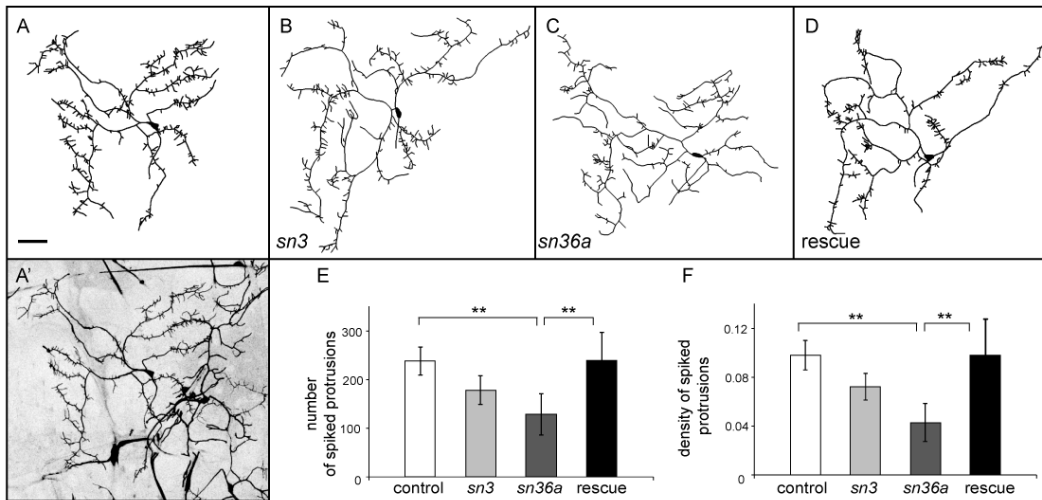


Figure 3.8: Loss of *singed* leads to the loss of class III spiked protrusions

(A-D) Tracings and original image (A') of class III *IdaB* neurons expressing *mCD8GFP* under the control of *c161Gal4* of third instar larvae of the following genotypes: (A, A') Wild-type, (B) *sn³*, (C) *sn^{36a}*. (D) Demonstrates the cell autonomous rescue of the *sn^{36a}* mutant phenotypes obtained by expressing *mKO::sn* in class III neurons. Scale bar: 50 μ m. (E) Quantification of the total number of spiked protrusions in class III *IdaB* neurons of wild-type, *sn³*, *sn^{36a}* and class III-rescued third instar larvae. The number of spiked protrusions is significantly reduced in the *sn^{36a}* mutant and is rescued to wild type levels by expressing one copy of *mKO::sn* with *c161Gal4*. (F) The density of spiked protrusions is significantly reduced in *sn^{36a}* mutant larvae compared to wild type and is cell autonomously rescued to wild type levels.

3.3.2 *Singed* controls terminal branchlet morphology and dendrite complexity

In class III neurons mutant for *singed*, not only the density of spiked protrusions was reduced, but also the morphology of the remaining spikes was altered. Instead of the short and straight appearance of the wild type spiked protrusions, the *sn^{36a}* mutant ones were longer and often bend (Fig. 3.9 A, B). The curvature of the terminal branchlets of *sn^{36a}* mutant class III *IdaB* neurons was significantly increased compared to the control (analyzed by Friedrich Förstner; Fig. 3.9 C). Interestingly, this parameter was lying between the values obtained of class III and class IV neurons (see also Fig. 3.7 B).

Additionally, the percentage of long spiked protrusions, longer than 10 μm , was significantly increased from 12% (± 3) in the control to 24% (± 5 ; $p < 0.01$) in the sn^3 mutant and to 20% (± 8 ; $p < 0.05$) in the sn^{36a} mutant. The increase in the fraction of long spikes was cell-autonomously rescued with one copy of the $mKO::sn$ construct to wild type levels (11% ± 2 ; $p > 0.5$; Fig. 3.9 D).

The increased curvature and length of the terminal branchlets in the *singed* mutant class III neurons represented a clear shift of terminal branchlet properties of class III to class IV neurons, which are longer and more bent.

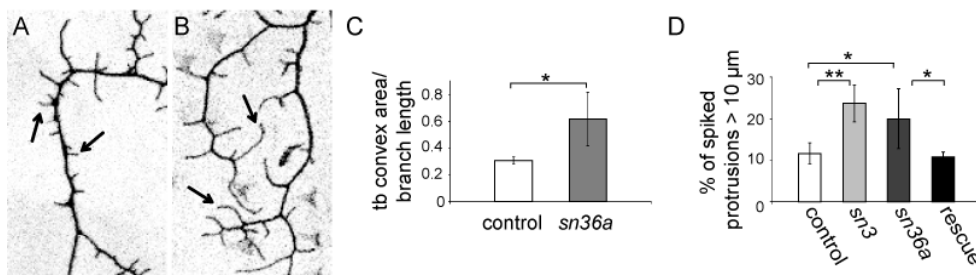


Figure 3.9: Singed controls spiked protrusion length and curvature

(A, B) Terminal branchlets of a wild type (A) and a sn^{36a} mutant (B) class III ldaB neuron expressing *mCD8GFP* under the control of *c161Gal4* (arrows). Scale bar: 10 μm . (C) Quantification of the curvature of terminal branchlets of wild type and sn^{36a} mutant class III ldaB neurons measured by the convex area spanning the branchlet, divided by its length. (D) Quantification of the spiked protrusions length distribution of wild type and sn^{36a} mutant branchlets. The percentage of spiked protrusions that are longer than 10 μm is significantly increased in sn^3 and sn^{36a} mutants. This sn^{36a} mutant phenotype is cell autonomously rescued by expressing *mKO::sn* under the control of the *c161Gal4* driver.

Additionally to the changes in the density and morphology of the spiked protrusions, the sn^{36a} class III neurons appeared to be more complex in the overall morphology of the dendritic tree than the control neurons. As a measure of the complexity of the dendritic tree, I quantified the number of all termini, excluding the spiked protrusions, which were defined as terminal branchlets of less than 30 μm (Fig 3.10 A-B'). As an increased complexity of the main branches would be masked by the massive loss of the spiked protrusions, I thereby eliminated the effect of the reduced spike density in the

sn^{36a} mutant. The number of these defined termini was significantly increased from 29 (±3) in the control to 40 (±4) in the *sn*^{36a} mutant ($p < 0.01$), demonstrating an increase in branching complexity (Fig. 3.10 C). Again this effect was rescued cell-autonomously by re-inserting one copy of the *mKO::sn* construct.

Taken together, loss of *singed* modified the number, density and morphology of the class III neuron terminal branchlets. In addition, it increased the complexity of the dendrite tree. It appeared that loss of *singed* in the class III neurons leads to a partial shift towards the class IV morphology, including longer terminal branchlets, a higher curvature of the terminal branchlets and an increased complexity of the dendritic tree.

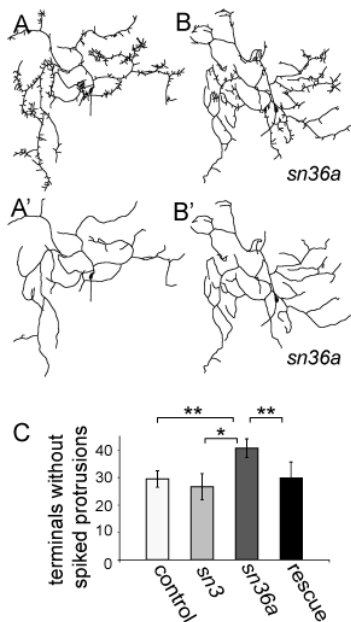


Figure 3.10: Singed controls dendrite complexity

(A-B') Tracing of a wild type (A) or of a *sn*^{36a} mutant (B) class III *l*daB neuron. (A' and B') The same tracings after eliminating the terminal branchlets shorter than 30 μm. (C) The number of terminals left after pruning the terminal branchlets below 30 μm is significantly increased in the *sn*^{36a} mutant and can be rescued cell autonomously.

3.3.3 *Singed* does not affect the general cytoskeletal organization in class III neurons

In the last section, I could show that in *sn^{36a}* mutants, class III spiked protrusions grow out longer and the main dendritic branching pattern gets more complex compared to control. In wild type class III neurons only the main branches show localization of microtubules and they never invade the spiked protrusions (Andersen, Li et al. 2005; Li, Li et al. 2005). In contrast actin-GFP is highly enriched in the spiked protrusions, nicely correlating with the localization of the actin bundling molecule *Singed*. Therefore, I was interested if the morphological changes were also accompanied by changes in the organisation of the cytoskeleton. First, I wanted to see if invasion of microtubules into the spiked protrusions lead to their increase in length and if microtubules are also responsible for the increased branching complexity. To label the microtubule positive domains of the dendritic tree I stained for Futsch, a MAP1B-like protein, that is specifically expressed in neurons (Hummel, Krukkert et al. 2000). However, the total extension of the futsch labelled, microtubule positive, dendrite domains was not increased in the *sn^{36a}* mutant compared to the control (Fig. 3.11 A-C, D-F and G). Also the number of futsch positive branches was not modified by the mutation in *singed* (Fig. 3.11 F). Finally, *singed* mutant spiked protrusions did not show any invasion of futsch labelled microtubules like in the control (Fig. 3.11 A'-C', D'-F').

These results show that the elongated branchlets resulting from the absence of *singed* do not contain microtubules. The morphological changes that lead to longer spiked protrusions and a more complex branching pattern seem to be all actin-based. Interestingly, *singed* mutant class III dendrites show larger regions that are devoid of microtubules as compared to wild type, a morphological feature that is again similar to class IV dendrites.

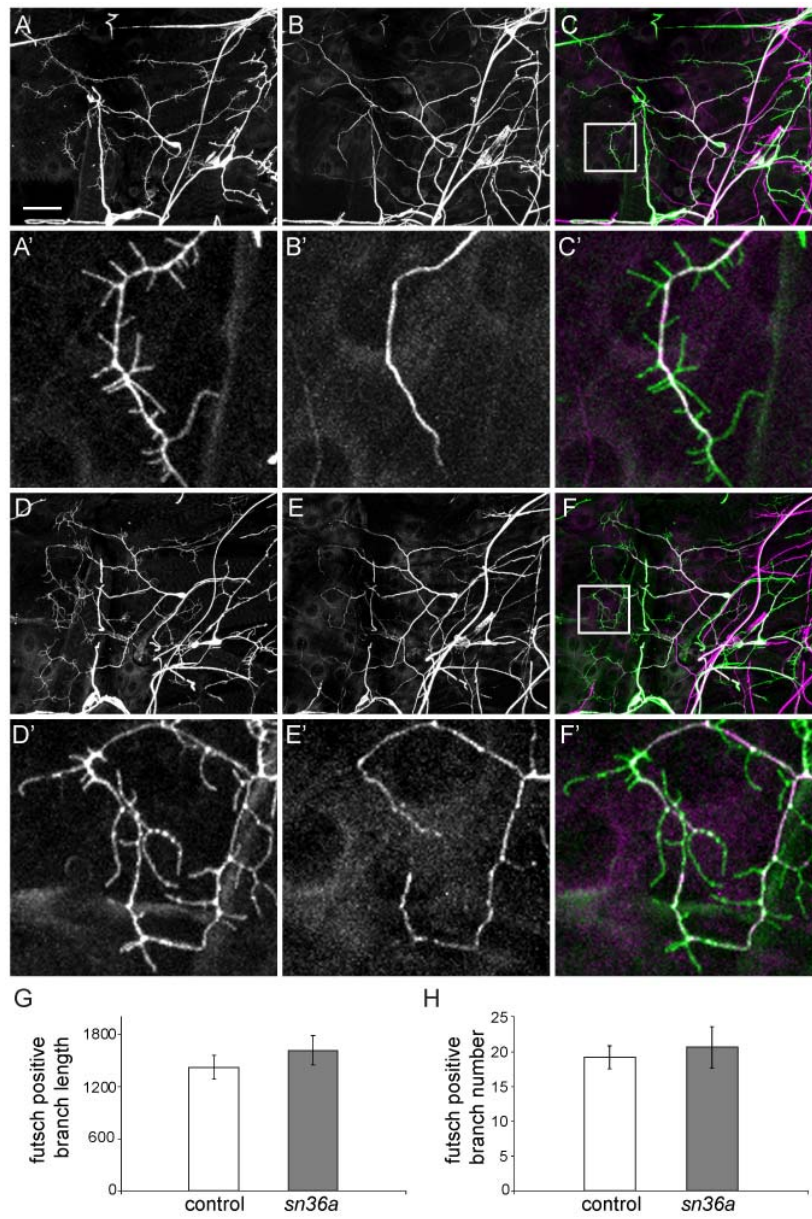


Figure 3.11: Futsch extension is not altered upon loss of *singed*

(A, F') Class III ldaB neurons expressing *UASmCD8GFP* under the control of *c161Gal4*. (A-C') Control and (D-F') *sn^{36a}* mutant larvae stained against GFP and Futsch. Scale bar: 50 μm. (G) Quantification of the total length of futsch-positive dendritic branches. (H) Quantification of the number of futsch-positive dendritic branches.

3.3.4 MARCM

By re-expressing *singed* specifically in class III neurons in otherwise full mutant sn^{36a} larvae, I could restore the wild type density and morphology of spiked protrusions, which demonstrated the cell autonomous effect of *singed* in this type of neurons. To confirm this mode of function, I additionally performed MARCM (Mosaic Analysis with a Repressible Cell Marker) analysis. With this system it is possible to generate mutant single cell clones that are at the same time labeled with GFP in a non-mutant, unlabeled background (Lee and Luo 1999). I analyzed single cell clones of class III *IdaB* neurons of the control and the sn^{36a} mutation and found a clear trend showing the reduction of the spiked protrusion density in the sn^{36a} mutant (0.06 ± 0.003) compared to wild type clones (0.11 ± 0.03). However, this difference was not significant (Fig. 3.12). In contrast to the results obtained by the analysis of the full mutant larvae, there was no difference in the length of the spiked protrusions. Moreover, single cell mutant clones did not show an increase in complexity of the main branches. This difference in the strength of the phenotype between single cell clones and full mutants might be due to higher protein levels remaining in the *singed* single cell clones compared to the full mutant larvae. Due to the genetics underlying MARCM, all cells are heterozygous for *singed* until the heat shock induces the recombination of paired chromosomal arms during mitosis. *Singed* protein and mRNA expressed from the wild type chromosome remain in the cytoplasm of the recombined *singed* mutant single cell clone. Thereby, additionally to the maternal contribution there is also contribution of *singed* from the mother cell, leading to a less pronounced phenotype.

Even though I found a reduced spike density in the sn^{36a} single cell clones, the reduction was not significant. Nevertheless, the specific rescue of *singed* in the class III neurons showed that *singed* acts cell autonomously in these neurons.

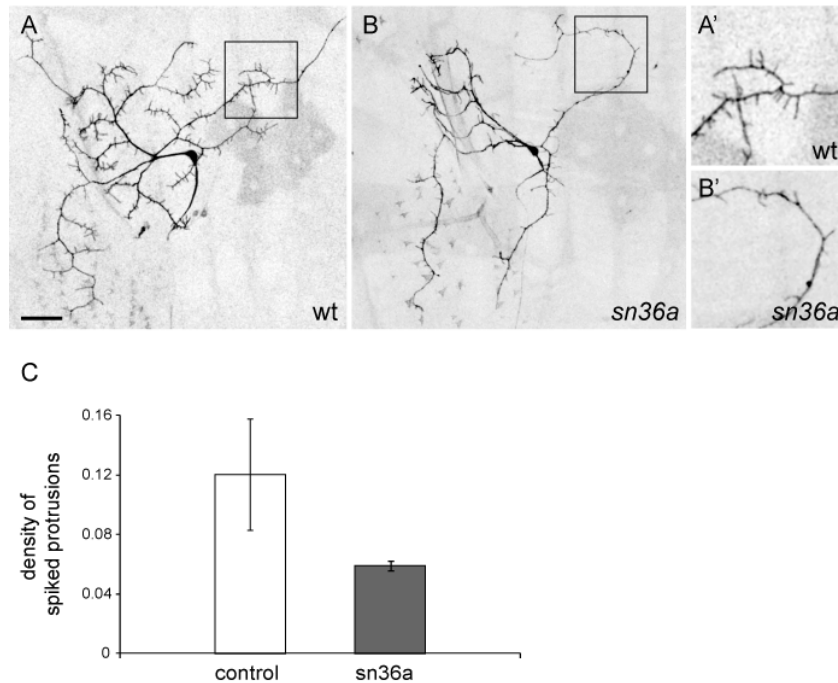


Figure 3.12: *singed* MARCM clones

Mosaic clones of class III *IdaB* neurons of (A) wild type and (B) *sn^{36a}* mutants. Scale bar: 50 μm . (A'-B') Blow up of the indicated squares in A and B. (C) There is a clear, though not significant trend showing the reduction of the spiky protrusion density in the *sn^{36a}* mutant clones compared to wild type clones

3.3.5 *Singed* accumulation is correlated with the outgrowth of spiky protrusions

Loss of function experiments revealed that *singed* is required for the density of spiky protrusions and their typical morphology, which is short and straight. It was already shown with time-lapse analysis that the spiky protrusions of class III neurons are very dynamic and constantly grow and retract (Andersen, Li et al. 2005). However, the question remains at which stage of spiky protrusion formation, or also maintenance, *Singed* is required. Therefore, I was interested if the dynamic morphological changes of class III spiky protrusions are accompanied with alterations in *Singed* accumulation. Using a mCD8cherry membrane marker and GFP tagged *Singed*, I investigated the specific localization of *Singed* during extension and retraction of the spiky protrusions by time-lapse imaging. However, with classical confocal imaging, bleaching impeded time-lapse imaging with two different fluorophores. To solve this problem, I employed

spinning disc confocal microscopy, a technique that allows much faster imaging and therefore also reduces bleaching. Second instar larvae expressing *mCD8cherry* and *GFP::sn* were imaged every 3 min over a time frame of 15 min. In these movies, I found a close correlation between the amount of Singed on a defined branchlet and its dynamic state (Fig. 3.13 A-C). While Singed accumulated on a large fraction of extending branches ($81\% \pm 7$), only a small fraction ($10\% \pm 11$) of the extending branchlets showed Singed enrichment before extension and a similar small fraction ($9\% \pm 10$) did not show any enrichment of Singed (Fig. 3.13 D). In contrast, retracting branchlets displayed a lower Singed signal that was either not detectable before ($16\% \pm 10$) or during the whole retraction ($38\% \pm 21$), or was shrinking while the process retracted ($46\% \pm 12$) (Fig. 3.13.E). I could not detect a clear accumulation of Singed predicting the site of new branch formation. However, this signal might have been well under detection levels.

Taken together, Singed enrichment was a feature of extending spiked protrusions, suggesting that actin-bundling through Singed is required for the formation and the straight outgrowth of the spiked protrusions. Retracting spiked protrusions instead correlated with a reduction of Singed signal. Less actin-bundling through Singed could possibly allow shrinking of the spiked protrusions.

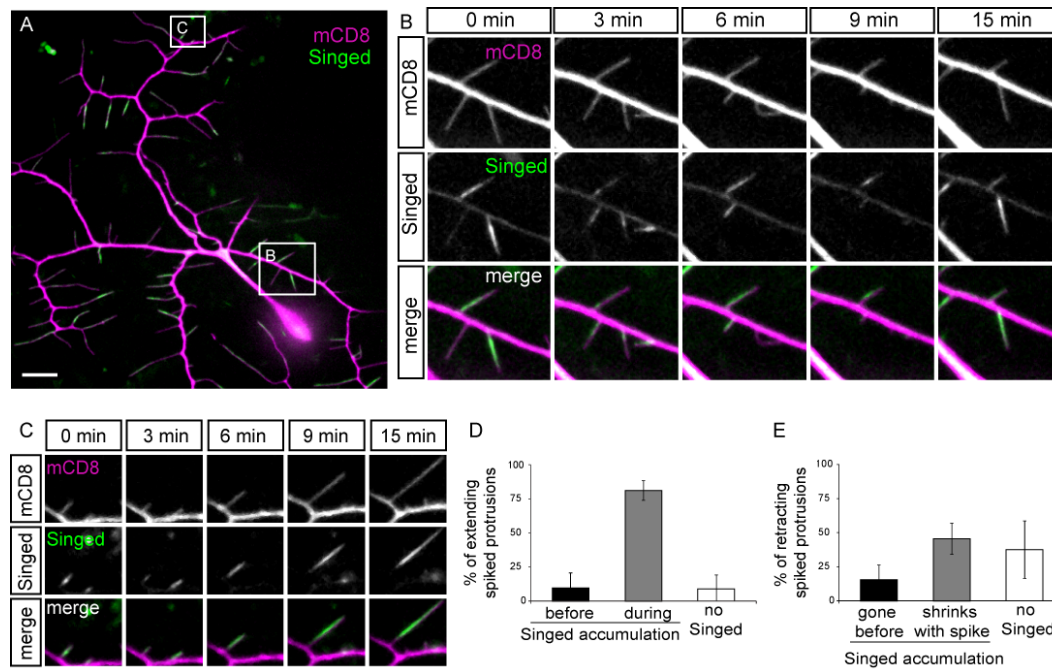


Figure 3.13: Singed accumulates within extending terminal branchlets of class III neurons

Time lapse analysis of Singed localization during terminal branchlet dynamics in class III neurons that express membrane-tagged cherry (mCD8) and GFP-Singed (Singed). (A) One of the imaged neurons at time point 0. Scale bar: 5 μ m. (B, C) Time lapse sequence of the regions boxed in (A). (D) Singed preferentially accumulates within extending terminal branchlets. (E) Singed localization is more variable in retracting terminal branchlets, including branchlets that do not contain detectable Singed, that lose the Singed signal before retraction and ones in which the Singed signal diminishes during retraction.

3.4 Singed in class IV neurons

3.4.1 Singed loss of function does not affect class IV dendritic branching

As class III neurons that lack *singed* show dendrite morphology that is quantitatively partially shifted towards class IV neurons characteristics, I examined whether Singed also plays a role during dendrite formation of class IV neurons. I could show that Singed is only localized to the spiked protrusions of class III neurons and not to the terminal branchlets of other classes of neurons. Nevertheless, it is expressed in class IV neuron cell bodies, even to comparable levels as in class III neurons.

To investigate the potential role of *singed* in class IV dendrite formation, I examined the effect of the severe *sn*^{36a} mutation in ddaC class IV neurons. First, I quantified the number of termini, which did not differ between the mutant (470±40) and the control (463±25; $p>0.5$; Fig. 3.14 A-C). To reveal a possible difference in the distribution of the branches, I analyzed tracings of the neurons with Sholl-Analysis, where concentric circles are drawn around the cell body spaced from one another by 10 μm . All intersections of the dendritic tree with the respective concentric circles were counted and represented the dendrite branch distribution. Using this analysis, I could show that the loss of *singed* did also not affect the distribution of branches in class IV ddaC neurons (Fig. 3.14 D).

Taken together, *singed* was necessary in class III neurons for proper terminal branchlet formation and to define tree complexity, but was dispensable in class IV neurons. Even though Singed was detectable within the cell body of class IV neurons, *sn*^{36a} mutants did not show any alteration in the branching pattern of class IV dendrites. A possible explanation could be that in these neurons Singed was not activated or localized appropriately to function in the formation of spiked protrusions like it does in class III neurons.

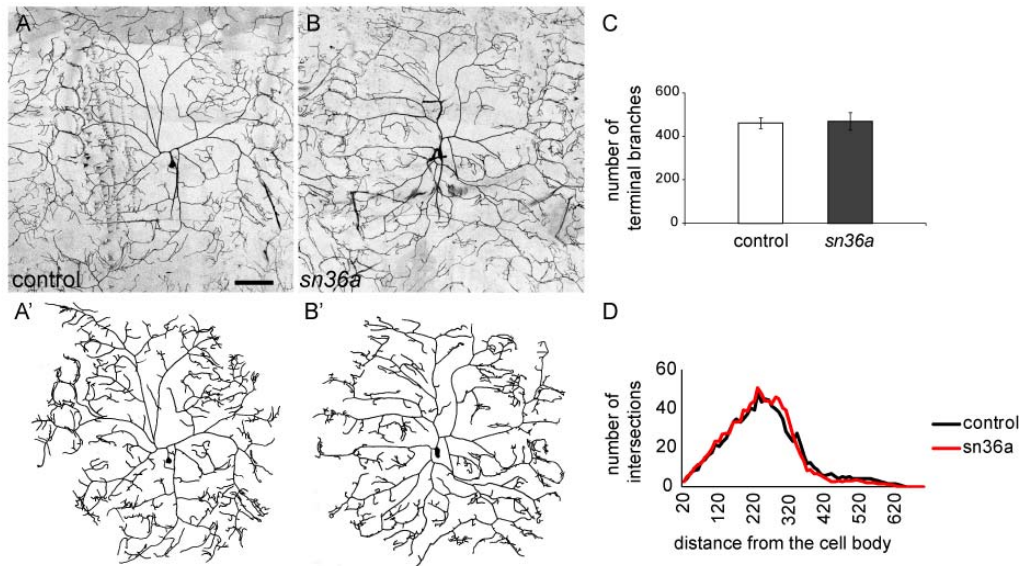


Figure 3.14: Singed is not required for class IV terminal branching

(A, B) Class IV ddaC neurons expressing *mCD8GFP* under the control of *477Gal4*. (A, A') Wild type and (B, B') *sn^{36a}* mutant neurons and their tracing. Scale bar: 100 μm. (C) There is no significant difference in the number of terminal branches between wild type and *sn^{36a}* mutant neurons. (D) The number of intersections of dendritic branches with concentric circles drawn around the cell body (Sholl Analysis) is not different between wild type and *sn^{36a}* mutant neurons.

3.4.2 Overexpression of Singed can induce spiked protrusions in class IV neurons

In the last section, I could show that loss of *singed* does not affect dendritic branching of class IV neurons. Since class IV neurons nonetheless express Singed, one could imagine that Singed is not activated or localized to function in dendritic development in this class of neurons. If this was the case, massive overexpression of Singed might overrule this internal regulation in class IV neurons. To test this possibility, I expressed *mKO::sn* at high levels in the ddaC class IV neurons. For stable and high expression of the construct, *mKO::sn* was inserted into a defined position in the fly genome with the *attP* landing site system. This system allows the insertion of transgenes into predetermined intergenic regions in the fly genome. Therefore selection of insertion sites with a defined expression level, which could be high, low or intermediate, is possible (Bischof, Maeda et al. 2007). For the overexpression of *mKO::sn* in class IV

neurons I chose the 51D landing site, which directs the insertion into a position in the fly genome that leads to high expression levels of the construct. With these high levels of expression, I could induce the formation of terminal branchlets that resembled spiked protrusions in class IV neurons in that they were shorter and straighter than terminal branchlets of the control (Fig. 3.15 A, B). There was a significant increase in the fraction of short terminal branchlets, measuring less than 10 μm in length (Fig. 3.15 C). Analysis of the curvature of the terminal branchlets confirmed that overexpression of *mKO::sn* in class IV neurons lead to a reduced curvature of the terminals than in the control (analyzed by Friedrich Förstner). The convex area spanned by the terminal branchlets of class IV neurons overexpressing Singed was shifted towards class III values (Fig. 3.15 D; see also Fig. 3.7). Importantly, numerous of these shorter terminal branchlets accumulated Singed. This was not the case when the *mKO::sn* construct was expressed with lower levels, or when *mKO* was expressed on its own (Fig. 3.15 E-J; see also Fig. 3.4 D-F).

Thus, it was possible to induce the formation of spiked protrusions in class IV neurons with high levels of Singed, showing that *singed* is not only necessary for spiked protrusion density and morphology, but also sufficient for their formation.

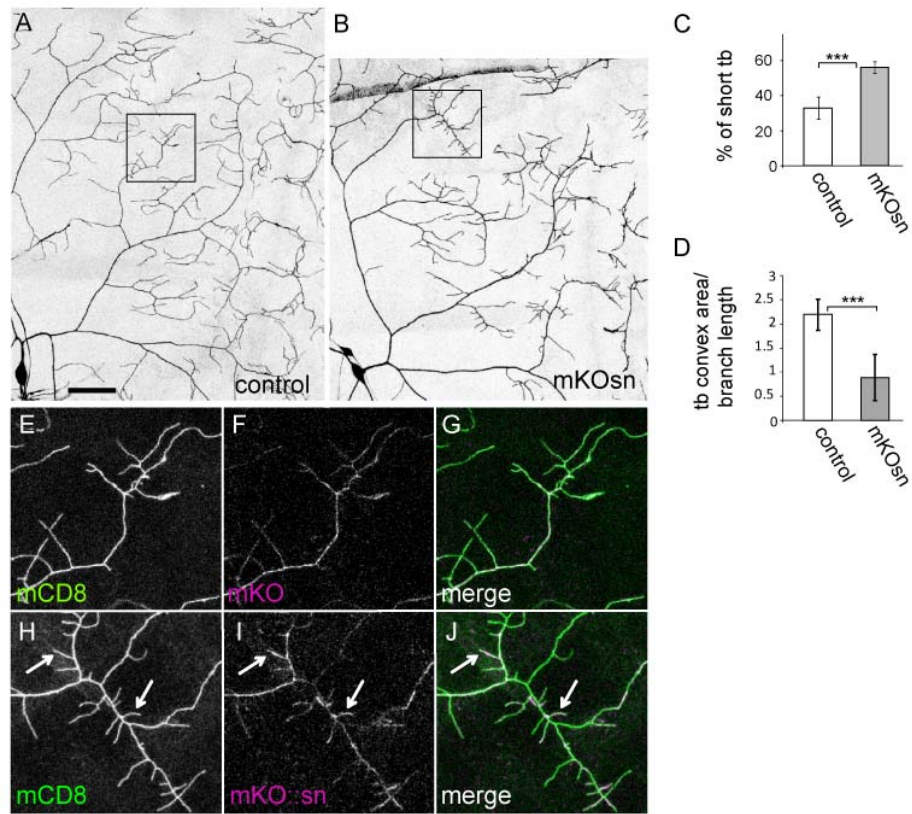


Figure 3.15: Singed overexpression in class IV neurons

(A, B) Class IV *ddaC* neurons expressing *mCD8GFP* under the control of *477Gal4*; the dorsal-posterior quarter of the dendritic tree is shown. Overexpression with *477Gal4* of the following constructs: (A) *mKO*, (B) *mKO::sn*. Scale bar: 50 μm . (C) Overexpression of *mKO::sn* induces significantly more terminal branchlets that are shorter than 10 μm . (D) Overexpression of *mKOsn* straightens the terminal branchlets significantly compared to *mKO* only. (See also Fig. 3.7). (E-G) Kushabira Orange protein is uniformly distributed and not enriched at terminal branches in control neurons. (H-J) Strong overexpression of *mKO::sn* that leads to the formation of short terminal branchlets is accompanied by recruitment of *mKO::sn* to the ectopic short branchlets (arrows). Compare to the absence of *mKOsn* enrichment in class IV neurons at low expression levels that does not induce a phenotype (Fig. 3.4 D-F).

3.5 Singed activity is modulated by phosphorylation

3.5.1 Regulation through phosphorylation in class III neurons

Several studies showed that fascin is negatively controlled by phosphorylation of a conserved Serine within the MARCKS homology domain. Phosphorylation of Serine-39 leads to a reduced capacity of actin binding, and therefore probably also reduced bundling (Yamakita, Ono et al. 1996; Ono, Yamakita et al. 1997; Adams, Clelland et al. 1999; Vignjevic, Kojima et al. 2006). In the *Drosophila* Singed protein, this Serine is located at position 52 and has been shown to be important for the role of Singed in bristle formation (Holthuis, Schoonderwoert et al. 1994; Zanet, Stramer et al. 2009). To address the regulation of phosphorylation at Ser52 in the formation of spiked protrusions, I generated phosphomimetic and non-phosphorylatable Singed constructs by site-directed mutagenesis. To mimic the phosphorylation of Serine 52, I replaced it with Aspartic Acid. This amino acid has a similar size and structural properties as Serine, but additionally an oxygen molecule and a negative charge, which leads to almost identical structural properties as phosphorylated Serine. For the generation of a non-phosphorylatable construct, I replaced Serine 52 with Alanine, which lacks the hydroxyl group where the phosphorylation of Serine usually takes place. To obtain similar expression levels, both constructs were inserted in the same landing site, 51D, which lead to high expression.

First, I tested these constructs for their ability to rescue the *sn*^{36a} mutant phenotype in class III neurons. As expected, the non-modified Singed, also inserted in the 51D landing site, was able to rescue the density of spiked protrusions to control levels. The same was true for the non-phosphorylatable *mKO::snS52A*. Surprisingly, also the phosphomimetic *mKO::snS52D* construct was able to rescue the spike density phenotype (Fig. 3.16 A-C). However, when I compared the spike densities rescued by the different constructs, it was obvious that the phosphomimetic *mKO::snS52D* construct resulted in a significant lower spiked protrusion density compared to the other two constructs. This might be due to a lower capacity to induce actin bundling (*mKO::sn*: 0.13 ±0.01; *mKO::snS52A*: 0.12 ±0.02; *mKO::snS52D*: 0.9 ±0.01; p<0.05; Fig. 3.16 D). These results show that phosphorylation is part of the control mechanism

for Singed activity in class III spike formation; however it seems not to be the major one, as all three constructs can rescue the phenotype.

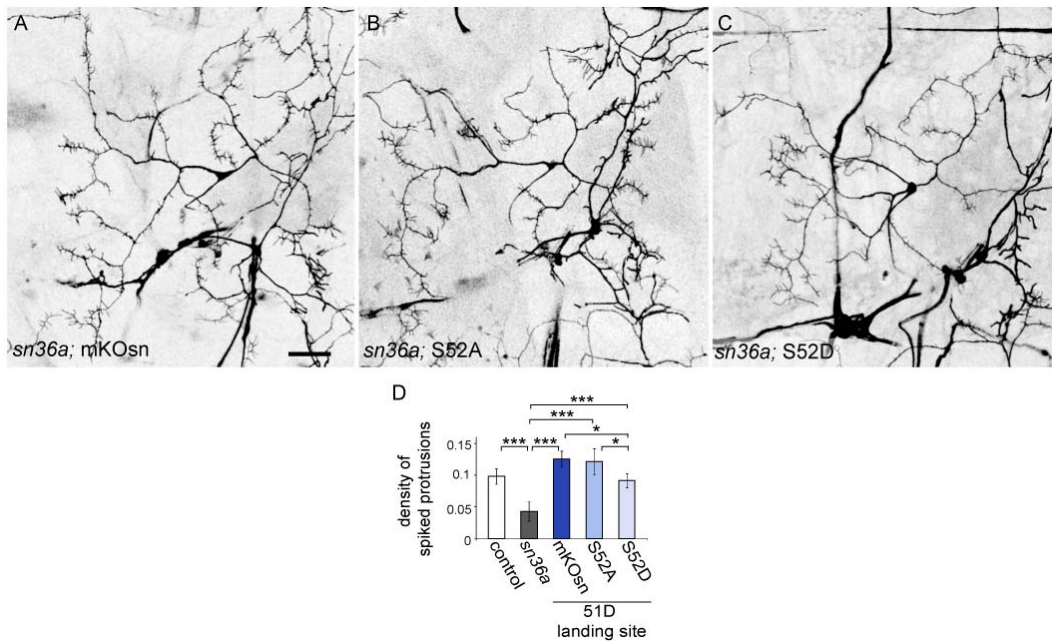


Figure 3.16: Singed is partially regulated by phosphorylation

(A-C) Rescue of the spiked protrusion density phenotype of *sn^{36a}* mutant class III ldaB neurons with Singed wild-type or phosphovariant constructs inserted at the 51D landing site and expressed with *c161Gal4*. (A) Rescue with unmodified *mKO::sn*. (B) Rescue with non-phosphorylatable *mKO::snS52A* or (C) with phosphomimetic *mKO::snS52D*. Scale bar: 50 μ m. (D) Quantification of the density of spiked protrusions of wild-type, *sn^{36a}* mutant and landing site construct rescue in the *sn^{36a}* mutant background. Unmodified *mKO::sn*, non-phosphorylatable *mKO::snS52A* and phosphomimetic *mKO::snS52D* rescue the spiked protrusion density defect of the *sn^{36a}* mutants. However rescue with the phosphomimetic *mKO::snS52D* results in a significantly lower spiked protrusion density compared to the rescue with unmodified *mKO::sn* and non-phosphorylatable *mKO::S52A*.

3.5.2 Regulation through phosphorylation in class IV neurons

Overexpression of full length *mKO::sn* at high levels in class IV neurons resulted in the formation of terminal branchlets that resembled class III spiked protrusions. Since in

the wild type Singed is expressed in class IV neurons, but does not play a role in the formation of terminal branchlets, it might be possible that Singed activity is downregulated in class IV neurons. As shown above, in class III neurons, regulation through phosphorylation at Serine 52 is not the major control mechanism for the formation of spiked protrusions. However, it is partially involved, since the phosphomimetic *mKO::snS52D* construct is not able to rescue the density of spiked protrusions to the same extent as full length and the non-phosphorylatable *mKO::snS52A* construct. To test, if this regulation is also involved in the suppression of Singed function in class IV neurons, I analyzed the effects of overexpressing phosphomimetic and non-phosphorylatable Singed in this class of neurons. Similar to the full length version of Singed, both phospho-variants were able to induce the formation of terminal branchlets that resembled spiked protrusions (Fig. 3.17 A, B; see also Fig. 3.15). Interestingly, overexpression of the non-phosphorylatable *mKO::snS52A* construct also induced increased formation of terminal branchlets compared to the control (Fig. 3.17 C). The non-phosphorylatable *mKO::snS52A* and the phosphomimetic *mKO::snS52D* constructs both increased the fraction of terminal branchlets shorter than 10 μm significantly compared to the control, but no difference was found in the fraction of short terminal branchlets compared to *mKO::sn* overexpression (Fig. 3.17 D). Also the convex area spanned by the terminal branchlets, as a measure of curvature, was reduced in a comparable range to *mKO::sn* overexpression using *mKO::snS52D* and *mKO::snS52A* constructs (analyzed by Friedrich Förstner; Fig. 3.17 E).

Taken together, overexpression of Singed is sufficient to induce shortening and straightening of the class IV terminal branchlets. This effect is independent of the phosphorylation state of Singed. Still, regulation through phosphorylation restricts the capacity of Singed to induce high order branching in these neurons. Since all three phosphovariants can induce the formation of short, straight terminal branchlets in class IV neurons, it is unlikely that regulation through phosphorylation mediates the class III specificity of Singed function.

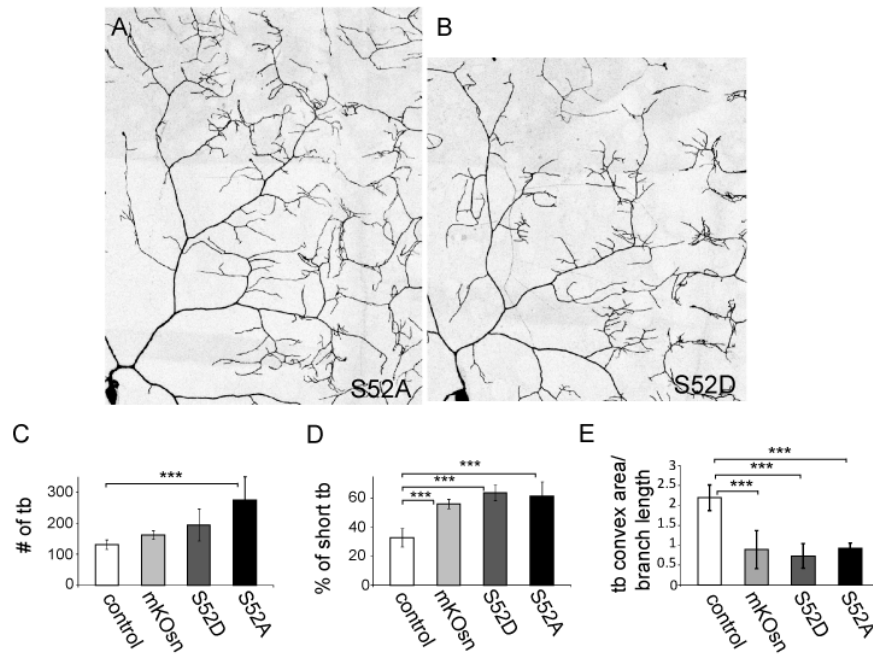


Figure 3.17: Singed is partially regulated by phosphorylation in class IV neurons

(A, B) Class IV ddaC neurons expressing *mCD8GFP* under the control of *477Gal4*; the dorsal-posterior quarter of the dendritic tree is shown. Overexpression with *477Gal4* of the following constructs: (A) *mKO::snS52A* and (B) *mKO::snS52D*. Scale bar: 50 μm . (C) Overexpression of *mKO::SnS52A* induces significantly more terminal branches compared to *mKO* only. Overexpression of the unmodified *mKO::sn* and the phosphomimetic *mKO::snS52D* constructs does not induce a significant increase in terminal branchlets. (D) There is a significant increase of terminal branches shorter than 10 μm upon overexpression of *mKO::sn*, *mKO::snS52A* and *mKO::snS52D*. (E) Overexpression of *mKO::sn*, *mKOsnS52A* and *mKO::snS52D* straightens the terminal branchlets significantly compared to *mKO* only. See also Fig. 3.15.

3.6 The transcription factor Cut is acting through Singed in spiked protrusion formation

The transcription factor Cut has been described to be part of the transcriptional code that defines class III versus class IV morphology. In class III neurons Cut is expressed at very high levels and loss of *cut* leads to the complete loss of spikes and to defects in dendrite complexity. Overexpression of Cut in class I neurons, which is usually not expressed in this class of neurons, leads to an increased dendrite complexity and the formation of short terminal protrusions that are devoid of the microtubule binding protein Futsch (Grueber, Jan et al. 2003; Jinushi-Nakao, Arvind et al. 2007). Cut is also expressed in class IV neurons, however, at lower levels. Overexpression of Cut in these neurons also results in a partial shift to class III morphology, with numerous short terminal branchlets, but in contrast to class I neurons, not to an increase in dendritic complexity (Grueber, Jan et al. 2003).

Here, I could show that *singed* is required for the formation of class III spiked protrusions and that is sufficient to induce short terminal branchlets in class IV neurons. These Singed-induced effects are similar to the morphological changes induced by *cut*. Therefore, I tested if Singed might be an effector of Cut, using the simple class I neurons, that usually do not express Cut as a model system. First, I investigated if *singed* itself has an effect on the branching pattern of class I neurons. Using *sn^{36a}* mutant class I neurons, I could show that the gross morphology of the dendritic tree was not affected (Fig. 3.18 A, B). However, there was a slight increase in the number of termini compared to the control (control: 23 ± 4 ; *sn^{36a}*: 28 ± 4 ; $p < 0.05$), suggesting that Singed might be required to suppress branching in class I neurons. Overexpression of Cut in otherwise wild type class I neurons resulted, as shown before, in the formation of lots of short terminal branchlets (134 ± 30 ; Fig. 3.18 C, C', E). Using the same approach in the *sn^{36a}* mutant background, the number of ectopic short terminal branchlets was clearly reduced by more than 40% (79 ± 20 ; $p < 0.01$; Fig. 3.18 D, D', E). As reported before, overexpression of Cut also lead to a massive increase in the total branch length of the class I dendrites. But, in contrast to the formation of short terminal branchlets, this effect was not suppressed in the *sn^{36a}* mutant (Fig. 3.18 F).

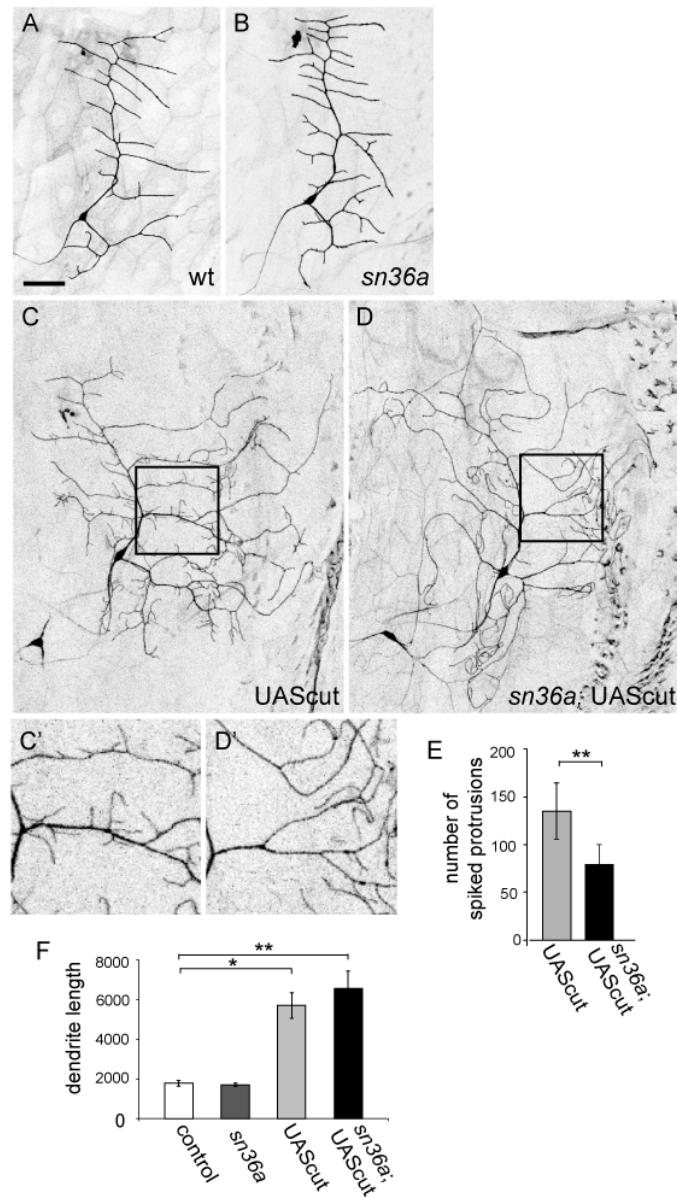


Figure 3.18: Singed is essential for the formation of Cut-induced spiked protrusions

(A-D) Class I vpd neurons expressing *mCD8GFP* under the control of *2-21Gal4*. (A) Wild type and (B) *sn^{36a}* mutant class I neurons. Loss of *singed* does not visibly affect the morphology of the class I neurons. (C-D) Overexpression of the transcription factor Cut in the wild type or in the *sn^{36a}* mutant background. Scale bar: 50 μ m. (C'-D') blow up of the indicated regions from (C-D). (E) The number of ectopically formed short terminal branchlets upon Cut overexpression in class I neurons is significantly reduced in the *sn^{36a}* mutant background. (F) There is a significant increase in dendrite length upon Cut overexpression, very prominent also in the *sn^{36a}* mutant background.

Overexpression of Cut in class I neurons induces formation of short, terminal branchlets devoid of microtubules (Jinushi-Nakao, Arvind et al. 2007). However, these short terminal branchlets seem not to be as straight as class III spiked protrusions (Fig. 3.18 C'). I therefore wanted to examine if Singed can be detected at the ectopically formed termini, as it is the case in the spiked protrusions of class III neurons. By antibody staining I found some ectopically formed spiked protrusions containing Singed (Fig. 3.19). This was in clear contrast to control class I neurons, where endogenous Singed or fluorescently tagged Singed constructs never localized to terminal branchlets (Fig. 3.2 J-L and Fig. 3.4 G-I).

These experiments show that Singed is a special effector of Cut in the formation of spiked protrusions, however, not in the promotion of dendritic complexity.

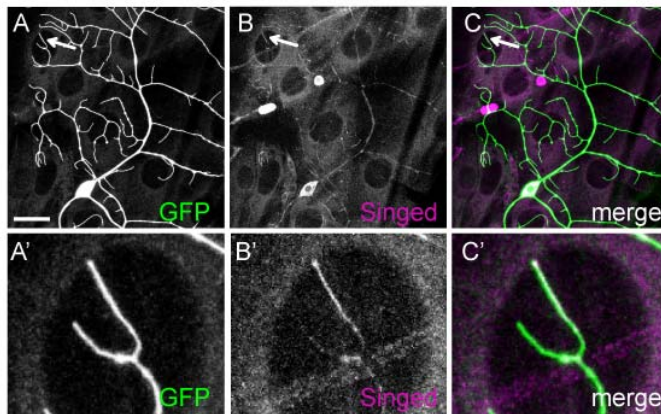


Figure 3.19: Singed localizes to ectopic spiked protrusions induced by Cut

(A-C) Cut overexpressing class I vpda neurons show localization of endogenous Singed at several ectopically formed terminal branchlets. Scale bar: 25 μ m. (A'-C') Blow up regions marked with arrows in (A-C).

4 Discussion

4.1 Summary of the results

In this work, I have investigated how the specific morphologies of dendrites of distinct neuronal classes are formed. Using the md-da neurons of the *Drosophila* PNS as a model system I showed that the actin bundling molecule fascin, called Singed in *Drosophila*, is an important determinant of class III neuron dendrite morphology. Singed is necessary for the formation of the class III terminal branchlets, the spiked protrusions, and acts as an effector of the transcription factor Cut. In addition, loss of *singed* induces a partial transformation of class III neurons towards class IV neuron morphology and Singed overexpression in class IV neurons results in the formation of class III-typical spiked protrusions, indicating that *singed* is part of the distinction between these two neuronal types.

I questioned whether the mechanisms that underlie the formation of different dendrite branch types are similar and rely on the same molecular factors. My loss- and gain-of-function experiments indicate that the precise molecular composition of the terminal branchlets can strongly influence their morphology. In fact, Singed strongly contributes to the morphology of a specific neuronal type and helps defining the distinction between two classes of neurons. Similar effects have been previously mainly ascribed to transcription factors.

4.2 The role of Singed in class III neurons

4.2.1 Singed is required for the bundling of actin-filaments in class III neurons

Loss of *singed* drastically affected the morphology of class III neurons, most strikingly, the density of the spiked protrusions was reduced. This phenotype could be due to a defect in spiked protrusion formation or also maintenance. In both cases, loss of *singed* would result in a decreased number and density of spiked protrusions at later developmental stages. In several cell culture systems, depletion of fascin results in a decreased number of filopodia. EM studies could show that the actin filaments of these cells were only loosely bundled and laying wavy along the cell edge, suggesting that they failed to bulge out the membrane to give rise to a mature filopodium. Also in *singed* mutant class III neurons, reduced actin bundling during spiked protrusion formation is likely the cause of the reduced spiked protrusion density. Indeed, time-lapse experiments done by Yun Zhang (PhD student in the lab of Gaia Tavosanis, MPI of Neurobiology) showed that the formation of new spiked protrusions was drastically reduced in the *singed* mutant class III neurons (data not shown).

In addition to the decreased spiked protrusion density, the remaining spiked protrusions of *singed* mutant larvae were longer and more bended instead of being short and straight like in the wild type. Similarly, the straight bristles of *Drosophila*, become curved and gnarled upon loss of *singed*, a phenotype that was linked to reduced bundling of actin filaments during bristle development (Cant, Knowles et al. 1994). Also *singed* mutant mushroom body neurons in culture form abnormal curls and hooks if they are mutant for *singed*. These morphological changes are again accompanied with altered F-actin distribution (Kraft, Escobar et al. 2006). Therefore, the increased curvature of *singed* mutant spiked protrusions is also likely a direct result of reduced actin bundling. Still, the question remains why the spiked protrusions grow out longer in the *singed* mutant. Typically, class III neurons have the actin enriched spiked protrusions that are devoid of microtubules. One could imagine, that the tight actin-bundling through Singed prevents microtubule invasion into the spiked protrusions, what could possibly allow for

increased elongation of the branchlets. However, microtubule invasion seems not to be the reason for the elongated spiked protrusions in the *singed* mutant, because they still do not contain microtubules. A reasonable theory explaining the increased length of the *singed* mutant spiked protrusions could be found in their dynamic behavior. Singed is highly enriched on the elongating spiked protrusions and less abundant on the retracting ones (Fig. 3.13). It might be that the actin filaments bundled by Singed in the spiked protrusions are only able to reach a certain length before Singed comes off and allows for retraction. Without Singed the remaining spiked protrusions might be controlled molecularly in a different way, allowing for prolonged elongation.

4.2.2 Singed does not influence the overall dendrite extension

Interestingly, all morphological transitions observed upon loss of *singed* did not result in changes of the overall length of the dendritic branches. The reduction in spiked protrusion density combined with an increased length of the remaining ones and a higher number of terminal branchlets without spiked protrusion character equal out to the overall dendrite length of wild type neurons (Fig. 3.9). These results suggest an internal control mechanism independent of *singed* that regulates the overall dendrite length in class III neurons. To reach the final and predetermined total dendrite length, a defect in spiked protrusion formation was effectively rescued by the elongation of the existing dendritic branches. Similarly, in class IV neuron *slit* and *robo* mutants a reduction in the dendritic branching level was shown to be accompanied by an increased branch elongation rate, also suggesting a homeostatic regulation to reach the desired total dendrite length (Dimitrova, Reissaus et al. 2008). One possible candidate for regulating the overall length of the dendritic tree in class III neurons is the transcription factor Cut. In addition to the loss of spiked protrusions, *cut* mutant class III neurons show severe defects in the general outgrowth and elongation of dendritic branches. Moreover ectopic overexpression of *cut* in class I neurons leads to a huge increase in dendrite length which is not affected by *singed* (Grueber, Jan et al. 2003)(Fig. 3.18 F).

4.2.3 Dynamic Singed accumulation on dynamic spiked protrusions

Previous studies showed that the md-da neurons of the *Drosophila* PNS have very dynamic terminal branchlets in the second instar larvae (Andersen, Li et al. 2005; Dimitrova, Reissaus et al. 2008). Especially the class III spiked protrusions were reported to be constantly formed and retracted. It seems that for the dynamic outgrowth of the spiked protrusions, for their formation and elongation, actin bundling through Singed is required to generate a force to protrude the membrane. Loss of this tight bundling could instead allow for the retraction of the spiked protrusions.

During the formation of spiked protrusions also dynamic changes in the actin-cytoskeleton were observed. Patches of F-actin accumulation predicted the sites of new spiked protrusion formation (Andersen, Li et al. 2005). However, I never observed Singed accumulation before a new spiked protrusion was formed. One could imagine that this very initial step of spiked protrusion formation is independent of Singed and can be therefore not detected at this stage. But possibly, there is still Singed accumulation, though at too low levels to be detected. Specifically the “convergent elongation model” for the formation of filopodia is suggesting that bundling through Fascin of the constantly elongated actin filaments in the cell cortex leads to the protrusive force for to push the membrane outwards (Vignjevic, Kojima et al. 2006). Since upon loss of *singed* the formation of spiked protrusions is impaired, it is very likely that Singed is required for the initial bundling of actin filaments, probably at low levels which could not be detected at this stage with the implemented imaging technique.

4.3 Molecular regulation of Singed

4.3.1 Regulation through phosphorylation of the conserved Serine52

Fascin activity can be regulated by phosphorylation at Ser39, which leads to a lower binding affinity of fascin-1 to actin in vitro and to reduced formation of fascin protrusions in matrix-adherent cells (Yamakita, Ono et al. 1996; Ono, Yamakita et al. 1997; Adams, Clelland et al. 1999). Expression of a fascin Ser39 phosphomimetic mutant in B16F1 cells yielded reduced formation of filopodia. Moreover, in N2a cells the association of fascin specifically to filopodial actin bundles was promoted by dephosphorylation (Vignjevic, Kojima et al. 2006; Aratyn, Schaus et al. 2007). Although phosphorylation of the conserved Serine seems to play an important role in cell culture systems, the regulation of fascin activity seems to be more complex in vivo. In *Drosophila* it was shown that regulation through phosphorylation of Serine 52 is not required for blood migration or oogenesis, but for the bristle formation. The authors of this study argue, that regulation through phosphorylation is mainly required for a long and stable association of actin with fascin (Zanet, Stramer et al. 2009).

Also in the md-da neurons phosphorylation of Serine 52 does not represent the main regulatory switch for Singed function. In class III and also class IV neurons both phosphovariants can fulfil nearly the same functions as the wild type protein. However, the minor differences between the constructs show that regulation through phosphorylation takes part in the formation of spiked protrusions. Possibly, the partial effect of Serine 52 phosphorylation reflects the dynamics of class III neuron branchlets that perhaps do not need prolonged association of fascin with actin bundles (Vignjevic, Kojima et al. 2006).

4.3.2 Regulation by small GTPases

Other candidates for Singed regulation are the small GTPases. In cell culture systems the formation of fascin-containing microspikes was shown to be dependent on Rac1 and Cdc42. Moreover, overexpression of Rac1 in the md-da neurons results in the formation of numerous short filopodia that reminded of class

III spiked protrusions in all classes (Andersen, Li et al. 2005). To test if the Rac1 induced filopodia are dependent on *singed*, our collaborators Caroline Delandre and Adrian Moore (RIKEN Brain Science Institute, Japan) compared Rac1 overexpression in the wild type and *singed* mutant background of class III neurons. Strikingly, they did not observe any difference in filopodia formation between mutant and wild type background, showing that Rac1 can induce filopodia without Singed. Of course, this data does not rule out that in the wild type class III neurons, spiked protrusion formation is Rac1 independent. To investigate this further, *rac1* loss of function analysis is needed. *rac1* mutant class IV neurons were shown to have reduced branching, but so far no data for class III neurons is available that could support the Rac1 overexpression data, which is suggesting that Rac1 is also required for spiked protrusion formation (Lee, Li et al. 2003). To test for a genetic interaction between *rac1* and *singed*, one could investigate if the loss of function phenotype of *rac1* or *singed* is successfully rescued by overexpression of the other protein. In further studies also Cdc42 should be investigated for its role in class III spiked protrusion formation.

4.4 Singed and the transcription factor Cut

4.4.1 Cut is acting through Singed in the formation of spiked protrusions

The transcription factor Cut is an important part of the transcriptional codex defining the class specific dendritic morphology of the md-da neurons. Particular high levels of Cut can be detected in the class III neurons and loss of *cut* leads to the complete loss of the spiked protrusions and to a defect in dendrite outgrowth in this class of neurons (Grueber, Jan et al. 2003).

Implementing the Cut-negative class I neurons as a model system, I could clearly show that the ectopic formation of spiked protrusions induced by Cut expression is dependent on Singed (Fig. 3.18). However, to reveal that Singed is a downstream effector of Cut in the formation of class III spiked protrusions, it would necessary to show that overexpression of Singed can rescue the class III *cut* mutant phenotype. Though, this experiment might be challenging because *cut* mutant class III neurons have in addition to the loss of spiked protrusions severe defects in general dendrite outgrowth (Grueber, Jan et al. 2003). It might well be that in the absence of the transcription factor Cut, more of the environment than only Singed or its activation is missing that is required for the formation of spiked protrusions. In the simplest scenario, the lack of properly formed main branches would also impede the formation of spiked protrusions. If so, *cut* loss of function could be not rescued by Singed overexpression, even though it was a real downstream effector of *cut* in class III neurons. Interestingly, even strong overexpression of Singed in class I neurons that do not express Cut is not able to induce the formation of spiked protrusions (data not shown). In class IV neurons in contrast, *cut* is expressed at intermediate levels and high levels of Singed can lead to the formation of spiked protrusions, suggesting that Singed needs Cut expression to form the spiked protrusions (Fig. 3.15).

Taken together, it is well possible that Cut even though it acts through Singed in the formation of spiked protrusions, additionally generates an environment that allows Singed to act in this pathway by switching on or off other essential factors. One possibility to solve this problem experimentally would be instead of using a

cut loss of function mutant, implementing *cut* RNAi to reduce Cut levels and try to rescue a possibly intermediate phenotype with Singed overexpression.

4.4.2 Possible regulation of Singed by Cut

As discussed in the last section, the transcription factor *cut* is acting through Singed in the formation of short, actin-rich dendritic protrusions. However, the question remains if *singed* is also directly regulated by *cut*. Cut belongs to the CDP/Cut/Cux protein family of homeodomain transcription factors. Different members of the family were reported to be able to repress and most probably also activate the expression of target genes. DNA binding of these molecules can occur through different domains, three Cut repeats and one Cut-type homeodomain that can either act independently or cooperative (reviewed in (Nepveu 2001). Interestingly, a consensus sequence that can be bound by Cut repeats is also present in the first large intron of the *singed* gene locus. Therefore, it might be possible that *singed* is directly upregulated by *cut*. High levels of Cut in class III neurons could lead to high levels of Singed in class III neurons and finally to the formation of spiked protrusions. Arguing against this hypothesis, is the fact that Singed is expressed in all cell bodies of the md-da neurons at similar levels, independent of *cut* expression levels (Grueber, Jan et al. 2003)(Fig. 3.1). Nevertheless, the information obtained by immunohistochemistry might not be solid enough to rule out the possibility of a direct upregulation of Singed through Cut. An easy possibility to test this hypothesis is the analysis of the correlation of Singed protein levels with ectopic overexpression of Cut. However, overexpression of Cut with a panneural driver line and subsequent western blot analysis of single larval lysates did not show any alteration of the Singed protein levels, as shown by Anastasia Tartanikova (PhD student in the lab of Gaia Tavosanis, MPI of Neurobiology). A drawback of this approach is that Cut might not regulate Singed expression in all neuronal cells, but rather only affects Singed levels in the md-da neurons. Upregulation of Singed, just in this small subset of cells, would be masked by the general expression of Singed in the larva. For a final conclusion if Singed levels are regulated by Cut, investigation of only the md-da neurons would

be necessary. With md-da neuron specific driver lines it is possible to FACS sort GFP positive cells from homogenized embryos and therefore enrich neuronal cells of the PNS (Jinushi-Nakao, Arvind et al. 2007). Subsequent western blot analysis of wild type and Cut overexpressing sorted cells could possibly help to detect changes in the levels of Singed in the md-da neurons.

4.5 What is the difference in class IV neurons?

4.5.1 Distinct and similar properties of class III and class IV dendrites

Class III and class IV neurons exhibit the most complex dendritic trees among the md-da neurons. Nevertheless their branching patterns are quite distinct, including the dendritic field size, branching order and number of dendritic termini (Grueber, Jan et al. 2002). Moreover the terminal branchlets of these two classes show very distinctive characteristics. Class IV terminal branchlets are longer and more bended than class III terminal branchlets (Fig. 3.7). Also during development the dynamic behavior of these distinct types of terminal branchlets is qualitatively different. Yun Zhang did detailed analysis of class IV terminal branchlet dynamics and most strikingly they seem to probe the environment to grow out suddenly into their preferred direction. This is in clear contrast to class III terminal branchlets that constantly grow and retract on a linear slope.

Still, class III and class IV neurons also share similar properties. Both neuronal classes have terminal branchlets that are enriched in actin and both of them express the transcription factor cut, though at different levels (Grueber, Jan et al. 2003)(Fig. 3.5). Most strikingly, they both express Singed, which can be detected at the cell bodies at comparable levels (Fig. 3.1). However, only class III neurons and not class IV neurons need Singed for the formation of their terminal branchlets (Fig. 3.14). Singed is only localized to class III terminal branchlets, but upon strong Singed overexpression in class IV neurons it can be also detected at class IV terminal branchlets, which are at the same time transformed to a class III spiked protrusion morphology, showing that in principle Singed can fulfill similar functions in class IV as in class III neurons (Fig. 3.15).

4.5.2 Singed in class IV neurons

As discussed above, class IV neurons express Singed, but do not need it for the elaboration of their specific dendritic branching pattern. However, strong overexpression of Singed can induce spiked protrusions also in class IV neurons. Likely, in wild type class IV neurons Singed is not activated or localized properly

to induce spiked protrusions. My experiments showed that this activation does not depend on the phosphorylation state of the conserved Serine 52, because phosphomimetic and non-phosphorylatable versions of Singed both can induce the formation of spiked protrusions upon strong overexpression just as wild type Singed.

A promising candidate, that could be responsible for the specific localization of Singed to class III spiked protrusions, is Rab35. It has been shown that Rab35 can recruit fascin and that fascin acts as an effector of Rab35 in filopodia induction. Interestingly, a dominant negative version of Rab35 affects *Drosophila* bristle morphology and results into loosely bundled actin filaments during bristle development just as in mutants of *singed* (Cant, Knowles et al. 1994; Zhang, Fonovic et al. 2009). It would be interesting to test if Rab35 is also involved in class III spiked protrusion formation.

4.5.3 Possible mechanisms for terminal branchlet formation in class IV neurons

In class IV neuron dendritic development, growth cone splitting as well as interstitial branching can be observed (Sugimura, Yamamoto et al. 2003; Dimitrova, Reissaus et al. 2008). Both are processes, which are thought to require filopodia formation. Interestingly, the major actin crosslinking protein of filopodia, fascin/Singed is not required class IV dendritic branching. Still, class IV neurons have actin-enriched, dynamic terminal branches, suggesting that other actin bundling molecules might play a role in their terminal branchlet formation.

In *Drosophila*, there are numerous actin-bundling or crosslinking proteins including espin/Forked, filamin/Cheerio, fimbrin, α actinin and of course fascin/Singed. In bristle formation, oogenesis and spermatid individualization, it has been shown that several, and not only one, actin-bundling molecules are involved (Tilney, Connelly et al. 2000; Hudson and Cooley 2002; Noguchi, Lenartowska et al. 2008). For example, *forked* mutant flies have also defects in the tight actin-bundling required for bristle formation and oogenesis. In bristle formation, *forked* is required to form the initial actin-bundles that are later on

bundled by Singed (Tilney, Connelly et al. 2000). Different dendritic morphologies might be also established by diverse actin regulating molecules. Therefore, investigation of actin-bundling molecules other than Singed would give important information about how the actin-enriched terminal branchlets of class IV neurons are formed.

4.6 Singed as a molecular switch between class III and class IV dendritic branching pattern

4.6.1 Singed defines class III characteristic morphology

One distinctive characteristic of class III and class IV neurons is the morphology of their terminal branchlets. Class III typical spiked protrusions are short and straight, whereas class IV terminal branchlets are longer and more bended (Fig. 3.7). Interestingly, the morphological changes in class III neurons, observed by *singed* loss of function, gave rise to a dendritic branching pattern that was shifted to the morphology of a class IV dendritic tree: the class III typical spiked protrusions were dramatically reduced and the remaining ones were longer and showed a higher curvature (Fig. 3.8 and 3.9). Moreover, the main branching pattern of the *singed* mutant class III neurons got more complex, representing another morphological trait resembling class IV neurons (Fig. 3.10). By gain of function analysis I could show that Singed can also induce class III characteristics in class IV neurons: high levels of Singed lead to terminal branchlets that resemble spiked protrusions in that they are short, straight and localize Singed (Fig. 3.15).

Singed seems to act as a molecular switch defining part of the morphological distinction of class III and class IV neurons, especially the terminal branchlets of these neurons. So far, the feature as a molecular switch between class specific morphologies was only assigned to transcription factors, the more surprising it is that a regulator of the actin cytoskeleton can fulfill this function.

4.6.2 Singed does not facilitate a complete transformation between the two classes

Singed acts as a molecular switch between class III and class IV dendritic morphology. However, it is not able to fulfill a complete transformation between the two classes. There are still differences in the terminal branchlets formed upon loss of *singed* in the class III neurons compared to class IV neurons. First, the values describing the curvature of the branchlets lie in between the ones obtained from control class III and class IV neurons. Moreover, *singed* mutant spiked

protrusions grow out longer, but they do not reach the diversity of different lengths observed in class IV neurons. Therefore, class III *singed* mutant spiked protrusions are only shifted to a class IV typical morphology. Second, even though *singed* spiked protrusions resemble morphologically class IV terminal branchlets, they show in contrast to class IV terminals drastically reduced dynamics. It seems that an additional factor is missing that could provide complete transformation from class III to class IV terminal branchlets. A possible candidate for this missing factor is the transcription factor Knot, which is part of the transcriptional code that defines class IV morphology. Interestingly, overexpression of Knot in class III neurons results in increased dendrite length and a reduction of the number of spiked protrusions (Jinushi-Nakao, Arvind et al. 2007). It would be interesting to investigate the class III terminal branchlets in the *singed* mutant while overexpressing Knot, to see if a complete transformation to class IV terminal branchlets could be achieved.

Also overexpression of Singed in class IV neurons only partially converts terminal branchlets to spiked protrusion morphology. Just a fraction of the terminal branchlets become short and straight upon Singed overexpression. Lots of terminal branchlets still resemble the ones of wildtype class IV neurons. Consequently, also the curvature values of the terminal branchlets are lying in between the ones of class III and class IV neurons. Time-lapse analysis of the morphologically transformed class IV branchlets could show if the morphologically transformed terminal branchlets are also acting in a class III typical manner, namely a rapid extension and retraction on a linear slope.

Again, one could imagine that additional factors are missing, allowing for a complete transformation. The transcription factor *cut* is responsible for the formation of spiked protrusions in class III neurons. It is also expressed in class IV neurons, but at lower levels. Strikingly, overexpression of *cut* in class IV neurons also leads to a morphological shift resembling class III neurons (Grueber, Jan et al. 2003). Maybe a complete transformation could be achieved if Cut and Singed are both co-overexpressed.

4.7 Specific versus general mechanisms in dendritic branch formation

Dendrites show a huge variety of different morphologies, they can be simple mono-ciliated processes like dendrites of type I *Drosophila* PNS neurons, or very complex and repeatedly branched like pyramidal neurons and *Drosophila* class IV neurons. Studies of the *Drosophila* md-da neurons showed that specific dendritic morphologies can be determined by different combinations of transcription factors, suggesting that certain types of branches could be also made by distinct molecular mechanisms (reviewed in (Jan and Jan 2010)). However, from the analysis of different cytoskeletal regulating molecules in this system, it seems that most regulators of the cytoskeleton fulfill similar functions in all classes of neurons. Most probably, the elaboration of distinct dendritic morphologies is based on general mechanisms of branching or extension of branches, combined with cell specific activities. For example, mutants of *ena*, which allows prolonged elongation of actin-bundles in filopodia formation, show reduced dendritic branching in all classes of md-da neurons (Li, Li et al. 2005). Also *tropomyosin* seems to have a conserved function in the morphologically very distinct class I and class IV neurons. Mutants of *tropomyosin* fail to restrict the dendritic field size in these two classes (Li and Gao 2003). Cytoskeletal molecules that regulate dendritic branching only in specific classes are largely unknown. However, I could show that mutations of *singed* are specifically affecting the class III spiked protrusions and not the branching pattern of other classes.

Future studies in the *Drosophila* md-da neurons could provide more information about general and specific mechanisms in dendritic branch formation. One promising way could be the analysis of targets of the transcription factors defining the class specific branching patterns. Another possibility would be to screen for regulators of the cytoskeleton to find molecules that can that either affect all classes in the same way, or only distinct neuronal types.

4.8 A model for Singed function in dendrite formation

Here, I have characterized for the first time the role of fascin/Singed in dendrite development. My data show that Singed is implementing part of the distinction between class III and class IV dendritic morphology. So far, class specific dendritic branching patterns were only linked to transcription factors, not to effector molecules acting directly on the cytoskeleton. Indeed, Singed is acting downstream to the previously described transcription factor Cut.

Singed is localized to the class III spiked protrusions and required for their formation and typical morphology. Upon loss of *singed*, less spiked protrusions are formed and the remaining ones grow out longer and become more bended. Moreover, the intrinsic dynamic behavior of the spiked protrusions is lost. In class IV neurons, instead, *singed* is not required for the dendritic branching pattern. Interestingly, strong overexpression of Singed leads to the transformation of the long and bended terminal branchlets to a shorter and straight appearance, similar to the one of class III spiked protrusions (Fig. 4.1). Nevertheless, the mechanisms why Singed is not localized or activated in wild type class IV neurons remain to be elucidated.

Regarding the wide expression of fascin in neural tissue of several species, it is likely that fascin is also responsible for dendritic morphologies, other than *Drosophila* md-da class III neurons. Further studies on fascin in dendrite development could help to understand the general and specific mechanisms underlying the formation of dendritic branches.

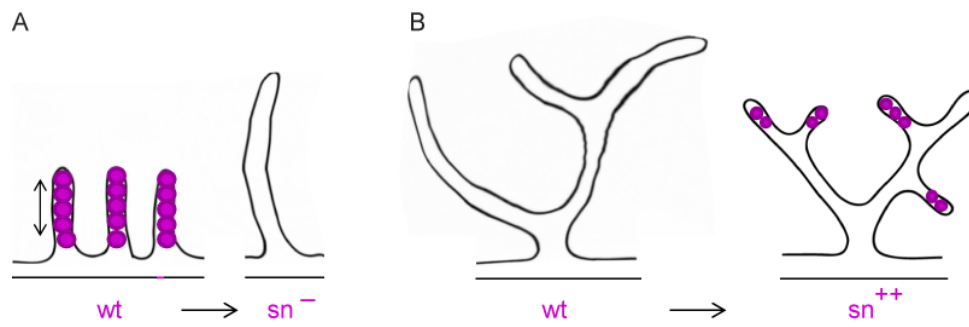


Figure 4.1: Model for Singed in dendrite formation

(A) In class III wild type neurons, Singed is localized to the short and straight spiky protrusions. Upon loss of *singed*, the spiky protrusions grow out longer and become more bent. On top, they lose their dynamics. (B) In class IV wild type neurons, Singed is not localized to terminal branchlets. Upon Singed overexpression, class IV terminal branchlets become short, straight and do localize Singed.

5 Materials and Methods

5.1 Materials

5.1.1 Chemicals

Table 5.1: Chemicals used in this study

Chemical	Supplier
Acetic Acid	MERCK
Agarose, high electroendosmosis	Biomol
Ampicillin	Roche
dNTP set	Roche
EDTA	GIBCO
Ethanol	Riedel - de Haën
Ethidium Bromide	Roth
Fetal Calf Serum (FCS)	Perbio
Formaldehyde (Methanol free) 10%	Polysciences
Glycerine	MERCK
Glycerine for fluorescence microscopy	VWR international
Halocarbon oil Volatof S3	Lehmann & Voss & Co
Hydrochloric acid (HCL, 1M)	VWR international
p Hydroxybenzoic acid	Sigma
Methanol	VWR international
Methyl paraben	Sigma
Phosphoric acid	VWR international
Potassium dihydrogen phosphate	MERCK
Potassium chloride (KCl)	MERCK
Propionic acid	VWR international
Sodium dihydrogen phosphate	MERCK
Sodium chloride (NaCl)	MERCK
Tris	BioRad
Triton-X100	Roth

5.1.2 Buffers and Solutions

Blocking Solution

5% FCS was diluted in 0.3% PBT.

Fly water

8 ml propionic acid was filled up to 1L with H₂O.

Formaldehyde (FA) 4% for fixation

For 50 ml final solution 20 ml 10% FA were mixed with 25 ml distilled water and 5 ml 10xPBS.

Phosphate buffered saline (PBS)

NaCl (137 mM)

KCl (2.7 mM)

Na₂HPO₄ (8 mM)

KH₂PO₄ (1.5 mM)

For 1L 8g NaCl, 0.2g KCl, 1.15g Na₂HPO₄ and 0.24g KH₂PO₄ were dissolved in 800 ml distilled water. The pH was adjusted with HCl to 7.4 and the volume with distilled water to 1L. The final solution was sterilized by autoclaving and stored at room temperature. For 10xPBS 10-fold amounts of salts were solved in 1L distilled H₂O.

Squishing Buffer

Tris-Cl, pH 8.2 (10 mM)

EDTA (1 mM)

NaCl (25 mM)

Poteinase K was freshly added to a final concentration of 200 µg/ml.

PBT (0.3%)

0.3% Triton-X100 was dissolved in PBS.

TAE (50x)

Tris base 242g

Glacial acetic acid 57.1 ml

EDTA (0.5 M, pH 8.0) 100 ml

All ingredients were dissolved in distilled H₂O to obtain a final volume of 1L. For 1xTAE 20 ml of 50xTAE were mixed with 980 ml distilled H₂O.

5.1.3 Media

Table 5.2: Media

Medium	Supplier
Instant blue Drosophila medium	Fisher Scientific
Instant dry yeast	Fermipan Inc.

Apple agar plates

To prepare apple agar 40 g agarose were slowly added to a boiling mixture of 500 ml commercially available apple juice and 480 ml of distilled water. After cooling down to 60°, 10.5 ml of 95% ethanol and 10 ml of 100% acetic acid were added. The pH was adjusted to 4.2 and the apple agar was poured into plates.

Fly Food

To obtain a final volume of 50 L, 585 g agar (Probio GmbH) were dissolved in 30 L of 93°C hot water. Meanwhile, 5 kg maize flour (Prima Vera), 925 g yeast (Probio GmbH) and 500 g soy flour (Hofbräuhaus-Kunstmühle GmbH & Co. KG) were mixed with cold water to obtain a homogeneous broth. 2 kg sugar beet molasses (Grafschafter Krautfabrik) and 2 kg Diamalt (BIB Bake Mark Deutschland GmbH) were mixed in warm water. Finally, the yeast-flour broth and the molasses-Diamalt solution were mixed.

As soon as the agar was dissolved, temperature was reduced to 90 °C and all prepared ingredients were added. The volume was adjusted to 50 L with water, and the solution was cooked for 2 h under constant mixing.

When the temperature cooled down to 50 °C, 125 g Methyl paraben solved in 11 ml 20% Ethanol and 500 ml 10% Phosphoric acid were added.

LB (Luria-Bertani) medium and plates

1% (w/v) Bacto-Trypton

0.5% (w/v) Yeast extract

0.5% (w/v) NaCl

Distilled H₂O was added to obtain the final volume. If necessary the pH was adjusted to 7.5. Finally, the solution was sterilized by autoclaving and stored at room temperature. LB plates were supplemented with 1.5% Bacto-Agar before autoclaving. To allow for selection of Ampicillin resistant bacteria Ampicillin was added to LB media and plates in a 1:1000 dilution of a 100 mg/ml stock solution.

Yeast

Instant dry yeast was mixed with Instant blue Drosophila medium and fly water to obtain a paste of the consistency of peanut butter.

5.1.4 Enzymes and DNA standards

Table 5.3: Enzymes and DNA standards

Enzyme/Standard	Supplier
Pfu DNA Polymerase	Promega
Proteinase K	Sigma
Restriction Endonucleases	NEB
T4 DNA Ligase	Roche
Taq Polymerase	NEB
1 kb ladder	NEB
100 bp ladder	NEB

5.1.5 Plasmids and DNA library

Table 5.4: Plasmids and DNA library

Vector/Library	Supplier/Donor
Drosophila cDNA clone LD16477	BioCat
pP{UAST}	Juh Nung Jan
pP{UAST} attB	Johannes Bischof
pRmHa3-GFP-actin	Hiroki Oda
pmKO1-MN1	MBL

5.1.6 Primer

Table 5.5: Primer

primer	sequence 5' – 3'	use
GT684	ATAAGAATGCGGCCGCGGAAACGGC CAGGGCTGCGAGC	singed for N-terminal KO tag (forward)
GT685	GCTCTAGATTAGAACTCCCACTGTGT GGCC	singed for N-terminal KO tag (reverse)
GT681	CGGAATTCGACCATGGTGAGTGTGAT TAAACCAGAGATG	KO N-terminal tag (forward)
GT682	ATAGTTTACGCGGCCCGGAATGAGC TACTGCATCTTCTACC	KO N-terminal tag (reverse)
GT765	ACCTTTCATCCTACATAAATAGAC	FRT19A (forward)
GT766	ACATTATGAAGAGCAGCATATTAC	FRT19A (reverse)
GT827	GCTCAACGCCAATGGCGCCGCCCTGA AGAAGAAGCAACTGTGG	Site directed mutagenesis Ser52 → Ala (forward)
GT828	CCACAGTTGCTTCTTCTTCAGGGCGG CGCCATTGGCGTTGAGC	Site directed mutagenesis Ser52 → Ala (reverse)
GT829	GCTCAACGCCAATGGCGCCGACCTGA AGAAGAAGCAACTGTGG	Site directed mutagenesis Ser52 → Asp (forward)
GT830	CCACAGTTGCTTCTTCTTCAGGTCGGC GCCATTGGCGTTGAGC	Site directed mutagenesis Ser52 → Asp (reverse)

All primers were synthesized by Eurofins MWG Operon. The primers GT827-
GT830 were additionally HPLC (high performance liquid chromatography)
purified.

5.1.7 Antibodies

Table 5.6: Antibodies

Antibody	Supplier
mouse anti-Singed 7C	DSHB
mouse anti-22C10	DSHB
donkey anti-mouse-Cy3	Jackson Laboratories
donkey anti-rabbit-Cy2	Jackson Laboratories
rabbit anti-GFP	Living Colors

5.1.8 Commercial kits

Table 5.7: Commercial kits

Commercial Kits	Supplier
QIAquick Gel Extraction Kit	Qiagen
QIAprep Spin Miniprep Kit	Qiagen
QIAGEN Plasmid Midi Kit	Qiagen
Quick Change II XL Site directed mutagenesis Kit	Stratagene

5.1.9 Equipment

Table 5.8: Microscope systems

Microscope	Supplier
Coolsnap HQ2 camera	Photometrics
CSU Real-Time Confocal System	Visitron
Leica MZ16 Fluorescent Dissectoscope	Leica GmbH
Leica SP2 Confocal Microscope	Leica GmbH
Schott KL 1500 LCD Light Source	Schott
Zeiss Observer 1 Microscope	Zeiss GmbH
Zeiss Stemi 2000-C Dissectoscope	Zeiss GmbH

Table 5.9: Consumables

Consumables	Supplier
Electrocompetent cells TOP10	Invitrogen
Electroporation cell	BioRad
Doppelband Fotostrip (double sided tape)	Tesa AG
Foreceps DuMont Nr. 5	FST
Immersion oil	Leica GmbH
Insect pins	FST
Microscope cover glasses 24 mm x 40 mm	Menzel Gläser
Microscope sildes 76 mm x 26 mm	Menzel Gläser
Sylgard 184 Silicone Elastomere	SASCO GmbH
Small petri dishes	Mat Tek Corporation
Vectashield mounting medium	Vector Laboratories

5.2 Drosophila stocks

5.2.1 Fly stocks

Table 5.10: Fly stocks

Stock	Donor/Source
<i>2-21Gal4</i> (Ye, Petritsch et al. 2004)	Juh Nung Jan
<i>80G2</i> (Gao, Brenman et al. 1999)	Juh Nung Jan
<i>c161Gal4</i> (Shepherd and Smith 1996)	Wesley Grueber
<i>477Gal4</i> (Grueber, Jan et al. 2003)	Bloomington Stock Center
<i>109(2)80Gal4</i> (Gao, Brenman et al. 1999)	Juh Nung Jan
OregonR	Bloomington Stock Center
<i>actinGal4</i>	Bloomington Stock Center
<i>UASmCD8::cherry</i>	Takashi Suzuki
<i>UAScut^{EHK}</i> (Grueber, Jan et al. 2003)	Adrian Moore
<i>FRT19A</i>	Bloomington Stock Center
<i>tubGal80 hsFLP FRT19A; 109(2)80Gal4 UASmCD8GFP</i>	Wesley Grueber
<i>UAS-Act5C.T::GFP</i>	Bloomington Stock Center
<i>UAS-GFP S65C tub84B</i> (Grieder, de Cuevas et al. 2000)	Nicole Gieser
<i>w¹¹¹⁸</i>	Bloomington Stock Center
<i>sn³</i> (Paterson and O'Hare 1991)	Bloomington Stock Center
<i>sn³⁶</i> (Paterson and O'Hare 1991)	Bloomington Stock Center
<i>UASmCD8::GFP</i>	Bloomington Stock Center

5.2.2 Genotypes analysed

Table 5.11: Genotypes analyzed in this study

Genotype
80G2/+
<i>sn</i> ^{36a} ; 80G2/+
+/ <i>Y</i> or <i>sn</i> ³ / <i>Y</i> or <i>sn</i> ^{36a} / <i>Y</i> ; <i>UASmCD8GFP</i> /+; <i>c161Gal4</i> /+
<i>sn</i> ^{36a} / <i>Y</i> ; <i>UASmCD8GFP/UAS-mKO::sn</i> ; <i>c161Gal4</i> /+
<i>UAS-GFP::sn</i> /+; <i>c161Gal4 UASmCD8cherry</i> /+
+/ <i>Y</i> or <i>sn</i> ^{36a} / <i>Y</i> ; <i>477Gal4 UASmCD8GFP</i>
<i>attPUAS::mKOsn/477Gal4 UASmCD8GFP</i>
<i>attPUAS::mKOsnS52A/477Gal4 UASmCD8GFP</i>
<i>attPUAS::mKOsnS52D/477Gal4 UASmCD8GFP</i>
<i>sn</i> ^{36a} / <i>Y</i> ; <i>attPUAS::mKOsn/UASmCD8GFP</i> ; <i>c161Gal4</i> /+
<i>sn</i> ^{36a} / <i>Y</i> ; <i>attPUAS::mKOsnS52A/UASmCD8GFP</i> ; <i>c161Gal4</i> /+
<i>sn</i> ^{36a} / <i>Y</i> ; <i>attPUAS::mKOsnS52D/UASmCD8GFP</i> ; <i>c161Gal4</i> /+
+/ <i>Y</i> ; <i>UAS-cutEHK</i> /+; <i>2-21 UASmCD8GFP</i> /+
<i>sn</i> ^{36a} / <i>Y</i> ; <i>UAS-cutEHK</i> /+; <i>2-21 UASmCD8GFP</i> /+
<i>sn</i> ^{36a} / <i>Y</i> ; <i>2-21 UASmCD8GFP</i> /+
<i>109(2)80Gal4/UAS-actinGFP</i> ; <i>UASmCD8cherry</i> /+
<i>109(2)80Gal4/UAS-tubulinGFP</i> ; <i>UASmCD8cherry</i> /+
<i>UAS-mKO::sn/80G2</i>
<i>UAS-mKO::sn/UASmCD8GFP</i> ; <i>c161Gal4</i> /+
<i>UAS-mKO::sn</i> /+; <i>477Gal4 UASmCD8GFP</i> /+
<i>sn</i> ^{36a} <i>FRT19A</i> ; <i>109(2)80Gal4 UASmCD8::GFP</i> /+
<i>FRT19A</i> ; <i>109(2)80Gal4 UASmCD8::GFP</i> /+

5.3 Methods

5.3.1 Molecular procedures

Fluorescently tagged Singed constructs

For the fluorescently tagged versions of Singed, mKO (GFP) and Singed were cloned in two steps into the pP{UAST} vector. The sites for restriction endonucleases and other additional nucleotides were introduced by appropriate primer design. For mKO (GFP) the restriction sites EcoRI and NotI were added and the STOP codon was eliminated. An additional guanosine nucleotide upstream of the NotI restriction site was necessary to maintain the open reading frame. For Singed the restriction sites NotI and XbaI were added and the first AUG was eliminated. GGA, coding for Glycine, was introduced downstream the NotI site and should provide flexibility between the mKO (GFP) and the Singed part of the protein.

For each construct at least 3 independent lines were generated by Best Gene.

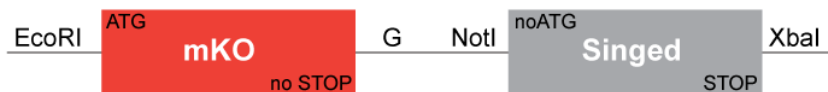


Figure 5.1: Cloning strategy for mKO tagged Singed

Polymerase Chain Reaction (PCR)

PCR was used to amplify the DNA fragments of interest. The template for the PCR amplification of singed was the *Drosophila* cDNA clone LD16477. For the amplification of mKO the pmKO1-MN1 plasmid was used and for the amplification of GFP the pRmHa3-GFP-actin plasmid. The GFP tagged Singed was cloned by Jana Lindner using the same cloning strategy as described for the mKO tagged Singed.

PCR singed

1 μl cDNA clone LD16477 (0,1 $\mu\text{g}/\mu\text{l}$)
2 μl Primer GT684 (10 pmol/ μl)
2 μl Primer GT685 (10 pmol/ μl)
5 μl dNTPs (5 mM)
0.5 μl Pfu DNA Polymerase (3000 U/ml)
5 μl Pfu Buffer

ad 50 μl dH₂O

Cycling conditions

95 °C	2 min	
<hr/>		
95 °C	30 sec	
62 °C	45 sec	34 cycles
72 °C	2 min	
<hr/>		
72 °C	10 min	
10 °C	∞	

PCR KO

1 μl pmKO1-MN1 (0,143 $\mu\text{g}/\mu\text{l}$)
2 μl Primer GT681 (10 pmol/ μl)
2 μl Primer GT682 (10 pmol/ μl)
5 μl dNTPs (5 mM)
1 μl Taq Polymerase (5000 U/ml)
5 μl 10x ThermoPol Reaction Buffer

ad 50 μl dH₂O

Cycling conditions

95 °C	2 min	
95 °C	30 sec	
62 °C	45 sec	34 cycles
72 °C	45 sec	
72 °C	10 min	
10 °C	∞	

Site directed mutagenesis

For the generation of the Singed phosphovariants, mKO tagged Singed was subcloned into the pP{UAST} attB vector (Bischof, Maeda et al. 2007).

To exchange the conserved Serine at position 52 with Alanine or Arspatic Acid I performed site directed mutagenesis by PCR using the Stratagene Quick Change II XL Site directed mutagenesis Kit as described in the manual. To achieve comparable levels of expression all constructs were inserted into the 51D attP landing site (Bischof, Maeda et al. 2007). At least 3 independent lines were generated by Best Gene.

PCR for site directed mutagenesis

10 ng dsDNA template (attPUASmKO::sn)

5 µl 10x Reaction Buffer

1 µl Primer GT827 or GT829 (100pmol/µl)

1 µl Primer GT828 or GT830 (100pmol/µl)

1 µ dNTP Mix

3 µl Quick Solution Reagent

1 µl Ultra Pfu

ad 50 µl dH₂O

Cycling conditions

95 °C	1 min	
<hr/>		
95 °C	50 sec	
60 °C	50 sec	18 cycles
68 °C	13 min	
<hr/>		
68 °C	7 min	
4 °C	∞	

Gelelectrophoresis

Depending on the size of the DNA fragments of interest 0,8 %-1,2 % agarose in TAE buffer was used for the gels. Before pouring the gel, 0,5 µg/ml ethidium bromide were added to the hand-hot agarose to visualize the DNA under UV light. TAE Buffer was used as running Buffer. The gel was run for 30-60 min at 200V. For documentation a picture of the gel was taken under UV light.

Gel extraction of DNA

To purify the specific PCR DNA fragments, the DNA was separated on a agarose gel. The fragment of interest was cut out of the gel under UV-light with a sterile razor blade and purified with QIAquick Gel Extraction Kit following the manufacturer's manual. DNA was eluted with 30 µl dH₂O instead of elution buffer.

Restriction Digests of DNA

Restriction digests with endonucleases were performed in a 20-45 µl reaction volume using buffer conditions and incubation temperatures according to the manufacturer's manual. Digests were incubated 1-4 h. Enzymes were heat inactivated if necessary according to the manufacturer's manual.

Estimation of DNA concentration on a agarose gel

The concentration of DNA can be estimated on an agarose gel. Therefore DNA was loaded on a gel together with a standard curve of DNA of a known concentration. The intensities of their bands were compared and the concentration of the sample DNA estimated. As reference DNA 1 kb DNA ladder at a concentration of 0,1 µg/µl was used. Its 1,6 kb band corresponds to 10% of the total DNA.

Ligation

Ligations were carried out in a 10 µl reaction volume, containing 1 µl T4 DNA Ligase, 1 µl 10x T4 DNA Ligase Buffer, vector and fragment. Vector and fragment (“insert”) concentrations were estimated on an agarose gel and used in an approximate ratio of 1:5 in the reaction, their molecular weight taken to account. The reaction was incubated at 16° C overnight.

Electroporation

After thawing 50 µl electrocompetent bacteria (TOP10, Intritrogen) from a frozen stock (-80° C) for 15 min on ice, 50-150 ng DNA were added. The mixture was transferred to a chilled electroporation cell, avoiding formation of air bubbles. Electroporation was conducted at 2,5V, 25 µF capacity and 200Ω resistance. Directly after electroporation 250-350 µl LB-medium was added and the bacteria were transferred to a 1,5 ml reaction tube and incubated at 37°C for 60 min to allow expression of resistance genes in transformed cells. Afterwards the bacteria were plated on selective LB plates and incubated at 37°C overnight.

DNA Miniprep

The DNA of a 4 ml bacterial overnight culture in selective LB medium was extracted using the QIAprep Spin Miniprep Kit as described in the manual. DNA was eluted with 30 µl dH₂O. DNA purification was verified on an agarose gel.

DNA Midiprep

The DNA of a 50 ml bacterial overnight culture in selective LB medium was extracted using the QIAGEN Plasmid Midi Kit as described in the manual. The DNA pellet was dissolved in 100 μ l dH₂O. DNA concentration was determined with a UV spectrometer.

Determination of DNA concentration

The final concentration of Plasmid DNA was measured using a UV spectrometer. The extinction of 1 at a wavelength of 260 nm corresponds to a concentration of 50 ng/ μ l.

(dsDNA: OD x 50 x dilution factor = X ng/ μ l) The quotient of optical density from 260 nm and 280 nm depends on the quality of the DNA. Pure DNA results in values between 1,8 and 2,0

Culture and conservation of E. coli strains

Bacteria were either cultured in LB-Medium containing selective antibiotics in a shaking incubator at 37° C or on LB-agar plates containing selective antibiotics in an incubator at 37° C. For short time periods bacteria were stored at 4° C, for longer periods they were stored in 45 % Glycerol at -80° C.

Sequencing

The all cloned vectors were verified by sequencing in house or were sent to Eurofins MWG operon.

5.3.2 Gal4 UAS system

With the Gal4 UAS system it is possible to restrict the expression of genes spatially and temporally (Brand and Perrimon 1993). Therefore I implemented this system to visualize different subsets of md-da neurons in the living animal. Gal4 enhancer trap lines combined with UAS coupled fluorophores like mCD8::GFP or mCD8::cherry allowed for labeling of the membrane in the neurons of interest. Moreover, I used the Gal4 UAS system to express UAS coupled genes ectopically.

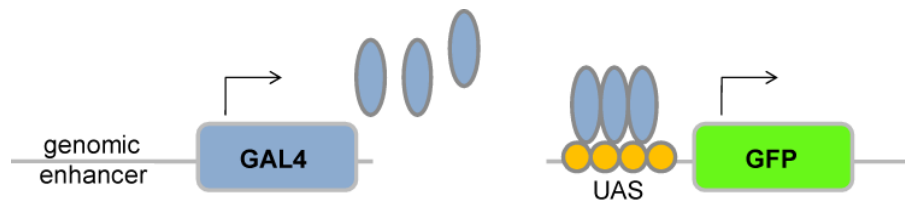


Figure 5.2: Gal4 UAS system

The Gal4 protein is expressed under the control of a tissue specific genomic enhancer. It can bind to upstream activation sequences (UAS) and activate the expression of genes downstream of UAS.

5.3.3 MARCM

The MARCM (mosaic analysis with a repressible cell marker) system is used to create genetic mosaics with unlabeled and labeled cells. Initially all cells in the MARCM system have the potential for the expression of a UAS coupled marker gene: they carry the UAS coupled marker gene and express Gal4, however they are unlabeled because of the existence of a Gal80 repressor. Upon mitotic recombination the repressor can be lost in one daughter cell, allowing for labeling of this cell (Lee and Luo 1999). The mitotic recombination is mediated by the FLP recombinase, which catalyses the recombination at specific FRT sites (Golic and Lindquist 1989). Mutations of interest that were located in *trans* to the Gal80 repressor on the same chromosome arm, and distal to the homozygous insertions of FRTs, should become homozygous in the uniquely labeled cells after the recombination event (Lee and Luo 1999).

For *singed* loss-of-function analysis by MARCM, sn^{36a} was recombined with *FRT19A*. Single male recombinants were checked for the *singed* mutant bristle phenotype to verify the existence of the sn^{36a} p-element insertion. The *FRT19A* insertion was verified by PCR. Therefore single males were frozen at -20°C for 3 h. To extract the genomic DNA frozen single males were squished in 50 μl squishing buffer in PCR tubes. Followed by incubation in the PCR heating block:

37°C	30 min
95°C	2 min
10°C	∞

1 µl of the extracted DNA was used for the PCR.

PCR FRT19A

1 µl extracted DNA
 1 µl Primer GT765 (100 pmol/µl)
 1 µl Primer GT766 (100 pmol/µl)
 10 µl dNTPs (5mM)
 2 µl Taq Polymerase (5000 U/ml)
 10 µl 10x ThermoPol Reaction Buffer

ad 100 µl dH₂O

Cycling conditions

95 °C	5 min	
95 °C	30 sec	
57 °C	30 sec	39 cycles
72 °C	1 min	
72 °C	10 min	
10 °C	∞	

The existence of the 500 bp PCR product was checked by gelelectrophoresis.

tub-Gal80, *hsFLP*, *FRT19A*; *109(2)80Gal4 UASmCD8GFP/CyO* virgins were crossed to *sn^{36a} FRT19A/Y* and *FRT19A/Y* males. Out of this cross an egg collection on apple agar plates was done for two hours at 25°C, followed by a 3 h incubation time at 25°C. Heat shock was performed in a 38°C water bath for 45

min followed by a 30 min incubation time at RT and a final heat shock at 38°C for 30 min (Grueber, Jan et al. 2002). Third instar larvae were directly examined for clones under the confocal microscope (Leica SP2).

5.3.4 Immunohistochemistry

For antibody staining wandering third instar larvae were pinned down on sylgard dishes at their anterior and posterior ends with insect pins. The larvae were then covered with PBS and cut ventral along their long body axis with dissection scissors. The larval body wall, consisting of epidermis and muscles was opened and pinned down to obtain a flat open book preparation. The interior of the larvae, including trachea, CNS and digestive system, was removed (Grueber, Jan et al. 2002).

For Singed antibody staining, filleted third instar larvae were fixed for 1 h at RT in 4% formaldehyde, incubated for 45 min in 1% PBT afterwards incubated in blocking solution for 30 min and probed with the following primary antibodies: mouse anti-Singed 7C (1:20) and rabbit anti-GFP (1:1000); followed by the secondary antibodies: Cy3-conjugated donkey anti-mouse (1:200) and Cy2-conjugated anti-rabbit (1:200).

For Futsch antibody staining filleted third instar larvae were fixed for 5 min in -20°C Methanol, followed by three rehydration steps in 75%, 50% and 25% Methanol at RT for 5 min each. Afterwards they were incubated in blocking solution for 30 min and probed with the following primary antibodies: mouse anti-22C10 (1:20) and rabbit anti-GFP (1:1000); followed by the secondary antibodies: Cy3-conjugated donkey anti-mouse (1:200) and Cy2-conjugated anti-rabbit (1:200).

The larva filets were mounted in Vectashield and analyzed by confocal microscopy (Leica SP2) using a 40x objective.

5.3.5 Confocal imaging

To image the da neurons in abdominal segments A3-A6, wandering third instar larvae were immersed in 90% glycerol and pressed between glass slide and cover slip using double sided tape as spacer. Confocal images were obtained (Leica TCS SP2) using a 20x objective for class I and class III neurons, and a 40x objective for class IV neurons. Maximum projections of the confocal stacks were further processed with Photoshop (Adobe).

For time-lapse imaging *UAS-GFP-sn/+; C161Gal4 UAS-mCD8-cherry/+* second instar larvae (~ 48 h AEL) were mounted in S3 Voltalef halocarbon oil and immobilized with an air-permeable sieve as described before (Dimitrova, Reissaus et al. 2008). For imaging a spinning disc confocal (CSU10 Real-Time Confocal System by Visitron Systems, mounted on a Zeiss Observer 1 microscope) with a Photometrics Coolsnap HQ2 camera was used. Confocal stacks of the same region of the neuron were taken every 3 min over a period of 15 min with a 63x objective. Laser power was set to 80%, exposure time to 900 ms for 561nm laser and 1200 ms for 488nm laser and every stack consists of 10 slices (distance 1µm).

To avoid movement of the larvae they were anesthetized in ether as described before (Zito, Parnas et al. 1999) and immediately imaged. Thereafter each larva was checked for vitality. Maximum projections of the individual time-points were further processed with Photoshop (Adobe). Single time-points were deleted if the larval movement interfered with proper confocal imaging.

5.3.6 Image analysis and statistics

Images were analyzed with ImageJ software (National Institutes of Health, Bethesda, Maryland, USA, <http://rsb.info.nih.gov/ij/>), using the NeuronJ Plug-in (Meijering, Jacob et al. 2004) to trace the dendritic branches. In class III neurons, spiked protrusions were counted as unbranched terminal processes that are no longer than 30 µm. If there was a branch point that gave rise to two terminal branches, the shorter one of these branches was counted as a spiked protrusion, the longer one was considered to be part of the main dendritic tree. To analyze the branch distribution in class IV neurons I used Sholl-Analysis (ImageJ, NeuronJ

plug-in Sholl-Analysis). Neuron J tracings were measured to quantify dendrite length, spiked protrusion and terminal branch number and length and spiked protrusion density. At least 5 different animals per genotype were used for quantification. Statistical analysis was done using Student's t-test for comparing two groups. When more than two groups were compared we did One Way Anova and a Bonferroni's Multiple Comparison Test for normally distributed samples and Dunn's Multiple Comparison Test for non-normally distributed samples.

To calculate the convex hulls defining the curvature of terminal branchlets, NeuronJ reconstructions were exported to tiff images and imported to Matlab. To make the reconstructions accessible to graph theoretical calculations, cells were automatically reconstructed to vectorized directed binary tree structures using the TREES toolbox (Cuntz, Forstner et al. 2010). Terminal branchlets were defined from the terminal tip to the closest branch point along the path to the soma of a cell. Convex hulls enclosing the complete terminal branchlets were computed individually for each terminal using built-in Matlab functions. The polygon area was calculated and normalized by the specific terminal path length.

6 References

- Adams, J. C. (2004). "Roles of fascin in cell adhesion and motility." *Curr Opin Cell Biol* **16**(5): 590-596.
- Adams, J. C., J. D. Clelland, et al. (1999). "Cell-matrix adhesions differentially regulate fascin phosphorylation." *Mol Biol Cell* **10**(12): 4177-4190.
- Adams, J. C. and M. A. Schwartz (2000). "Stimulation of fascin spikes by thrombospondin-1 is mediated by the GTPases Rac and Cdc42." *J Cell Biol* **150**(4): 807-822.
- Ahnert-Hilger, G., M. Holtje, et al. (2004). "Differential effects of Rho GTPases on axonal and dendritic development in hippocampal neurones." *J Neurochem* **90**(1): 9-18.
- Andersen, R., Y. Li, et al. (2005). "Calcium/calmodulin-dependent protein kinase II alters structural plasticity and cytoskeletal dynamics in *Drosophila*." *J Neurosci* **25**(39): 8878-8888.
- Aratyn, Y. S., T. E. Schaus, et al. (2007). "Intrinsic dynamic behavior of fascin in filopodia." *Mol Biol Cell* **18**(10): 3928-3940.
- Baas, P. W., J. S. Deitch, et al. (1988). "Polarity orientation of microtubules in hippocampal neurons: uniformity in the axon and nonuniformity in the dendrite." *Proc Natl Acad Sci U S A* **85**(21): 8335-8339.
- Balcer, H. I., A. L. Goodman, et al. (2003). "Coordinated regulation of actin filament turnover by a high-molecular-weight Srv2/CAP complex, cofilin, profilin, and Aip1." *Curr Biol* **13**(24): 2159-2169.
- Bear, J. E., T. M. Svitkina, et al. (2002). "Antagonism between Ena/VASP proteins and actin filament capping regulates fibroblast motility." *Cell* **109**(4): 509-521.
- Bender, H. A. (1960). "Studies on the Expression of Various Singed Alleles in *Drosophila Melanogaster*." *Genetics* **45**(7): 867-883.
- Bentley, D. and A. Toroian-Raymond (1986). "Disoriented pathfinding by pioneer neurone growth cones deprived of filopodia by cytochalasin treatment." *Nature* **323**(6090): 712-715.
- Bischof, J., R. K. Maeda, et al. (2007). "An optimized transgenesis system for *Drosophila* using germ-line-specific phiC31 integrases." *Proc Natl Acad Sci U S A* **104**(9): 3312-3317.
- Blanchoin, L. and T. D. Pollard (2002). "Hydrolysis of ATP by polymerized actin depends on the bound divalent cation but not profilin." *Biochemistry* **41**(2): 597-602.
- Bodmer, R., S. Barbel, et al. (1987). "Transformation of sensory organs by mutations of the cut locus of *D. melanogaster*." *Cell* **51**(2): 293-307.
- Branco, T., B. A. Clark, et al. (2010). "Dendritic discrimination of temporal input sequences in cortical neurons." *Science* **329**(5999): 1671-1675.
- Brand, A. H. and N. Perrimon (1993). "Targeted gene expression as a means of altering cell fates and generating dominant phenotypes." *Development* **118**(2): 401-415.
- Brierley, D. J., E. Blanc, et al. (2009). "Dendritic targeting in the leg neuropil of *Drosophila*: the role of midline signalling molecules in generating a myotopic map." *PLoS Biol* **7**(9): e1000199.

- Brown, J. A. and P. C. Bridgman (2009). "Disruption of the cytoskeleton during Semaphorin 3A induced growth cone collapse correlates with differences in actin organization and associated binding proteins." *Dev Neurobiol* **69**(10): 633-646.
- Bryan, J., R. Edwards, et al. (1993). "Fascin, an echinoid actin-bundling protein, is a homolog of the *Drosophila* *singed* gene product." *Proc Natl Acad Sci U S A* **90**(19): 9115-9119.
- Bryan, J. and R. E. Kane (1978). "Separation and interaction of the major components of sea urchin actin gel." *J Mol Biol* **125**(2): 207-224.
- Cant, K. and L. Cooley (1996). "Single amino acid mutations in *Drosophila* fascin disrupt actin bundling function in vivo." *Genetics* **143**(1): 249-258.
- Cant, K., B. A. Knowles, et al. (1994). "*Drosophila* *singed*, a fascin homolog, is required for actin bundle formation during oogenesis and bristle extension." *J Cell Biol* **125**(2): 369-380.
- Carrier, M. F. and D. Pantaloni (1988). "Binding of phosphate to F-ADP-actin and role of F-ADP-Pi-actin in ATP-actin polymerization." *J Biol Chem* **263**(2): 817-825.
- Cheng, L. E., W. Song, et al. (2010). "The role of the TRP channel NompC in *Drosophila* larval and adult locomotion." *Neuron* **67**(3): 373-380.
- Cohan, C. S., E. A. Weinhofner, et al. (2001). "Role of the actin bundling protein fascin in growth cone morphogenesis: localization in filopodia and lamellipodia." *Cell Motil Cytoskeleton* **48**(2): 109-120.
- Corty, M. M., B. J. Matthews, et al. (2009). "Molecules and mechanisms of dendrite development in *Drosophila*." *Development* **136**(7): 1049-1061.
- Crozatier, M. and A. Vincent (2008). "Control of multidendritic neuron differentiation in *Drosophila*: the role of *Collier*." *Dev Biol* **315**(1): 232-242.
- Cubelos, B., A. Sebastian-Serrano, et al. (2010). "Cux1 and Cux2 regulate dendritic branching, spine morphology, and synapses of the upper layer neurons of the cortex." *Neuron* **66**(4): 523-535.
- Cuntz, H., F. Forstner, et al. (2010). "One rule to grow them all: a general theory of neuronal branching and its practical application." *PLoS Comput Biol* **6**(8).
- Dailey, M. E. and S. J. Smith (1996). "The dynamics of dendritic structure in developing hippocampal slices." *J Neurosci* **16**(9): 2983-2994.
- De Arcangelis, A., E. Georges-Labouesse, et al. (2004). "Expression of fascin-1, the gene encoding the actin-bundling protein fascin-1, during mouse embryogenesis." *Gene Expr Patterns* **4**(6): 637-643.
- DeRosier, D. J. and K. T. Edds (1980). "Evidence for fascin cross-links between the actin filaments in coelomocyte filopodia." *Exp Cell Res* **126**(2): 490-494.
- Dimitrova, S., A. Reissaus, et al. (2008). "Slit and Robo regulate dendrite branching and elongation of space-filling neurons in *Drosophila*." *Dev Biol* **324**(1): 18-30.
- Edwards, R. A., H. Herrera-Sosa, et al. (1995). "Cloning and expression of a murine fascin homolog from mouse brain." *J Biol Chem* **270**(18): 10764-10770.
- Eriksson, A. E., L. S. Cousens, et al. (1991). "Three-dimensional structure of human basic fibroblast growth factor." *Proc Natl Acad Sci U S A* **88**(8): 3441-3445.

- Faix, J., D. Breitsprecher, et al. (2009). "Filopodia: Complex models for simple rods." Int J Biochem Cell Biol **41**(8-9): 1656-1664.
- Feller, M. B. (1999). "Spontaneous correlated activity in developing neural circuits." Neuron **22**(4): 653-656.
- Fujiwara, I., S. Takahashi, et al. (2002). "Microscopic analysis of polymerization dynamics with individual actin filaments." Nat Cell Biol **4**(9): 666-673.
- Furrer, M. P., S. Kim, et al. (2003). "Robo and Frazzled/DCC mediate dendritic guidance at the CNS midline." Nat Neurosci **6**(3): 223-230.
- Furrer, M. P., I. Vasenkova, et al. (2007). "Slit and Robo control the development of dendrites in Drosophila CNS." Development **134**(21): 3795-3804.
- Gao, F. B., J. E. Brenman, et al. (1999). "Genes regulating dendritic outgrowth, branching, and routing in Drosophila." Genes Dev **13**(19): 2549-2561.
- Golic, K. G. and S. Lindquist (1989). "The FLP recombinase of yeast catalyzes site-specific recombination in the Drosophila genome." Cell **59**(3): 499-509.
- Govek, E. E., S. E. Newey, et al. (2005). "The role of the Rho GTPases in neuronal development." Genes Dev **19**(1): 1-49.
- Graves, B. J., M. H. Hatada, et al. (1990). "Structure of interleukin 1 alpha at 2.7-A resolution." Biochemistry **29**(11): 2679-2684.
- Grieder, N. C., M. de Cuevas, et al. (2000). "The fusome organizes the microtubule network during oocyte differentiation in Drosophila." Development **127**(19): 4253-4264.
- Grueber, W. B., L. Y. Jan, et al. (2002). "Tiling of the Drosophila epidermis by multidendritic sensory neurons." Development **129**(12): 2867-2878.
- Grueber, W. B., L. Y. Jan, et al. (2003). "Different levels of the homeodomain protein cut regulate distinct dendrite branching patterns of Drosophila multidendritic neurons." Cell **112**(6): 805-818.
- Gundersen, R. W. and J. N. Barrett (1980). "Characterization of the turning response of dorsal root neurites toward nerve growth factor." J Cell Biol **87**(3 Pt 1): 546-554.
- Gupton, S. L. and F. B. Gertler (2007). "Filopodia: the fingers that do the walking." Sci STKE **2007**(400): re5.
- Hand, R., D. Bortone, et al. (2005). "Phosphorylation of Neurogenin2 specifies the migration properties and the dendritic morphology of pyramidal neurons in the neocortex." Neuron **48**(1): 45-62.
- Hartwig, J. H. and T. P. Stossel (1975). "Isolation and properties of actin, myosin, and a new actinbinding protein in rabbit alveolar macrophages." J Biol Chem **250**(14): 5696-5705.
- Hashimoto, Y., M. Parsons, et al. (2007). "Dual actin-bundling and protein kinase C-binding activities of fascin regulate carcinoma cell migration downstream of Rac and contribute to metastasis." Mol Biol Cell **18**(11): 4591-4602.
- Hattori, Y., K. Sugimura, et al. (2007). "Selective expression of Knot/Collier, a transcriptional regulator of the EBF/Olf-1 family, endows the Drosophila sensory system with neuronal class-specific elaborated dendritic patterns." Genes Cells **12**(9): 1011-1022.

- Heiman, M. G. and S. Shaham (2010). "Twigs into branches: how a filopodium becomes a dendrite." Curr Opin Neurobiol **20**(1): 86-91.
- Holthuis, J. C., V. T. Schoonderwoert, et al. (1994). "A vertebrate homolog of the actin-bundling protein fascin." Biochim Biophys Acta **1219**(1): 184-188.
- Hudson, A. M. and L. Cooley (2002). "Understanding the function of actin-binding proteins through genetic analysis of *Drosophila* oogenesis." Annu Rev Genet **36**: 455-488.
- Hughes, C. L. and J. B. Thomas (2007). "A sensory feedback circuit coordinates muscle activity in *Drosophila*." Mol Cell Neurosci **35**(2): 383-396.
- Hummel, T., K. Krukkert, et al. (2000). "*Drosophila* Futsch/22C10 is a MAP1B-like protein required for dendritic and axonal development." Neuron **26**(2): 357-370.
- Hwang, R. Y., L. Zhong, et al. (2007). "Nociceptive neurons protect *Drosophila* larvae from parasitoid wasps." Curr Biol **17**(24): 2105-2116.
- Jan, Y. N. and L. Y. Jan (2010). "Branching out: mechanisms of dendritic arborization." Nat Rev Neurosci **11**(5): 316-328.
- Jinushi-Nakao, S., R. Arvind, et al. (2007). "Knot/Collier and cut control different aspects of dendrite cytoskeleton and synergize to define final arbor shape." Neuron **56**(6): 963-978.
- Kane, R. E. (1975). "Preparation and purification of polymerized actin from sea urchin egg extracts." J Cell Biol **66**(2): 305-315.
- Katz, L. C. and C. J. Shatz (1996). "Synaptic activity and the construction of cortical circuits." Science **274**(5290): 1133-1138.
- Kim, M. D., L. Y. Jan, et al. (2006). "The bHLH-PAS protein Spineless is necessary for the diversification of dendrite morphology of *Drosophila* dendritic arborization neurons." Genes Dev **20**(20): 2806-2819.
- Komiyama, T., L. B. Sweeney, et al. (2007). "Graded expression of semaphorin-1a cell-autonomously directs dendritic targeting of olfactory projection neurons." Cell **128**(2): 399-410.
- Korobova, F. and T. Svitkina (2008). "Arp2/3 complex is important for filopodia formation, growth cone motility, and neuritogenesis in neuronal cells." Mol Biol Cell **19**(4): 1561-1574.
- Kraft, R., M. M. Escobar, et al. (2006). "Phenotypes of *Drosophila* brain neurons in primary culture reveal a role for fascin in neurite shape and trajectory." J Neurosci **26**(34): 8734-8747.
- Krause, M., E. W. Dent, et al. (2003). "Ena/VASP proteins: regulators of the actin cytoskeleton and cell migration." Annu Rev Cell Dev Biol **19**: 541-564.
- Kuhn, T. B., P. J. Meberg, et al. (2000). "Regulating actin dynamics in neuronal growth cones by ADF/cofilin and rho family GTPases." J Neurobiol **44**(2): 126-144.
- Kureishy, N., V. Sapountzi, et al. (2002). "Fascin, and their roles in cell structure and function." Bioessays **24**(4): 350-361.
- Lee, A., W. Li, et al. (2003). "Control of dendritic development by the *Drosophila* fragile X-related gene involves the small GTPase Rac1." Development **130**(22): 5543-5552.
- Lee, T. and L. Luo (1999). "Mosaic analysis with a repressible cell marker for studies of gene function in neuronal morphogenesis." Neuron **22**(3): 451-461.

- Lee, T., C. Winter, et al. (2000). "Essential roles of Drosophila RhoA in the regulation of neuroblast proliferation and dendritic but not axonal morphogenesis." *Neuron* **25**(2): 307-316.
- Lewis, A. K. and P. C. Bridgman (1992). "Nerve growth cone lamellipodia contain two populations of actin filaments that differ in organization and polarity." *J Cell Biol* **119**(5): 1219-1243.
- Li, L., V. Mauric, et al. (2010). "Olfactory bulb proteins linked to olfactory memory in C57BL/6J mice." *Amino Acids*.
- Li, W. and F. B. Gao (2003). "Actin filament-stabilizing protein tropomyosin regulates the size of dendritic fields." *J Neurosci* **23**(15): 6171-6175.
- Li, W., Y. Li, et al. (2005). "Abelson, enabled, and p120 catenin exert distinct effects on dendritic morphogenesis in Drosophila." *Dev Dyn* **234**(3): 512-522.
- Li, Z., L. Van Aelst, et al. (2000). "Rho GTPases regulate distinct aspects of dendritic arbor growth in Xenopus central neurons in vivo." *Nat Neurosci* **3**(3): 217-225.
- London, M. and M. Hausser (2005). "Dendritic computation." *Annu Rev Neurosci* **28**: 503-532.
- Luo, L. (2000). "Rho GTPases in neuronal morphogenesis." *Nat Rev Neurosci* **1**(3): 173-180.
- Luo, L., Y. J. Liao, et al. (1994). "Distinct morphogenetic functions of similar small GTPases: Drosophila Drac1 is involved in axonal outgrowth and myoblast fusion." *Genes Dev* **8**(15): 1787-1802.
- Mabuchi, I. and R. E. Kane (1987). "A 250K-molecular-weight actin-binding protein from actin-based gels formed in sea urchin egg cytoplasmic extract." *J Biochem (Tokyo)* **102**(4): 947-956.
- Maekawa, S., S. Endo, et al. (1982). "A protein in starfish sperm head which bundles actin filaments in vitro: purification and characterization." *J Biochem (Tokyo)* **92**(6): 1959-1972.
- Magee, J. C. (2000). "Dendritic integration of excitatory synaptic input." *Nat Rev Neurosci* **1**(3): 181-190.
- Mattie, F. J., M. M. Stackpole, et al. (2010). "Directed microtubule growth, +TIPs, and kinesin-2 are required for uniform microtubule polarity in dendrites." *Curr Biol* **20**(24): 2169-2177.
- Mattila, P. K. and P. Lappalainen (2008). "Filopodia: molecular architecture and cellular functions." *Nat Rev Mol Cell Biol* **9**(6): 446-454.
- Mauss, A., M. Tripodi, et al. (2009). "Midline signalling systems direct the formation of a neural map by dendritic targeting in the Drosophila motor system." *PLoS Biol* **7**(9): e1000200.
- McAllister, A. K., D. C. Lo, et al. (1995). "Neurotrophins regulate dendritic growth in developing visual cortex." *Neuron* **15**(4): 791-803.
- Medalia, O., M. Beck, et al. (2007). "Organization of actin networks in intact filopodia." *Curr Biol* **17**(1): 79-84.
- Medina, P. M., L. L. Swick, et al. (2006). "A novel forward genetic screen for identifying mutations affecting larval neuronal dendrite development in Drosophila melanogaster." *Genetics* **172**(4): 2325-2335.
- Medina, P. M., R. J. Worthen, et al. (2008). "The actin-binding protein capulet genetically interacts with the microtubule motor kinesin to maintain neuronal dendrite homeostasis." *PLoS One* **3**(8): e3054.

- Meijering, E., M. Jacob, et al. (2004). "Design and validation of a tool for neurite tracing and analysis in fluorescence microscopy images." *Cytometry A* **58**(2): 167-176.
- Mogilner, A. and B. Rubinstein (2005). "The physics of filopodial protrusion." *Biophys J* **89**(2): 782-795.
- Moriyama, K. and I. Yahara (2002). "Human CAP1 is a key factor in the recycling of cofilin and actin for rapid actin turnover." *J Cell Sci* **115**(Pt 8): 1591-1601.
- Mosialos, G., S. H. Hanissian, et al. (1994). "A Ca²⁺/calmodulin-dependent protein kinase, CaM kinase-Gr, expressed after transformation of primary human B lymphocytes by Epstein-Barr virus (EBV) is induced by the EBV oncogene LMP1." *J Virol* **68**(3): 1697-1705.
- Mrkusch, E. M., Z. B. Osman, et al. (2010). "Netrin-guided accessory cell morphogenesis dictates the dendrite orientation and migration of a Drosophila sensory neuron." *Development* **137**(13): 2227-2235.
- Nepveu, A. (2001). "Role of the multifunctional CDP/Cut/Cux homeodomain transcription factor in regulating differentiation, cell growth and development." *Gene* **270**(1-2): 1-15.
- Ng, J., T. Nardine, et al. (2002). "Rac GTPases control axon growth, guidance and branching." *Nature* **416**(6879): 442-447.
- Niell, C. M., M. P. Meyer, et al. (2004). "In vivo imaging of synapse formation on a growing dendritic arbor." *Nat Neurosci* **7**(3): 254-260.
- Noguchi, T., M. Lenartowska, et al. (2008). "Proper cellular reorganization during Drosophila spermatid individualization depends on actin structures composed of two domains, bundles and meshwork, that are differentially regulated and have different functions." *Mol Biol Cell* **19**(6): 2363-2372.
- Ono, S., Y. Yamakita, et al. (1997). "Identification of an actin binding region and a protein kinase C phosphorylation site on human fascin." *J Biol Chem* **272**(4): 2527-2533.
- Otto, J. J., R. E. Kane, et al. (1979). "Formation of filopodia in coelomocytes: localization of fascin, a 58,000 dalton actin cross-linking protein." *Cell* **17**(2): 285-293.
- Parrish, J. Z., M. D. Kim, et al. (2006). "Genome-wide analyses identify transcription factors required for proper morphogenesis of Drosophila sensory neuron dendrites." *Genes Dev* **20**(7): 820-835.
- Parsons, M. and J. C. Adams (2008). "Rac regulates the interaction of fascin with protein kinase C in cell migration." *J Cell Sci* **121**(Pt 17): 2805-2813.
- Paterson, J. and K. O'Hare (1991). "Structure and transcription of the singed locus of Drosophila melanogaster." *Genetics* **129**(4): 1073-1084.
- Pilpel, Y. and M. Segal (2004). "Activation of PKC induces rapid morphological plasticity in dendrites of hippocampal neurons via Rac and Rho-dependent mechanisms." *Eur J Neurosci* **19**(12): 3151-3164.
- Pollard, T. D. (1986). "Rate constants for the reactions of ATP- and ADP-actin with the ends of actin filaments." *J Cell Biol* **103**(6 Pt 2): 2747-2754.
- Pollard, T. D. and G. G. Borisy (2003). "Cellular motility driven by assembly and disassembly of actin filaments." *Cell* **112**(4): 453-465.

- Pollard, T. D. and J. A. Cooper (2009). "Actin, a central player in cell shape and movement." Science **326**(5957): 1208-1212.
- Polleux, F., T. Morrow, et al. (2000). "Semaphorin 3A is a chemoattractant for cortical apical dendrites." Nature **404**(6778): 567-573.
- Ponting, C. P. and R. B. Russell (2000). "Identification of distant homologues of fibroblast growth factors suggests a common ancestor for all beta-trefoil proteins." J Mol Biol **302**(5): 1041-1047.
- Pruyne, D. W., D. H. Schott, et al. (1998). "Tropomyosin-containing actin cables direct the Myo2p-dependent polarized delivery of secretory vesicles in budding yeast." J Cell Biol **143**(7): 1931-1945.
- Purdy, K. R., J. R. Bartles, et al. (2007). "Structural polymorphism of the actin-espino system: a prototypical system of filaments and linkers in stereocilia." Phys Rev Lett **98**(5): 058105.
- Rajan, I. and H. T. Cline (1998). "Glutamate receptor activity is required for normal development of tectal cell dendrites in vivo." J Neurosci **18**(19): 7836-7846.
- Rajan, I., S. Witte, et al. (1999). "NMDA receptor activity stabilizes presynaptic retinotectal axons and postsynaptic optic tectal cell dendrites in vivo." J Neurobiol **38**(3): 357-368.
- Ruchhoeft, M. L., S. Ohnuma, et al. (1999). "The neuronal architecture of Xenopus retinal ganglion cells is sculpted by rho-family GTPases in vivo." J Neurosci **19**(19): 8454-8463.
- Sasaki, Y., K. Hayashi, et al. (1996). "Inhibition by drebrin of the actin-bundling activity of brain fascin, a protein localized in filopodia of growth cones." J Neurochem **66**(3): 980-988.
- Schafer, D. A., P. B. Jennings, et al. (1996). "Dynamics of capping protein and actin assembly in vitro: uncapping barbed ends by polyphosphoinositides." J Cell Biol **135**(1): 169-179.
- Schirenbeck, A., T. Bretschneider, et al. (2005). "The Diaphanous-related formin dDia2 is required for the formation and maintenance of filopodia." Nat Cell Biol **7**(6): 619-625.
- Scott, E. K., J. E. Reuter, et al. (2003). "Small GTPase Cdc42 is required for multiple aspects of dendritic morphogenesis." J Neurosci **23**(8): 3118-3123.
- Sedeh, R. S., A. A. Fedorov, et al. (2010). "Structure, Evolutionary Conservation, and Conformational Dynamics of Homo sapiens Fascin-1, an F-actin Crosslinking Protein." J Mol Biol.
- Sept, D. and J. A. McCammon (2001). "Thermodynamics and kinetics of actin filament nucleation." Biophys J **81**(2): 667-674.
- Shepherd, D. and S. A. Smith (1996). "Central projections of persistent larval sensory neurons prefigure adult sensory pathways in the CNS of Drosophila." Development **122**(8): 2375-2384.
- Shibayama, T., J. M. Carboni, et al. (1987). "Assembly of the intestinal brush border: appearance and redistribution of microvillar core proteins in developing chick enterocytes." J Cell Biol **105**(1): 335-344.
- Shin, H., K. R. Purdy Drew, et al. (2009). "Cooperativity and frustration in protein-mediated parallel actin bundles." Phys Rev Lett **103**(23): 238102.
- Small, J. V., G. Isenberg, et al. (1978). "Polarity of actin at the leading edge of cultured cells." Nature **272**(5654): 638-639.
- Small, J. V., A. Rohlf, et al. (1993). "Actin and cell movement." Symp Soc Exp Biol **47**: 57-71.

- Small, J. V., T. Stradal, et al. (2002). "The lamellipodium: where motility begins." Trends Cell Biol **12**(3): 112-120.
- Steffen, A., J. Faix, et al. (2006). "Filopodia formation in the absence of functional WAVE- and Arp2/3-complexes." Mol Biol Cell **17**(6): 2581-2591.
- Sugimura, K., D. Satoh, et al. (2004). "Development of morphological diversity of dendrites in *Drosophila* by the BTB-zinc finger protein abrupt." Neuron **43**(6): 809-822.
- Sugimura, K., M. Yamamoto, et al. (2003). "Distinct developmental modes and lesion-induced reactions of dendrites of two classes of *Drosophila* sensory neurons." J Neurosci **23**(9): 3752-3760.
- Svitkina, T. M., E. A. Bulanova, et al. (2003). "Mechanism of filopodia initiation by reorganization of a dendritic network." J Cell Biol **160**(3): 409-421.
- Teichmann, H. M. and K. Shen (2011). "UNC-6 and UNC-40 promote dendritic growth through PAR-4 in *Caenorhabditis elegans* neurons." Nat Neurosci **14**(2): 165-172.
- Threadgill, R., K. Bobb, et al. (1997). "Regulation of dendritic growth and remodeling by Rho, Rac, and Cdc42." Neuron **19**(3): 625-634.
- Tilney, L. G., P. S. Connelly, et al. (2000). "Regulation of actin filament cross-linking and bundle shape in *Drosophila* bristles." J Cell Biol **148**(1): 87-100.
- Tilney, L. G., M. S. Tilney, et al. (1992). "Actin filaments, stereocilia, and hair cells: how cells count and measure." Annu Rev Cell Biol **8**: 257-274.
- Tubb, B., D. J. Mulholland, et al. (2002). "Testis fascin (FSCN3): a novel paralog of the actin-bundling protein fascin expressed specifically in the elongate spermatid head." Exp Cell Res **275**(1): 92-109.
- Tubb, B. E., S. Bardien-Kruger, et al. (2000). "Characterization of human retinal fascin gene (FSCN2) at 17q25: close physical linkage of fascin and cytoplasmic actin genes." Genomics **65**(2): 146-156.
- Vignjevic, D., S. Kojima, et al. (2006). "Role of fascin in filopodial protrusion." J Cell Biol **174**(6): 863-875.
- Vignjevic, D. and G. Montagnac (2008). "Reorganisation of the dendritic actin network during cancer cell migration and invasion." Semin Cancer Biol **18**(1): 12-22.
- Vignjevic, D., D. Yarar, et al. (2003). "Formation of filopodia-like bundles in vitro from a dendritic network." J Cell Biol **160**(6): 951-962.
- Wada, Y., T. Abe, et al. (2001). "Mutation of human retinal fascin gene (FSCN2) causes autosomal dominant retinitis pigmentosa." Invest Ophthalmol Vis Sci **42**(10): 2395-2400.
- Whitford, K. L., V. Marillat, et al. (2002). "Regulation of cortical dendrite development by Slit-Robo interactions." Neuron **33**(1): 47-61.
- Wu, G. Y., D. J. Zou, et al. (1999). "Dendritic dynamics in vivo change during neuronal maturation." J Neurosci **19**(11): 4472-4483.
- Xiang, Y., Q. Yuan, et al. (2010). "Light-avoidance-mediating photoreceptors tile the *Drosophila* larval body wall." Nature **468**(7326): 921-926.

- Yamakita, Y., F. Matsumura, et al. (2009). "Fascin1 is dispensable for mouse development but is favorable for neonatal survival." *Cell Motil Cytoskeleton* **66**(8): 524-534.
- Yamakita, Y., S. Ono, et al. (1996). "Phosphorylation of human fascin inhibits its actin binding and bundling activities." *J Biol Chem* **271**(21): 12632-12638.
- Yamamoto, M., R. Ueda, et al. (2006). "Control of axonal sprouting and dendrite branching by the Nrg-Ank complex at the neuron-glia interface." *Curr Biol* **16**(16): 1678-1683.
- Yamashiro-Matsumura, S. and F. Matsumura (1985). "Purification and characterization of an F-actin-bundling 55-kilodalton protein from HeLa cells." *J Biol Chem* **260**(8): 5087-5097.
- Yamashiro-Matsumura, S. and F. Matsumura (1986). "Intracellular localization of the 55-kD actin-bundling protein in cultured cells: spatial relationships with actin, alpha-actinin, tropomyosin, and fimbrin." *J Cell Biol* **103**(2): 631-640.
- Yamashiro, S., Y. Yamakita, et al. (1998). "Fascin, an actin-bundling protein, induces membrane protrusions and increases cell motility of epithelial cells." *Mol Biol Cell* **9**(5): 993-1006.
- Ye, B., C. Petritsch, et al. (2004). "Nanos and Pumilio are essential for dendrite morphogenesis in Drosophila peripheral neurons." *Curr Biol* **14**(4): 314-321.
- Zanet, J., B. Stramer, et al. (2009). "Fascin is required for blood cell migration during Drosophila embryogenesis." *Development* **136**(15): 2557-2565.
- Zhang, F. R., L. H. Tao, et al. (2008). "Fascin expression in human embryonic, fetal, and normal adult tissue." *J Histochem Cytochem* **56**(2): 193-199.
- Zhang, J., M. Fonovic, et al. (2009). "Rab35 controls actin bundling by recruiting fascin as an effector protein." *Science* **325**(5945): 1250-1254.
- Zheng, J. Q., J. J. Wan, et al. (1996). "Essential role of filopodia in chemotropic turning of nerve growth cone induced by a glutamate gradient." *J Neurosci* **16**(3): 1140-1149.
- Zito, K., D. Parnas, et al. (1999). "Watching a synapse grow: noninvasive confocal imaging of synaptic growth in Drosophila." *Neuron* **22**(4): 719-729.

7 Acknowledgements

I like to thank Gaia Tavosanis for being an encouraging and caring supervisor. Thanks to all the current and previous members of the Tavosanis Lab for scientific and non-scientific discussion, you created a wonderful working atmosphere. For experimental support, I especially thank Jana Linder, Yun Zhang and Anastasia Tatarnikova.

I also owe very special thanks to Rüdiger Klein who always supported my work with useful discussion. Moreover, I thank Theresia Stradal, Adrian Moore, Caroline Delandre, Ilona Kadow and Takashi Suzuki for their great scientific advice. Finally, all the people from the MPI of Neurobiology who made every day work almost a pleasure – thank you! I am pretty sure that there is no working place in the whole wide world where I could have such a fun time.

Dodo, Flo, Daniel und Marion, ich bin überaus dankbar in euch wahre Freunde gefunden zu haben!

Der größte Dank gilt meiner Familie, weil sie einfach immer für mich da ist. Mama, Papa, Eva und Patrick...Danke!

Patrick, mit dem Abschluss dieser Arbeit geht eine lange und schwierige Zeit für uns zu Ende. Ich bin dankbar und stolz, dass wir es auch über die große Distanz geschafft haben uns im Laufe der Jahre nicht voneinander zu entfernen, sondern weiter zusammen zu wachsen.

8 Curriculum vitae

Personal data

Name Julia Nagel, née Negele
Date of birth 25th of February 1981 in Munich, Germany

Education

Since 04/2007 PhD thesis with Dr. Gaia Tavosanis under supervision of Prof. Dr. Rüdiger Klein at the Max Planck Institute of Neurobiology in Martinsried, Germany
03/2007 Diploma in Biology
06/2006 – 03/2007 Diploma Theses with Dr. Gaia Tavosanis at the Max Planck Institute of Neurobiology in Martinsried, Germany
09/2000 – 03/2007 Studies of Biology at the Ludwig Maximilians University München
06/2000 Allgemeine Hochschulreife

Scientific activities

09/2010 Talk at the Neurofly Meeting at the University of Manchester, UK
“The Specific Role of the General Actin Bundling Protein Fascin in Dendrite Differentiation”
10/2007 Talk at the 13th Regional *Drosophila* Meeting, Humbolt University, Berlin
“Studies on the Actin Regulation of Dendritic Branch Formation”